creative commons
COMMONS DEED

저작자표시-비영리-변경금지 2.0 대한민국

이용자는 아래의 조건을 따르는 경우에 한하여 자유롭게

- 이 저작물을 복제, 배포, 전송, 전시, 공연 및 방송할 수 있습니다.

다음과 같은 조건을 따라야 합니다:

저작자표시. 귀하는 원저작자를 표시하여야 합니다.

비영리. 귀하는 이 저작물을 영리 목적으로 이용할 수 없습니다.

변경금지. 귀하는 이 저작물을 개작, 변형 또는 가공할 수 없습니다.

- 귀하는, 이 저작물의 재이용이나 배포의 경우, 이 저작물에 적용된 이용허락조건을 명확하게 나타내어야 합니다.
- 저작권자로부터 별도의 허가를 받으면 이러한 조건들은 적용되지 않습니다.

저작권법에 따른 이용자의 권리는 위의 내용에 의하여 영향을 받지 않습니다.

이것은 이용허락규약(Legal Code)을 이해하기 쉽게 요약한 것입니다.

Disclaimer

dCollection

A Thesis for the Degree of Doctor of Philosophy

Genomic, Transcriptomic, and Metagenomic Analyses of *Vibrio* species and Microbial Community Composition of Crabs Harvested at Different Seasons and Locations

패혈증 비브리오균의 유전체 분석을 통한 꽃게 내 전사체 특성 규명 및 계절과 지역에 따른 미생물 균총 조성 분석

August, 2016

Suyeon Kim

Department of Agricultural Biotechnology

College of Agriculture and Life Sciences

Seoul National University

Genomic, Transcriptomic, and Metagenomic Analyses of *Vibrio* species and Microbial Community Composition of Crabs Harvested at Different Seasons and Locations

패혈증 비브리오균의 유전체 분석을 통한 꽃게 내 전사체 특성 규명 및 계절과 지역에 따른 미생물 균총 조성 분석

지도교수 최 상 호
이 논문을 농학박사학위논문으로 제출함

2016년 5월

서울대학교 대학원
농생명공학부
김 수 연

김수연의 박사학위논문을 인준함
2016년 6월

위 원 장 유 상렬 (인)
부위원장 최 상호 (인)
위 원 하 남출 (인)
위 원 이 주훈 (인)
위 원 김 봉수 (인)

Abstract

Genomic, Transcriptomic, and Metagenomic Analyses of *Vibrio* species and Microbial Community Composition of Crabs Harvested at Different Seasons and Locations

Suyeon Kim

Department of Agricultural Biotechnology

The Graduate School

Seoul National University

Vibrio vulnificus and *Vibrio parahaemolyticus* are gram-negative, motile, nonspore-forming opportunistic pathogens that causes foodborne illness associated with the consumption of contaminated seafood. Although many cases of foodborne outbreaks caused by *V. vulnificus* and *V. parahaemolyticus* have been reported, the genomes of only few of them have been completely sequenced and analyzed using bioinformatics. In order to characterize overall virulence factors and pathogenesis of *V. vulinificus* and *V. parahaemolyticus* associated with foodborne outbreak in South Korea, new strains *V. vulnificus* FORC_016 and *V. parahaemolyticus* FORC_008 were isolated from blood of food-poisoning patient or flounder fish and their genome

was completely sequenced. The genomic analysis of FORC_016 revealed that the genome consists of two circular DNA chromosomes, and contains 4,461 predicted open reading frames (ORFs), 129 tRNAs, and 34 rRNA genes. *V. parahaemolyticus* FORC_008 have two circular DNA chromosomes containing 4,494 predicted ORFs, 129 tRNAs, and 31 rRNA genes. The genomic analysis revealed that the *V. vulnificus* FORC_016 has major virulence genes such as RTX, cytolysin, and metalloprotases. Furthermore, comparative genome analysis identified unique virulence genes of FORC_016 strain, suggesting that this pathogen have unique pathogenesis mechanism which different from other *V. vulnificus*. While the strain FORC_008 does not have genes encoding thermo-stable direct hemolysin (TDH) and TDH-related hemolysin (TRH), its genome encodes many other virulence factors including hemolysins, pathogenesis-associated secretion systems, and iron acquisition systems, suggesting that it may be a potential pathogen. Subsequent cytotoxicity test of the strain FORC_008 revealed its high cytotoxicity activity, substantiating this. This report provides an extended understanding on *V. vulnificus* and *V. parahaemolyticus* in genomic level and would be helpful for rapid detection, epidemiological investigation, and prevention of foodborne outbreak in South Korea.

Because the foodborne illness occurs via consumption of contaminated food, it is important not only understanding of the virulence factors but also the transcriptome

alteration of pathogens caused by contacting with foods. To identify differentially expressed genes of pathogen under contact with foods, *V. vulnificus* FORC_016, an opportunistic marine pathogen, was selected for the transcriptome analysis. Swimming crab, a common niche of *V. vulnificus,* was selected for the model foods. The transcriptomic profiles of *V. vulnificus* exposed or unexporsed to crab in 1 or 4h were analyzed using a strand-specific RNA-sequencing. By analyzing RPKM (reads per kilobase of transcript per million reads) fold changes of each gene, I identified that 922 and 648 genes were differentially expressed under exposure to crab for 1h and 4h (P value < 0.05, 2 fold threshold). Regardless of incubation time, the genes related with energy production, cell growth, oligopeptide transport, and glucose metabolism were up-regulated, while genes associated with amino acid biosynthesis, nitrogen metabolism, and other sugar metabolism were down-regulated. These result suggested that *V. vulnificus* could metabolize the component of crab. Also, the genes encoding thermolabile hemolysin was up-regulated, suggesting this virulence gene might be have crucial role for pathogenesis of *V. vulnificus* FORC_016 when consumed the *V. vulnificus* FORC_016 contaminated crab.

The swimming crab, *Portunus trituberculatus,* is the most consumed edible crab in South Korea, and their production and consumption have been increased. Although the foodborne illness caused by consuming of swimming crab have been reported

each year, the bacterial community in swimming crab has not been fully understood yet. In order to identify the bacterial members in swimming crab depending on seasons and locations, the microbiota in 65 crabs which were collected from different locations in spring and autumn was analyzed by pyrosequencing. The bacterial communities in autumn crab were more diverse in than those in spring. *Psychrobacter, Vagococcus,* and *Carnobacterium* were the most abundant genera in spring, whereas *Roseovarius* was predominant in autumn, but their proportions were influenced by the pathogenic bacterial proportion. These results indicated that the microbiota in swimming crab significantly influenced by seasonal temperature change. The proportion analysis on *Vibrio* species indicated that intake of crab could cause the foodborne illness. This study provides the extended understanding on composition of bacterial community in swimming crab and the factors influencing crab microbiome.

Keywords: *Vibrio vulnificus, Vibrio parahaemolyticus,* Bioinformatics, Genomics, Transcriptomics, Metagenomics, Swimming crab

Student Number: 2010-21225

Contents

List of Figures

List of Tables

Chapter I.

Background

I-1. The genus *Vibrio*

I-1-1. Taxonomy of *Vibrio*

The phylum Proteobacteria is one of the largest phyla within Gram-negative bacteria. This phylum were divided into five subclasses, α, β, γ, δ, and ε, based on the phylogenetic analysis of rRNA superfamilies and protein signatures (Gupta 2000). Among the subclasses of Proteobacteria, the class γ-proteobacteria contains 14 orders including Vibrionales, which have been known to contain a family Vibrionaceae (Brenner, et al. 2005, Dikow, et al. 2013, Dryselius, et al. 2007, Gao, et al. 2009). Since *Vibrio* was firstly reported in 1854, the genus *Vibrio* was classified as the family Spirillaceae based on 7th edition of *Bergey's Mannual of Determinative Bacteriolgy* until 1957 (Farmer III 2006). In 1965, *Vibrio* was reclassified with *Aeromonas* and *Plesiomonas* as a new family Vibrionaceae based on their phenotypic properties such as fermentative activity, polar flagella, and positive oxidase reaction (Farmer III 2006).

I-1-2. General characteristics

The genus *Vibrio* is Gram-negative, motile, non-spore-forming, facultative anaerobic, and halophlic bacteria with various GC content ranged 38 to 51% (Brenner, et al. 2005, Dryselius, et al. 2007, Farmer III 2006). The cell morphology of *Vibrio* commonly appeared as slightly curved or curved-shaped rods with 0.5-0.7 μm in width and 1.5-2 μm in height (Brenner, et al. 2005, Farmer Iii, et al. 2006). These bacteria widely occur in marine and estuarine environment and have multiple lifestyles including a planktonic, free-swimming state or attached state to the organic or inorganic surface (Brenner, et al. 2005). Most of them are oxidase positive and could reduce nitrate to nitrite, and could utilizing glucose and ammonium as sole carbon and nitrogen source, respectively (Brenner, et al. 2005). All members of genus *Vibrio* have unique two chromosomes which is distinguish them from other bacterial family (Dikow, et al. 2013, Dryselius, et al. 2007, Egan, et al. 2003, Okada, et al. 2005)**.** .

I-2. *Vibrio vulnificus*

Vibrio vulnificus is Gram-negative, motile, and curved rod-shaped bacteria with a single polar flagellum. The bacterium is found in coastal or estuarine environment worldwide and frequently contaminates seafood like oysters (Hor, et al. 1995, Horseman, et al. 2011, Linkous, et al. 1999, Wright, et al. 1996). This bacterium could be differentiated from *Vibrio parahaemolyticus* by a lower tolerance for NaCl and fermentation of lactose. The water temperature in which *V. vulnificus* is usually found is from 9 to 31°C. The water temperatures above 18°C and salinities between 15 to 25 parts per thousand (ppt) have been reported as a preferred habitat. Salinities at or greater than 30 ppt will substantially reduce the growth of *V. vulnificus* regardless of the water temperature (Kaspar, et al. 1993).

I-2-1. Disease caused by *V. vulnificus*

V. vulnificus is a causative agent of foodborne diseases, such as life-threatening septicemia and possibly gastroenteritis (Gulig, et al. 2005). Consumption of seafood containing *V. vulnificus* is capable of causing a severe, fulminant systemic infection. The infection results in illness ranging from fever, chills, nausea, gastroenteritis to primary septicemia (Horseman, et al. 2011, Strom, et al. 2000b). In most of the cases involving *V. vulnificus* infection have underlying predisposed conditions, including

liver damage, excess levels of iron, and immunocompromised conditions (Oliver 2005a, Strom, et al. 2000b). The symptoms are typically observed within 36 hours to 10 days. The mortality from the primary septicemia is very high (>50%) and death can occur within one to two days after the first signs of illness (Horseman, et al. 2011, Jones, et al. 2009, Strom, et al. 2000b). The majority of all cases of primary septicemia by *V. vulnificus* has been reported to occur in males over the age of 50. Although the reason for the age risk factor is not known, estrogen, the major female hormone, appears to be a protective material after exposure to endotoxin (Merkel, et al. 2001, Oliver 2005a).

In addition to septicemia, *V. vulnificus* can produce serious wound infections that are resulted from contact of open wounds with water containing the bacterium and/or shellfish contaminated with the bacterium (Oliver 2005b). Symptoms of *V. vulnificus*-induced wound infections include pain, erythema, and edema at the wound site. It can progress rapidly to cellulitis, ecchymoses and bullae which can progress to necrotizing fasciitis at the site of infection. Although the mortality for the wound infection is lower than primary septicemia, ranging from 20 to 30%, even healthy people are susceptible to a serious wound infection (Oliver 2005b, Strom, et al. 2000b).

Since 2013 to date (Nov 2015), total number of reported *V. vulnificus* infection is 151 for the last three years in South Korea, among which 71 were dead (47%) (Korea Centers for Disease Control and Prevention, KCDC; http://is.cdc.go.kr/nstat/index.jsp). In Japan, approximately 400 persons were estimated to suffer from *V. vulnificus*-induced septicemia annually (Osaka, et al. 2004). According to estimates from U. S. Food and Drug Administration the average of 34 cases of *V. vulnificus* infection was reported annually in the United States (Jones, et al. 2009).

I-2-2. Virulence factors of *V. vulnificus*

The pathogenesis of *V. vulnificus* is a multifactorial and complex phenomenon that involves many genes. Here, some of important virulence factors of *V. vulnificus* are described: capsular polysaccharides (CPS), cytolysin (VvhA), MARTX toxin (RtxA1), pili, and flagella.

Capsular polysaccharide (CPS)

V. vulnificus is an extracellular pathogen that uses it CPS to avoid phagocytosis by host immune cells and complement. Encapsulation by CPS masks immunogenic structures that would normally activate nonspecific host response (Linkous, et al. 1999, Strom, et al. 2000b). Therefore, CPS allows the *V. vulnificus* cells to be more

invasive in subcutaneous tissue and to be more slowly cleared from the bloodstream than unencapsulted cells (Yoshida, et al. 1985). The presence of a capsule is involved in colonies morphology; encapsuled strain is opaque and unencapsuled strain is translucent (Wright, et al. 1999, Yoshida, et al. 1985). Indeed, unencapsulated mutants exhibited attenuated mortality in mouse models (Simpson, et al. 1987). Consistently, inactivation of a CPS transport gene (*wza*) of *V. vulnificus* abolished capsule expression and resulted in an dicreased mortality (Wright, et al. 2001).

Metalloprotease (VvpE)

VvpE is a nonspecific extracellular pretease and involves in *V. vulnificus* virulence. Purified VvpE cuase tissue necrosis and cutaneous lesions and increases vascular permeability (Chang, et al. 2005). The enhanced vascular permeability cause by VvpE is occurred through the generation of bradykinin, a known vasodilator, and is known to be important for invasion of the pathogen (Miyoshi, et al. 2006). However, inactivation of the *vvpE* gene did not show andy difference in LD_{50} (Jeong, et al. 2000), indicating VvpE is not a major virulence factor of *V. vulnificus*. More recently, it has been suggested that SmcR enhances the detachment of *V. vulnificus* biofilm by upregulating expression of VvpE that dissoves established biofilms directly, and thereby may promote the dispersal of the pathogen to new colonizationi site (Kim, et al. 2013)

Cytolysin (VvhA) and RtxA1 toxin

VvhA, an extracellular cytolysin encoded by *vvhA*, contributes to the virulence of *V. vulnificus* not only through the hemolytic activity but also through other cytotoxic effects (Wright, et al. 1991). VvhA causes cell death by pore formation in the cellular membrane followed by an increase of vascular permeability and hypotension (Kim, et al. 1993). Severe tissue necrosis, fluid accumulation, intestinal irregularities, partial paralysis, and lethality have also been demonstrated to be caused by VvhA (Gray, et al. 1987, Lee, et al. 2005). Other effects of VvhA include apoptosis of endothelial cells, and induction of inducible nitric oxide synthase (iNOS) activity (Kang, et al. 2002, Kim, et al. 2002, Kwon, et al. 2001). However, inactivation of *vvhA* did not affect the mortality of *V. vulnificus* in mouse model, suggesting that hemolysin is not solely responsible for the lethality and the tissue damage (Wright, et al. 1991).

RtxA1 is a multifunctional-autoprocessing RTX toxin (MARTX) encoded by *rtxA1*. Rtx toxins are made of repeated structural subunits and form pores in host cellular membranes (Gulig, et al. 2005, Satchell, et al. 2009). *V. vulnificus* RtxA1 is highly (80% ~ 90%) homologous with V. cholerae RtxA, and gene organization of the two rtx clusters is also similar (Kim, et al. 2008, Lee, et al. 2007). The strain deficient in this toxin was found to be less cytotoxic than wild type, and showed higher LD50s

upon intragastric or intraperitoneal injection to mice than those of wild type (Kim, et al. 2008). RtxA1 is considered to trigger excessive production of ROS by the host, leading to necrotic cell death and apoptosis (Lee, et al. 2007). RtxA1 also contributes to host cellular changes, including cytoskeleton rearrangement, bleb formation, and actin aggregation, which leads to cellular necrosis and enables V. vulnificus to invade the bloodstream by crossing the intestinal epithelium (Kim, et al. 2008). Recently, RtxA1 and VvhA have been demonstrated to play an additive role in causing intestinal tissue damage and inflammation that then promotes dissemination of the infecting bacteria to the bloodstream and other organs (Jeong, et al. 2012).

Pili and flagella

For most bacterial infections, attachment and colonization of host surfaces are important steps in the early phase of infections. Pili are proteinaceous fibers that stick out from the cell surface of bacteria, which often mediate the initial attachment to host surface. Likewise, *V. vulnificus* adherence has been demonstrated to correlate with increased piliation (Strom, et al. 2000b). Consistently, the absence of genes required for the biogenesis of type IV pili, *pilA* and *pilD* encoding the pilin structural protein and pre-pilin peptidase, respectively, resulted in a loss of attachment to epithelial cells as well as a slight increase in LD_{50} (Paranjpye, et al. 1998, Paranjpye, et al. 2005).

In addition, motility of pathogenic bacteria is essential in the process of infection as it allows adhesion and colonization to host cells (Ottemann, et al. 1997). Flagella-based motility is proposed to be another virulence determinant in *V. vulnificus*. Loss of each of two flagellar structural components, encoded by *flgC* and *flgE*, resulted in a significant decreases in motility, cellular adhesion, and cytotoxicity compared to wild type (Kim, et al. 2003b, Lee, et al. 2004).

I-3. *Vibrio parahaemolyticus*

V. parahaemolyticus is firstly discovered in Japan by an foodborne outbreak which caused by consumption of shirasu in 1950 (Shinoda 2011). This curved rod-shaped Gram-negative bacterium is an opportunistic pathogen that found in marine environment and seafood including oysters, clams, and crabs, etc.(Daniels, et al. 2000, Jun, et al. 2012, McCarter 1999). This bacterium has a single polar flagellum which is responsible for its motility that enables free-swimming state of *V. parahaemolyticus* (McCarter 1999). The temperature and salinity which *V. parahaemolyticus* could grow are ranged from 10 to 42°C and 1 to 7%, respectively, indicating that this bacterium is halophilic (Beuchat 1973, Joseph, et al. 1982, Kaneko, et al. 1973, Palasuntheram 1981).

I-3-1. Disease caused by *V. parahaemolyticus*

V. parahaemolyticus is a pathogen which cause the foodborne illness via consumption of contaminated water or seafood. Infection with *V. parahaemolyticus* can cause gastroenteritis and possibly life-threatening septicemia (Daniels, et al. 2000). The most common disease caused by *V. parahaemolyticus* infection is gastroenteritis accompanying with diarrhea, headache, vomiting, nausea, abdominal cramps and low fever (Su, et al. 2007). The symptoms are occurs within 96 hours

after consumption of contaminated foods, and can last for 3 to 12 days (Cabanillas-Beltrán, et al. 2006, Daniels, et al. 2000). Although the most of the infection with *V. parahaemolyticus* cause self-limited gastroenteritis, some of this infection could cause acute gastroenteritis, severe diarrhea, and furthermore, life-threatening septicemia to people who have underlying medical conditions, including liver disease or immune disorders (Daniels, et al. 2000, Su, et al. 2007).

The gastroenteritis outbreak which caused by *V. parahaemolyticus* have been reported over the world. In South Korea, total number of reported *V. parahaemolyticus* outbreaks is 23 during 2012 to 2014 (Ministry of Food and Drug Safety). In Mexico, approximately 100 patient who consumed raw or undercooked shrimp were infected by *V. parahaemolyticus* during 2003 to 2005 (Cabanillas-Beltrán, et al. 2006). According to U.S. Centers for Disease Control and Prevention (CDC), 40 outbreaks of *V. parahaemolyticus* including more than 1,000 illnesses were reported between 1973 and 1998 (Daniels, et al. 2000).

I-3-2. Virulence factors of *V. parahaemolyticus*

Although virulence factors of *V. parahaemolyticus* which is responsible for its virulence are still controversial, some genes have been considered to be related with its pathogenesis. Here, some of important virulence factors of *V. parahaemolyticus*

are described: Thermostable direct hemolysin (TDH), TDH-related hemolysin (TRH), and Type III secretion systems (T3SSs).

Thermostable direct hemolysin (TDH) and TDH-related hemolysin (TRH)

TDH is a pore-forming toxin of *V. parahaemolyticus* that occur beta-type hemolysis on a special blood agar medium, Wagatsuma agar (Nishibuchi, et al. 1995, Shirai, et al. 1990). Because most of clinical *V. parahaemolyticus* and only 1 to 2% of environmental strains have this hemolytic activity, which has been called the Kanagawa phenomenon (KP), TDH has been considered as an important virulence factors for *V. parahaemolyticus*. TDH was named on the basis of its heat-resistant characteristics, which was not inactivated at 100^{o}C for 10 min. Further biological analysis revealed that this hemolysin also has hemolytic activity on erythrocytes, cytotoxicity, cardiotoxicity, and enterotoxicity (Nishibuchi, et al. 1995, Raghunath 2014).

Although TDH is a major virulence factor of *V. parahaemolyticus*, some clinical isolates were KP-negative, which means absence of TDH. Instead, the KP-negative strains has other heat-labile hemolysin, TRH (Shirai, et al. 1990). The gene encoding TRH (*trh*) have approximately 70% of nucleotide sequence homology with gene encoding TDH (*tdh*), and TRH has immunological similarities with TDH (Honda, et

al. 1988, Nishibuchi, et al. 1995). Like TDH, TRH has hemolytic activities on erythrocytes from various animals such as sheep, chickens, and mice (Honda, et al. 1988).

Type III secretion system (T3SS)

T3SS is needle-like bacterial machinery used to inject bacterial toxins into the host, thus it has been recognized as a major virulence factors in various bacteria (Hueck 1998). *V. parahaemolyticus* have two non-redundant T3SSs on their chromosomes. T3SS1, which is present in all *V. parahaemolyticus* regardless of the presence of *tdh* or *trh*, is responsible for cytotoxic activity and induction of the rapid autophagy during infection by causing disruption of intracellular communications (Park, et al. 2004a, Zhang, et al. 2013). Unlike T3SS1, T3SS2 found in most of clinical isolates and some environmental strains (Raghunath 2014). The deletion mutation on T3SS2 resulted in loss of enterotoxicity, suggesting that T3SS2 is involved in enterotoxic activity of *V. parahaemolyticus* (Park, et al. 2004a). Further investigation revealed that the T3SS2 effectors manipulate the actin cytoskeleton of host cells that allows *V. parahaemolyticus* to invade and survive in non-phagocytic host cells (Zhang, et al. 2013).

I-4. The objective of this study

Bioinformatics including next-generation sequencing such as whole genome sequencing (WGS), RNA-seq and metagenomics is used as a powerful tool providing that further understanding on genetic properties and interpretation on characteristics of objects at genomic level. In the case of pathogens, bioinformatics could be used to identify whole putative virulence factors, explain its pathogenicity, and suppose the mechanisms of human infection. Also, the RNA-seq could identify the real genes that differentially expressed in specific circumstance, providing the clues about the target genes for effective regulation of pathogens. However, while the pathogenesis and its regulation of foodborne pathogens have been reported and well characterized in molecular level, the functions of its genome are not fully understood yet. For example, the pathogenesis of *V. vulnificus*, an opportunistic foodborne pathogen causing lethal primary septicemia, have been well-characterized, but only four complete genome sequences have been analyzed and reported. Therefore, to understand the genomic properties and characteristic of foodborne pathogens, I selected newly isolated noticeable foodborne pathogens, *V. vulnificus* FORC_016 and *V. parahaemolyticus* FORC_008, for WGS. The whole genomes of FORC_016 and FORC_008 were completely analyzed, and their virulence factors were analyzed. In addition, the genes of *V. vulnificus* FORC_016 that differentially

expressed under exposure to crab were identified. Also, the seasonal and locational microbial composition dynamics on crab were determined. These data would be useful for our understanding of virulence factors and their functions, and provide the basis of understanding about the interactions between *V. vulnificus* and contaminated crab.

Chapter II.

Genomic Analysis of Newly Isolated *Vibrio vulnificus* and *Vibrio parahaemolyticus* Related with Foodborne Outbreaks

A part of this chapter was published online in Pathog. Dis. May 2016

II-1. Introduction

Vibrio vulnificus and *Vibrio parahaemolyticus* are gram-negative pathogenic bacteria, causing a severe primary septicemia and seafoodborne gastroenteritis (Jones, et al. 2009, Joseph, et al. 1982). These microorganisms are generally detected in various seafood including oyster, flounder, clam, and crab. Therefore, consumption of raw or undercooked seafood contaminated with these *Vibrio* species possibly causes foodborne illnesses (Horseman, et al. 2011, Su, et al. 2007). These bacteria are found in coastal or estuarine environment worldwide and frequently contaminates seafood like oysters, clams, crabs, and flounder (Hor, et al. 1995, Horseman, et al. 2011, Linkous, et al. 1999, Wright, et al. 1996). The U. S. Food and Drug Administration reported that average of 34 cases of *V. vulnificus* infection were occurred annually in U. S (Jones, et al. 2009). Since the first foodborne outbreak by *V. parahaemolyticus* in 1950, numerous outbreaks have been reported over the worlds (Cabanillas-Beltrán, et al. 2006, Daniels, et al. 2000, Food, et al. 2005, Shinoda 2011, Wu, et al. 2014). In addition, approximately 150 cases of *V. vulnificus* and *V. parahaemolyticus* infection were reported during last three years in South Korea (KCDC; http://is.cdc.go.kr/nstat/index.jsp). These data suggest that both of *V. vulnificus* and *V. parahaemolyticus* is major foodborne pathogen.

While *V. vulnificus* and *V. parahaemolyticus* are one of the major pathogens causing seafood outbreaks, functions of its genome are not fully understood yet. To date, only four and five complete genome sequences for *V. vulnificus* and *V. parahaemolyticus* have been analyzed and reported (Chen, et al. 2003, Jensen, et al. 2013, Kalburge, et al. 2014, Kim, et al. 2003a, Lüdeke, et al. 2015, Lo, et al. 2014, Makino, et al. 2003, Park, et al. 2011). However, genome information of these *Vibrio* species was not completely interpret to understand its pathogenicity and virulence factors for human infections. Therefore, complete genome sequence analysis and functional interpretation needs to be conducted for further understanding of mechanisms of human infections and pathogenesis in genomic level.

To extend our knowledge about pathogenicity of *V. vulnificus* and *V. parahaemolyticus* in South Korea, the *V. vulnificus* FORC_016 and *V. parahaemolyticus* FORC_008 were newly isolated from blood of food-poisoning patient and a flounder fish, and their genomes were completely sequenced and analyzed. These genome information would be useful for our understanding of virulence factors and their functions for human infections. Furthermore, this report would provide extended genomic information for the epidemiological investigation and prevention of outbreak in South Korea.

II-2. Materials and Methods

II-2-1. Strains, culture conditions and genomic DNA isolation

V. vulnificus FORC_016 and *V. parahaemolyticus* FORC_008 was grown aerobically in modified Luria-Bertani medium (LB) supplemented with 2% (w/v) NaCl for 12 h at 30°C with shaking. Genomic DNA was isolated and purified using DNeasy Blood & Tissue Kit (QIAGEN, Valencia, CA) according to the manufacturer's protocol. The concentration of the purified genomic DNA was determined using a NanoVue spectrophotometer (GE Healthcare, Little Chalfont, UK).

II-2-2. Cytotoxicity test

Cytotoxicity was evaluated by measuring cytoplasmic lactate dehydrogenase (LDH) activity that is released from the human epithelial INT-407 cells by damage of plasma membrane. The INT-407 cells were grown in minimum essential medium containing 1% (v/v) fetal bovine serum (MEMF) (Gibco-BRL, Gaithersburg, MD) in 96-well culture dishes (Nunc, Roskilde, Denmark) as described previously (Kim, et al. 2014). Each well with 2×10^4 INT-407 cells was infected with the *V. vulnificus* strain FORC_016, MO6-24/O, and *V. parahaemolyticus* strain FORC_008 and KCTC 2471 at a various multiplicity of infection (MOI) for 2 h. The LDH activity released into the supernatant was determined using a cytotoxicity detection kit (Roche,

Mannheim, Germany).

Table II-1. Bacterial strains used in this study

Strain or plasmid	Relevant characteristics[a]	Reference or source
Bacterial strains		
V. vulnificus		
MO6-24/O	Clinical isolate; virulent	Laboratory collection
FORC_016	Clinical isolate; virulent	National Culture Collection for Pathogens
V. parahaemolyticus		
KCTC 2471	Clinical isolate; virulent	Korean Collection for Type Culture
FORC_008	Clinical isolate; virulent	Ministry of Food and Drug Safety

II-2-3. Genome sequencing and assembly

The whole genome sequencing and assembly were performed at the ChunLab Inc. (Seoul, South Korea) using combination of an Illumina MiSeq platform (Illumina, San Diego, CA) and a PacBio RS II platform (Pacific Biosciences, Menlo Park, CA) or combination of Illumina MiSeq platform (Illumina), a 454 Genome Sequencer Titanium FLX platform (Roche/454 Life Sciences, Branford, CT), and a PacBio RS II platform (Pacific Biosciences), respectively. To generate the 300 bp paired-end library for MiSeq platform, purified genomic DNA was fragmented and tagged with adapters using Nextera DNA sample prep kit (Illumina). The adaptor-tagged DNA fragments were amplified via a limited-cycle PCR using Nextera Index kit (Illumina), resulted in DNA library which has index on both ends of DNA fragments (dual-indexed). The draft DNA library was purified by using AMPure XP beads (Beckman Coulter, Brea, CA) for purification and size-selection of library DNA. The DNA library was sequenced using Illumina MiSeq sequencer. The sequencing reads from MiSeq platform were assembled using CLC Genomics Workbench ver. 7.0.4 (CLC bio, Aarhus, Denmark). For construction of 8 kb paired-end library which used in 454 platform, sample DNA was fragmented and ligated with circularization adaptors, which contain loxP sequence to make the fragmented DNA circular by intramolecular recombination of the loxP sites. The adaptor-ligated DNA fragments were separated and selected by size ranging from 6.5 kb to 9.5 kb using agarose gel

electrophoresis, and followed by intramolecular recombination which results in DNA circularization. The circularized DNA were fragmented by nebulization using GS FLX Titanium Nebulizer Kit (Roche), producing the 500 bp paired end DNA fragments that contain the circularization adaptor on center and genomic DNA on both ends. The paired end DNA fragments were immobilized on magnetic beads, ligated with library adaptors, amplified by PCR, and size-selected using AMPure XP beads (Beckman Coulter). Afterwards, the single-stranded paired end DNA library was isolated, and sequenced using 454 GS FLX Titanium platforms. The sequencing reads from 454 platform were assembled using Roche gsAssembler ver. 2.6 (Roche). The PacBio SMRTbellTM library for PacBio platform was prepared by using SMRTbell Template Prep Kit (Pacific Biosciences) and AMPure PB beads (Pacific Biosciences). The genomic DNA was fragmented, ligated with hairpin adaptors, and purified to produce double-stranded DNA templates capped with hairpin adaptors on both ends. The binding of DNA polymerase to the template DNA was conducted using DNA/Polymerase Binding Kit P6 v2 (Pacific Biosciences) and MagBead Kit (Pacific Biosciences). Sequencing was performed with a PacBio RS II platform. The sequencing reads from PacBio platform were assembled using PacBio SMRT Analysis ver. 2.0 software (Pacific Biosciences). All kits and sequencing platforms were used according to manufacturer's procedure.

II-2-4. Genome annotation and genome map construction

The open reading frames (ORFs) and tRNA/rRNA of the assembled genome were predicted using the Rapid Annotation using Subsystem Technology (RAST) server, and the predicted ORFs were manually curated with the ORF prediction result of GeneMarkS program (Aziz, et al. 2008, Besemer, et al. 2001). The manually curated ORFs were confirmed again using prediction of ribosome binding sites (RBS) by RBSfinder (J. Craig Venter Institute, Rockville, MD). All predicted ORFs was automatically annotated using the Global Annotation of Multiplexed On-site Blasted DNA-Sequences (GAMOLA). In addition, InterProScan5 with conserved protein domain databases and COG-based WebMGA program were used to further functional analysis of all annotated ORFs (Altermann, et al. 2003, Wu, et al. 2011, Zdobnov, et al. 2001). The circular genome maps including all predicted ORFs with COG functional assignments, RNA operons, GC-content, and gene cluster information were generated using GenVision program (DNASTAR, Madison, WI). The putative virulence genes of *V. vulnificus* FORC_016 and V. *parahaemolyticus* FORC_008 were identified using BLAST algorithm analysis with Virulence Factor Database (Chen, et al. 2011).

II-2-5. Comparative genome analysis

The complete sequences of 16S rRNA of *V. vulfnicus*, *V. parahaemolyticus* FORC_008 and other 12 *Vibrio* species were aligned by ClustalW (Thompson, et al. 2002). Phylogenetic trees were constructed from the aligned sequences using the Neighbor-joining method with 1,000 bootstrap replicates via MEGA6 software (Felsenstein 1985, Saitou, et al. 1987, Tamura, et al. 2013). For Average nucleotide identity (ANI) analysis, the whole genome sequences of *V. vulfnicus* and *V. parahaemolyticus* were fragmented into 1020 bp and compared to those of other *V. vulnificus* and *V. parahaemolyticus* species using JSpecies (http://imedea.uib-csic.es/jspecies/) based on BLAST algorism resulting in calculation of ANI values between *Vibrio* species. The tree was constructed using R program. The whole-genome alignment of *Vibrio* species for detection of unique gene were conducted using Artemis Comparison Tool (ACT) program (http://www.sanger.ac.uk/science/tools/artemis-comparison-tool-act).

II-3. Results and Discussion

II-3-1. Information of candidates for whole genome sequencing (WGS)

The *V. vulnificus* FORC_016 was isolated from blood of food-poisoning patient by Chonbuk national university hospital, Jeonju, South Korea. The *V. parhaemolyticus* FORC_008 was isolated from a patient who died after ingestion of flounder fish by Gyeongnam Health and Environmental Institute, Changwon, South Korea. The toxicity of these strains was confirmed using lactate dehydrogenase (LDH) assay (Fig. II-1), suggesting that they are potential foodborne pathogens possibly causing foodborne outbreak in South Korea.

II-3-2. Genome sequencing and assembly results

The whole genome of *V. vulnificus* FORC_016 and *V. parahaemolyticus* FORC_008 was sequenced using combination of an Illumina MiSeq platform (Illumina) and a PacBio RS II platform (Pacific Biosciences, Menlo Park, CA) and combination of Illumina MiSeq platform (Illumina), a 454 Genome Sequencer FLX Titanium platform (Roche, Branford, CT), and a PacBio RS II platform (Pacific Biosciences), respectively. The hybrid sequencing of MiSeq, 454, and PacBio platforms provided final 2 contigs for each *vibrio* species with total coverage of 345.04 and 451.98, respectively.

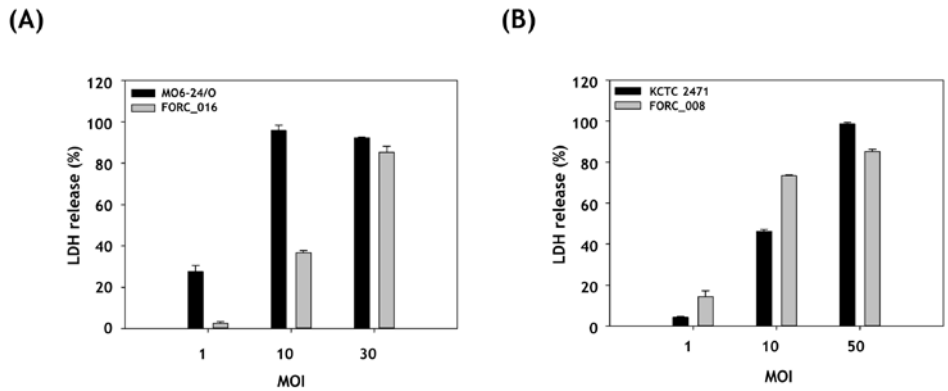

Figure II-1. Cytotoxicity of *V. vulnificus* FORC_016 and *V. parahaemolylticus* FORC_008. INT-407 cells were infected with *Vibrio* cells at various MOIs for 2h. The cytotoxicity was determined by an LDH release assay. 100% LDH release is determined when 1% Triton X-100 was treated for complete lysis of the cells instead of the specific bacterium. Error bars represent the standard errors of the means (SEM) (A) Cytotoxicity of *V. vulnificus* FORC_016 and *V. vulnificus* MO6-24/O (positive control), (B) Cytotoxicity of *V. parahamolyticus* FORC_008 and KCTC 2471 (positive control).

II-3-3. General genome properties of *V. vulnificus* FORC_016 and *V. parahaemolyticus* FORC_008.

The whole genome sequencing revealed that both of *V. vulfnicus* FORC_016 and *V. parahaemolyticus* FORC_008 has two circular chromosomes and no plasmid. For *V. vulnificus* FORC_016, the chromosome I consists of 3,234,424 bp with a GC contents of 46.60% containing 2,889 ORFs, 106 tRNA genes, and 31 rRNA genes. Among the predicted 2,889 ORFs, 2,298 ORFs (79.54%) were annotated to encode functional proteins and 591 ORFs were hypothetical proteins. Chromosome II consists of 1,837,945 bp with a GC content of 47.00% containing 1,572 ORFs, 13 tRNA genes, and 3 rRNA genes. Among the predicted 1,572 ORFs, 1,223 ORFs (77.80%) were annotated to encode functional proteins and 349 ORFs were hypothetical proteins. In addition, 2,711 ORFs on chromosome I and 1,453 ORFs on chromosome II were assigned to the specific COG functional categories. For *V. parahaemolyticus* FORC_008, the chromosome I consists of 3,266,132 bp with a GC content of 45.36% containing 2,909 ORFs, 115 tRNA genes, and 28 rRNA genes. Among the predicted 2,909 ORFs, 2,513 ORFs (86.39%) were annotated to encode functional proteins and 539 ORFs were hypothetical proteins. Chromosome II consists of 1,772,036 bp with a GC content of 45.53% containing 1,602 ORFs, 14 tRNA genes, and 3 rRNA genes. Among the predicted 1,585 ORFs, 1,245 ORFs (78.55%) were annotated to encode functional proteins and 340 ORFs

were hypothetical proteins. In addition, 2,744 ORFs on chromosome I and 1,458 ORFs on chromosome II were assigned to the specific COG functional categories. The general genome properties of *V. vulnificus* FORC_016 and *V. parahaemolyticus* FORC_008 were summarized in Table II-2, and the circular genome maps for FORC_016 and FORC_008 were generated based on the genome information (Fig. II-2 and 3).

Interestingly, both of *V. vulfnicus* FORC_016 and *V. parahaemolyticus* FORC_008 has an unusual large DNA fragment with low GC content (41.41% for FORC_016, FORC16_1435-1643; 38.67% for FORC_008, FORC8_1105 - 1246) on chromosome I, suggesting that it may be non-*Vibrio* DNA or may have been derived from different origin. Previously, this unusual DNA fragment was identified as super integron (SI), probably associated with various additional functions including antibiotic resistance, chaperone-like activity, glutathione transfer, plasmid partitioning, and DNA restriction activity (Fluit, et al. 2004, Stokes, et al. 1989). However, because most of ORFs (62.57% for FORC_016 and 77.46% for FORC_008) in SI are hypothetical proteins, the role of SI in the genome of the strain FORC_008 are unknown or need to be experimentally elucidated in near future.

Table II-2. General genome properties of *V. vulnificus* FORC_016 and *V. parahaemolyticus* FORC_008

Attribute	*V. vulnificus* FORC_016		*V. parahaemolyticus* FORC_008	
	Ch I	**Ch II**	**Ch I**	**Ch II**
Genome size (bp)	3,234,424	1,837,945	3,266,132	1,772,036
DNA G+C (%)	46.60	47.00	45.36	45.53
Total genes	3,026	1,588	3,052	1,602
Protein coding genes	2,889	1,572	2,909	1,585
tRNA genes	106	13	115	14
rRNA genes	31	3	28	3
Genes with function prediction	2,298	1,236	2,513	1,245
Genbank accession number	CP011775	CP011776	CP009982	CP009983

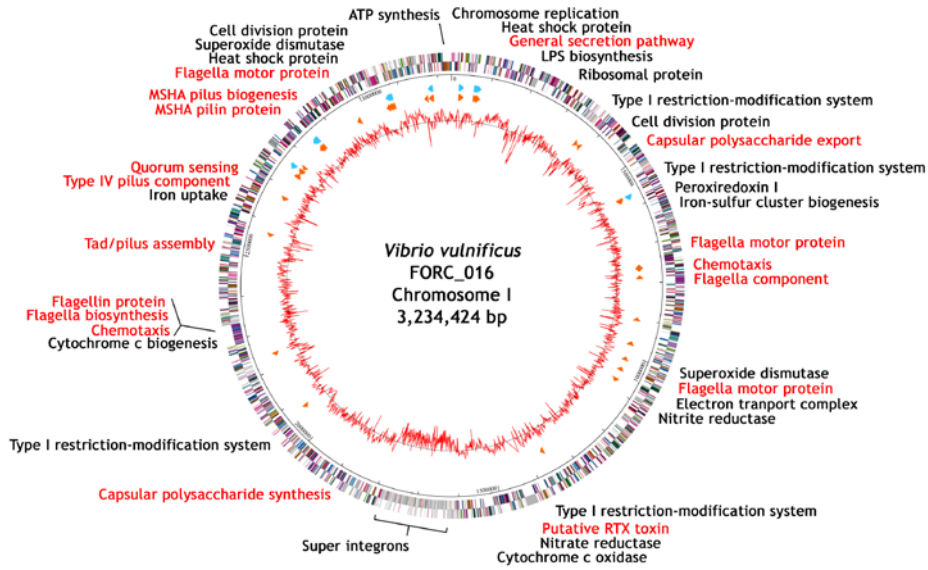

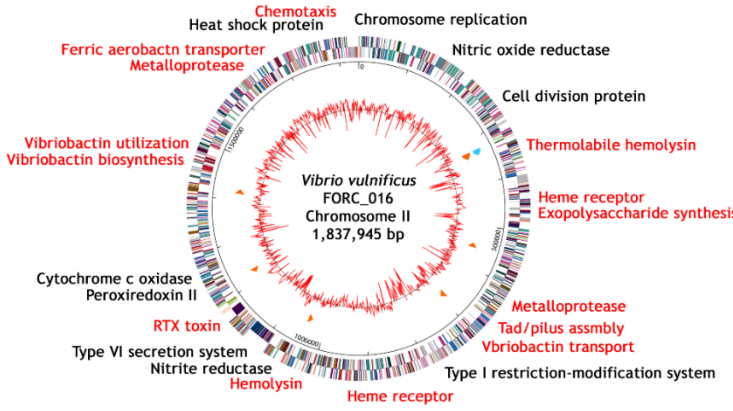

A RNA processing and modification
B Chromatin structure and dynimics
C Energy production and conversion
D Cell cycle control, cell division, chromosome partitioning
E Amino acid transport and metabolism
F Nucleotide transport and metabolism
G Carbohydrate transport and metabolism
H Coenzyme transport and metabolism
I Lipid transport and metabolism
J Translation, ribosomal structure and biogenesis
K Transcription
L Replication, recombination and repair
M Cell wall/membrane/envelope biogenesis
N Cell motility
O Posttranslational modification, protein turnover, chaperones
P Inorganic ion transport and metabolism
Q Secondary metabolites biosynthesis, transport and catabolism
R General function prediction only
S Function unknown
T Signal transduction mechanisms
U Intracellular trafficking, secretion, and vesicular transport
V Defense mechanisms
W Extracellular structures
No COG assignment

Figure II-2. Genome map of *V. vulnificus* FORC_016. The outer circle indicates the locations of all annotated ORFs, and the inner circle with the red peaks indicates GC content. Between these circles, sky blue arrows indicate the rRNA operons and orange arrows indicate the tRNAs. All annotated ORFs were colored differently according to the COG assignments. Genes with specialized functions labeled with different colors as follows; virulence-related genes in red and other functional genes in black.

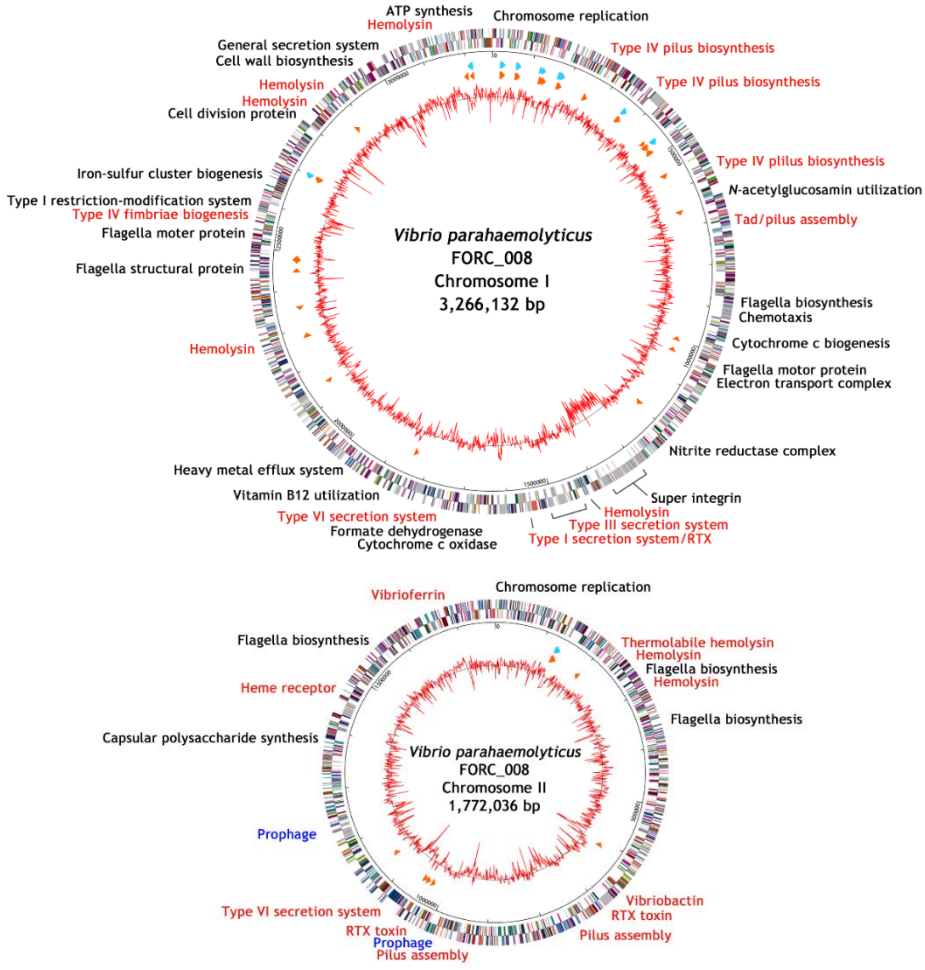
ATP synthesis
Hemolysin
Chromosome replication
General secretion system
Cell wall biosynthesis
Type IV pilus biosynthesis
Hemolysin
Type IV pilus biosynthesis
Hemolysin
Cell division protein
Type IV plilus biosynthesis
Iron-sulfur cluster biogenesis
N-acetylglucosamin utilization
Type I restriction-modification system
Type IV fimbriae biogenesis
Tad/pilus assembly
Flagella moter protein
Vibrio parahaemolyticus
FORC_008
Chromosome I
3,266,132 bp
Flagella structural protein
Flagella biosynthesis
Chemotaxis
Hemolysin
Cytochrome c biogenesis
Flagella motor protein
Electron transport complex
Nitrite reductase complex
Heavy metal efflux system
Vitamin B12 utilization
Super integrin
Type VI secretion system
Hemolysin
Type III secretion system
Formate dehydrogenase
Cytochrome c oxidase
Type I secretion system/RTX
Vibrioferrin
Chromosome replication
Flagella biosynthesis
Thermolabile hemolysin
Hemolysin
Flagella biosynthesis
Heme receptor
Hemolysin
Flagella biosynthesis
Capsular polysaccharide synthesis
Vibrio parahaemolyticus
FORC_008
Chromosome II
1,772,036 bp
Prophage
Vibriobactin
Type VI secretion system
RTX toxin
RTX toxin
Pilus assembly
Prophage
Pilus assembly
A RNA processing and modification
B Chromatin structure and dynimics
C Energy production and conversion
D Cell cycle control, cell division, chromosome partitioning
E Amino acid transport and metabolism
F Nucleotide transport and metabolism
G Carbohydrate transport and metabolism
H Coenzyme transport and metabolism
I Lipid transport and metabolism
J Translation, ribosomal structure and biogenesis
K Transcription
L Replication, recombination and repair
M Cell wall/membrane/envelope biogenesis
N Cell motility
O Posttranslational modification, protein turnover, chaperones
P Inorganic ion transport and metabolism
Q Secondary metabolites biosynthesis, transport and catabolism
R General function prediction only
S Function unknown
T Signal transduction mechanisms
U Intracellular trafficking, secretion, and vesicular transport
V Defense mechanisms
W Extracellular structures
No COG assignment

Figure II-3. Genome map of *V. parahaemolylticus* FORC_008. The outer circle indicates the locations of all annotated ORFs, and the inner circle with the red peaks indicates GC content. Between these circles, sky blue arrows indicate the rRNA operons and orange arrows indicate the tRNAs. All annotated ORFs were colored differently according to the COG assignments. Genes with specialized functions labeled with different colors as follows; virulence-related genes in red, prophage-related genes in blue, and other functional genes in black.

II-3-4. Comparative genome analysis

For comparative phylogenetic tree analysis, the complete 16S rRNA sequence of *V. vulnificus* FORC_016 and *V. parahaemolyticus* FORC_008 were compared to those of other *Vibrio* species, revealing that *V. vulnificus* FORC_016 and *V. parahaemolyticus* FORC_008 were closely related to other *V. vulnificus* and *V. parahaemolyticus* strains respectively (Fig. II-4). To further characterize the evolutionary relationship among them, average nucleotide identity (ANI) analysis was conducted. The ANI analysis showing that the strain FORC_016 has the highest ANI value of 98.07 with MO6-24/O, a clinical isolate from the patient with septicemia (Fig. II-5A) (Park et al. 2011). Also, the strain FORC_008 has the highest ANI value of 98.47 with CDC_K4557, a clinical isolate from the stool of a patient in Louisiana in 2007 (Fig. II-5B) (Lüdeke et al. 2015). These data suggest that FORC_016 and FORC_008 strain may be a potential pathogen causing foodborne outbreak, even though FORC_008 strain was originally isolated from the contaminated food.

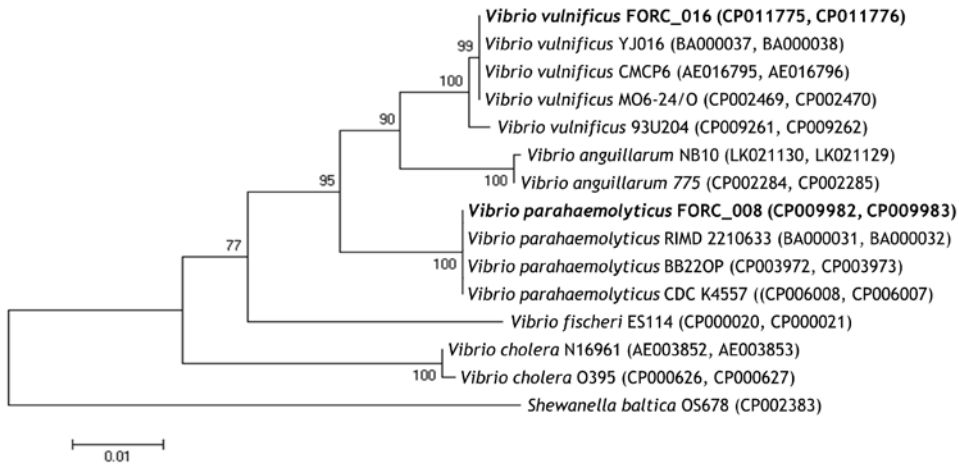

Figure II-4. 16S-based phylogenetic tree of *Vibrio* species. The 16S rRNA-based phylogenetic tree of *V. vulnificus* FORC_016, *V. parahaemolyticus* FORC_008 and other 12 *Vibrio* species were constructed using the Neighbor-joining method with 1,000 bootstrap replicates via MEGA6 software. *Shewanella baltica* OS678 was used as outgroup.

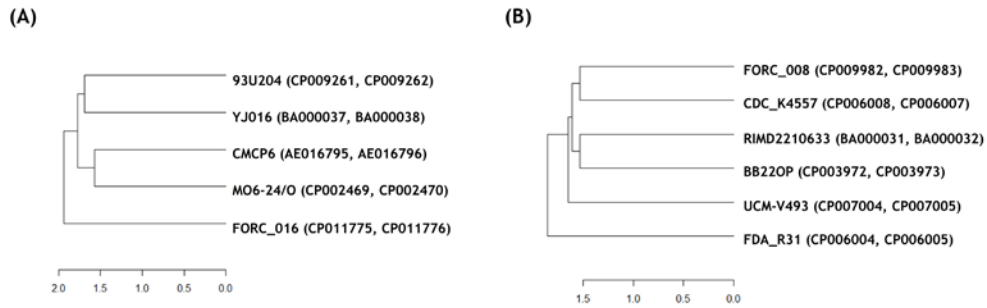

Figure II-5. ANI analysis of *Vibrio* species. The evolutionary relatedness between (A) *V. vulnificus* and (B) *V. parahaemolyticus* species were measured using the average nucleotide identity values. The average nucleotide identity values were calculated using JSpecies (Richter and Rosselló-Móra 2009) by comparing whole genome sequences of *V. parahaemolyticus*, which were fragmented into 1020 bp, based on BLAST algorism. The trees were constructed using R program.

II-3-5. Pathogenesis and virulence factors of *V. vulnificus* FORC_016.

V. vulnificus is an opportunistic foodborne pathogen that can cause primary septicemia with high mortality rate. As described in I-1, previous reports demonstrated that *V. vulniificus* has some of important virulence factors, such as CPS, cytolysin, RTX toxin, and metalloproteases (Chang, et al. 2005, Satchell, et al. 2009, Strom, et al. 2000a, Wright, et al. 1991). The genome analysis revealed that the strain FORC_016 has these virulence genes, suggesting that it is a virulent pathogen can cause foodborne outbreak.

To identify the unique virulence genes of *V. vulnificus* FORC_016, the whole genome sequences of *V. vulnificus* FORC_016 were aligned with those of *V. vulnificus* MO6-24/O using ACT program (Fig. II-6A-C). The whole genome alignment revealed that some genomic regions on chromosome of FORC_016 have low similarity with those of *V. vulnificus* MO6-24/O, suggesting that there might be some unique genes only FORC_016 have. From the further analysis of the unique genomic region of FORC_016, several genes were selected as putative unique virulence genes of FORC_016 (Fig. II-7).

V. vulnificus CPS provides resistance to opsonization by complement and subsequent phagocytosis by macrophages (Linkous, et al. 1999). The CPS operons in *V.*

vulnificus consist of two part; highly conserved *wza-wzb-wzc* transporter and polymorphic genes for CPS biosynthesis (Chatzidaki-Livanis, et al. 2006). The genomic analysis identified that the genome of *V. vulnificus* FORC_016 also contains the genes associated with CPS synthesis (FORC16_0182-0198), consisting the genes related with CPS transporter (FORC16_0182-0185) and genes encoding CPS synthesis genes (FORC_0186-0197). However, the comparative genome analysis and BLAST analysis revealed that the several genes belonging to CPS synthesis (FORC16_0186-196) have no homology with other *V. vulnificus* (Fig. II-6A and II-7 A), suggesting that the CPS production of FORC_016 is differ from those of the other *V. vulnificus.*

Pathogenesis and survival of *V. vulnificus* in host are highly associated with iron concentrations in infected individuals (Wright, et al. 1981). Since most iron in human exist as a transferrin-bound form, *V. vulnificus* has developed multiple system for iron acquisition. Previous studies have been reported that *V. vulnificus* have two types of siderophore, a catechol and a hydroxamate for iron acquisition, and several genes involved in catechol siderophore-associated genes are required for virulence (Simpson, et al. 1983, Webster, et al. 2000). From the genome analysis on FORC_016, it was revealed that the strain FORC_016 have the genes related with siderophore (FORC16_4130-4137, FORC16_4124-4125), suggesting that *V.*

vulnificus FORC_016 also has the ability to acquire iron from the host cells. In addition to genes associated with siderophore metabolism, several unique genes related with iron acquisition were present in *V. vulnificus* FORC_016. HupA is a heme receptor which is responsible for transport of non-transferrin-bound iron (Litwin, et al. 1998). The gene encoding HupA is present in strain FORC_016, but it has low similarity with in amino acid sequences with those of MO6-24/O (36%), YJ016 (36%), and CMCP6 (32%) (Fig II-7 B). Furthermore, FORC_016 have additional siderophore transport system which is not exist in MO6-24/O, YJ016, and CMCP6 (Fig II-7 C), suggesting that the iron acquisition system of FORC_016 would be different with other *V. vulnificus.*

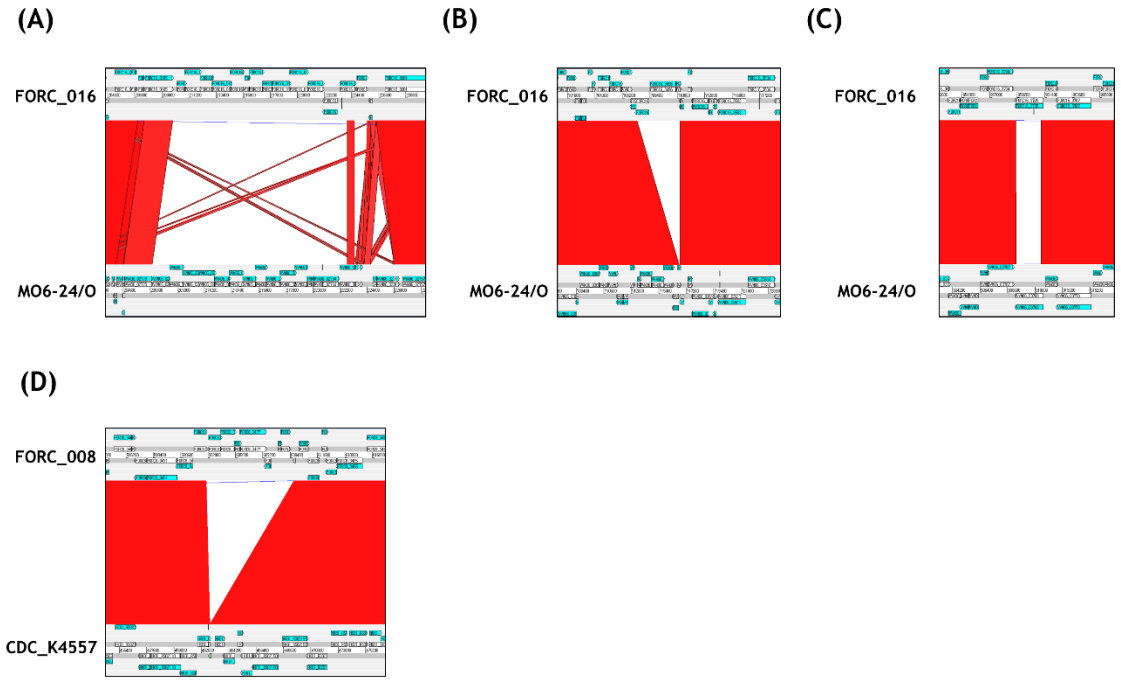

Figure II-6. Comparative analysis of *Vibrio* species. The whole genome sequences of *V. vulnificus* FORC_016 (A, B, and C) and *V. parahaemolyticus* FORC_008 (D) were aligned and compared to *V. vulnificus* MO6-24/O and *V. parahaemolyticus* CDC_K4557 by ACT, respectively. Conserved or highly related regions were indicated by red color, and unique regions with low homology were indicated by colorless.

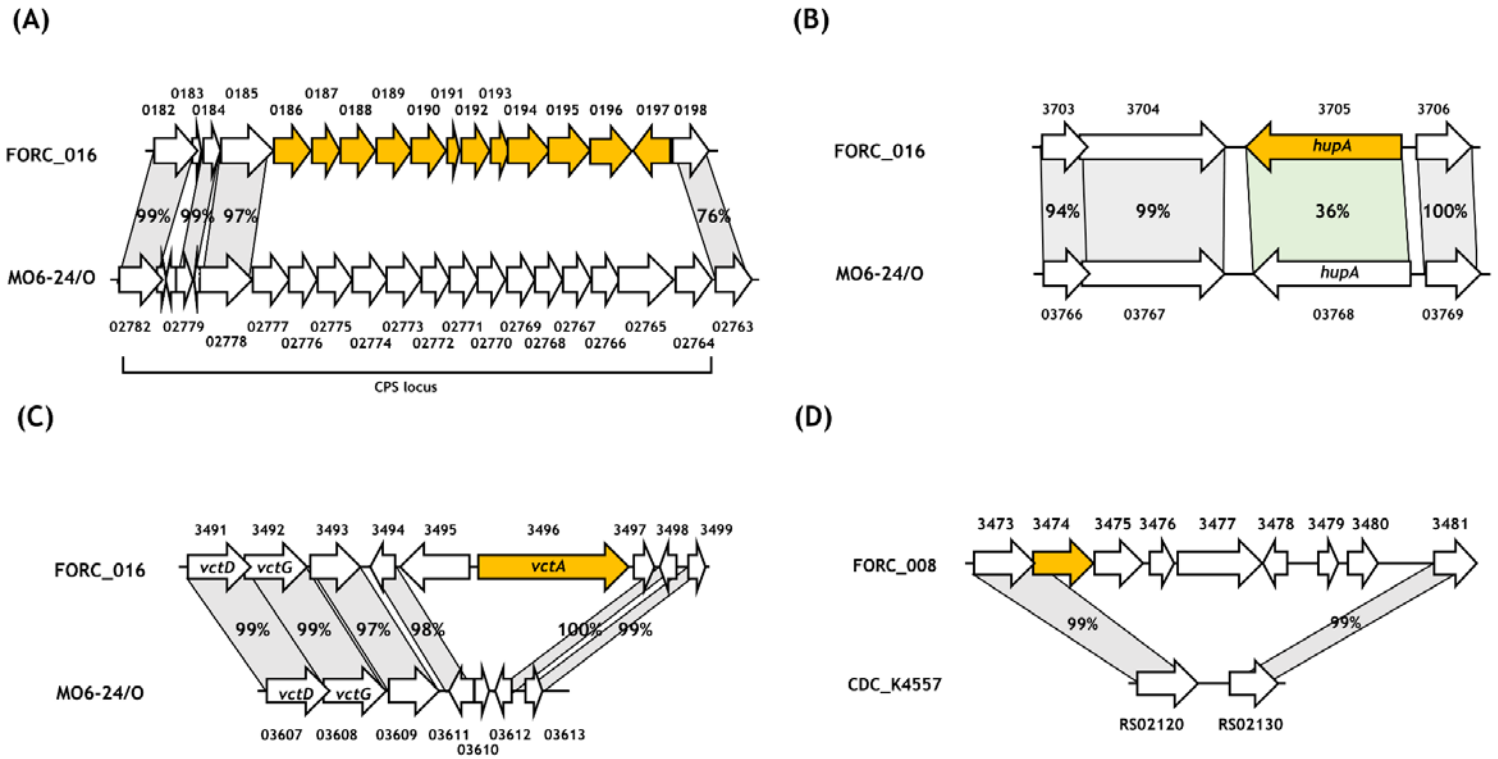
(A)
FORC_016
MO6-24/O
0182 0183 0184 0185 0186 0187 0188 0189 0190 0191 0192 0193 0194 0195 0196 0197 0198
99% 99% 97% 76%
02782 02779 02778 02777 02776 02775 02774 02773 02772 02771 02770 02769 02768 02767 02766 02765 02764 02763
CPS locus
(B)
FORC_016
MO6-24/O
3703 3704 3705 3706
hupA
94% 99% 36% 100%
hupA
03766 03767 03768 03769
(C)
FORC_016
MO6-24/O
3491 3492 3493 3494 3495 3496 3497 3498 3499
vctD vctG vctA
99% 99% 97% 98% 100% 99%
vctD vctG
03607 03608 03609 03611 03610 03612 03613
(D)
FORC_008
CDC_K4557
3473 3474 3475 3476 3477 3478 3479 3480 3481
99% 99%
RS02120 RS02130

Figure II-7. Unique genomic regions of *V. vulnificus* FORC_016 and *V. parahaemolyticus* FORC_008. The unique genomic region of *V. vulnificus* FORC_016 and *V. parahaemolyticus* FORC_008 were compared with similar region of *V. vulnificus* MO6-24/O and *V. parahaemolyticus* CDC_K4557, respectively. The arrows represent the coding regions of (A) CPS gene cluster, (B) heme receptor, and (C) enterobactin receptor in *V. vulnificus* FORC_016 and (D) β-lactamase in *V. parahaemolyticus* FORC_008. The middle line indicates amino acid sequence homology of each gene pair. The unique genes in *V. vulnificus* FORC_016 and *V. parahaemolyticus* FORC_008 were highlighted with orange color. The figure was derived using the nucleotide sequences of the *V. vulnificus* FORC_016 (GenBank™ CP011775, CP011776), *V. vulnificus* MO6-24/O (GenBank™ CP002469 and CP002470), *V. parahaemolyticus* FORC_008 (GenBank™ CP009982 and CP009983), and *V. parahaemolyticus* CDC_K4557 (GenBank™ CP006008 and CP006007) genome.

II-3-6. Pathogenesis and virulence factors of *V. parahaemolyticus* FORC_008.

V. parahaemolyticus is a foodborne pathogen causing acute gastroenteritis accompanied with diarrhea, abdominal cramps, nausea and vomiting (Su, et al. 2007). While the molecular pathogenesis of *V. parahaemolyticus* is not clearly demonstrated yet, two hemolysins, thermostable direct hemolysin (TDH) encoded by *tdh* and TDH-related hemolysin (TRH) encoded by *trh*, have been considered to play major roles in its virulence (Nishibuchi, et al. 1995, Shirai, et al. 1990). Interestingly, the genome analysis of *V. parhaemolyticus* FORC_008 revealed that FORC_008 do not contain both of *tdh* and *trh* genes. However, additional cytotoxicity test of the strain FORC_008 using LDH assay revealed that this strain may be pathogenic, suggesting that other unknown virulence factors may function for its pathogenesis (Fig. II-1). The mutants with *Δtdh/Δtrh* or some of clinical isolates without *tdh/trh* showed previously pathogenic activities, supporting this (Lynch, et al. 2005, Park, et al. 2004b, Pazhani, et al. 2014, Xu, et al. 1994). However, the strain FORC_008 has several other hemolysins (FORC8_2019, 2490, 2535, and 2869 in chromosome I; FORC8_3124, 3153, and 3182 in chromosome II), suggesting that they may be responsible for its virulence.

Chromosomes of the strain FORC_008 has various secretion systems including Type I, II, III, IV, and VI (T1SS, T2SS, T3SS, T4SS, and T6SS). The strain FORC_008

contains Type I secretion systems (T1SSs) with RTX toxin in both chromosome I and II (FORC8_1387-1392 in chromosome I; FORC8_3543, 3834, 3836, and 4213 in chromosome II), probably contributing to the pathogenesis of FORC_008. In addition, T3SS (FORC8_1322-1366 in chromosome I) has been known to be strongly correlated with highly adapted virulence mechanism to promote autophagy, membrane blebbing and cell lysis of host cell (Hueck 1998, Park, et al. 2004a, Zhang, et al. 2013). In addition to T1SS and T3SS, this strain has an additional secretion system, T2SS/Tad locus (FORC8_590-599 in chromosome I; FORC8_3593-3603 in chromosome II), probably associated with adherence to host cells by bacterial pili. While function of T6SSs (FORC8_1575-1605 in chromosome I and FORC8_3864-3881 in chromosome II) has not been clearly understood yet, it was reported to be probably involved in the adhesion to the host cells (Yu, et al. 2012). Therefore, these secretion systems may contribute to the pathogenesis of *V. parahaemolyticus* FORC_008.

As described above, iron acquisition from the host cells is an important strategy of pathogenic bacteria for survival. Because the loss of iron from heme proteins could affect the host cells, iron uptake of the bacteria indicates the bacterial pathogenesis. The strain FORC_008 has two iron-acquiring gene clusters, vibriobactin

(FORC8_3533-3536 in chromosome II) and vibrioferrin (FORC8_4412-4422 in chromosome II).

The comparative analysis between *V. parahaemolyticus* FORC_008 and CDC_K4557 identified that the strain FORC_008 possess a putative β-lactamase which did not identified in strain CDC_K4557 (Figs. II-6D and II-7D). The β-lactamase inactivates β-lactam antibiotics including penicillin by hydrolyzing the peptide bond of four-membered beta-lactam ring (Majiduddin, et al. 2002). Therefore, production of β-lactamase would be helpful to survival of *V. parahaemolyticus* FORC_008 by providing resistance to the β-lactam antibiotics during host infection.

Chapter III.

Transcriptome Analysis of *Vibrio vulnificus* in Response to Crab Exposure

III-1. Introduction

Vibrio vulnificus is an opportunistic marine pathogen that can cause primary septicemia accompanied with fever, gastroenteritis, diarrhea, and vomiting (Jones, et al. 2009). This organism occurs in marine environment and seafood such as oyster, clam, and crab, so *V. vulnificus* infection could occur via consumption of raw or undercooked seafood (Hor, et al. 1995). Because the most infections of *V. vulnificus* were mediated by food consumption, it is also important to understand and identify the especially expressed genes of the pathogens in response to exposure to foods. The study on differentially expressed genes in response to foods would provide the understanding on bacterial life cycle on food and information of putative target genes which must be regulated to prevention of infections.

The development of next-generation sequencing (NGS) techniques allow sensitive and precise examination of transcriptome profile and genome-side gene expression studies in particular physiological conditions. RNA-sequencing (RNA-seq) is one of the NGS techniques for transcriptome analysis, and provide the ability that sequence RNA in a strand-specific manner, identify transcriptional start sites, identify ncRNA, and defining the operons to which genes belong (Croucher, et al. 2010).

In this study, I analyzed the entire transcriptome of newly isolated *V. vulnificus* FORC_016 in response to exposure to crab using a strand-specific RNA-seq method. The differentially expressed genes under exposure to crab were identified and analyzed. These results would provide some clues for further understand the interaction of *V. vulnificus* in response to exposure to food.

III-2. Materials and Methods

III-2-1. Strains, plasmids, and culture conditions

The strain used in this study is listed in Table II-1. Unless otherwise noted, the *V. vulnificus* strains were grown aerobically in Luria-Bertani (LB) medium supplemented with 2% (w/v) NaCl (LBS) at 30°C. The cells grown to log phase (A_{600} of 0.8) were harvested and washed with PBS buffer and subcultured ($4x10^9$ CFU / 250 ml) in either *Vibrio fischeri* minimal medium containing 32.6mM glycerol (VFMG) or VFMG containing crab as final concentration of and incubated for 1 or 4 h at 30°C. After incubation, the bacteria culture were filtrated with syringe with sterilized gauze and vacuum filter with Whatman no. 1 filter paper (Whatman, Maidstone, UK). Subsequently, RNAprotect® Bacteria Reagent (Qiagen) was added to the culture to stabilize RNA. Total RNAs were isolated using miRNeasy Mini Kit (Qiagen) according to the manufacturer's procedure. The quality of total RNAs was verified using Agilent 2100 Bioanalyzer and Agilent RNA 6000 Nano reagents (Agilent Technologies, Waldbronn, Germany) by Chunlab (Seoul, South Korea).

III-2-2. Strand-specific cDNA library construction and RNA-seq.

The procedures for a strand-specific cDNA library construction and RNA-seq were conducted by Chunlab. mRNA was selectively enriched by depleting ribosomal RNAs by using Ribo-ZeroTM rRNA Removal Kits (Epicentre, Madison, WI). Enriched mRNA was subjected to the cDNA library construction using TruSeq Stranded mRNA Sample Prep Kit (Illumina) following manufacturer's instruction. The quality of cDNA libraries were evaluated as described above for the quality verification of total RNA, except that Agilent DNA 1000 Reagents (Agilent Technologies) was used. Strand-specific and paired-ended 100 nucleotide reads from each cDNA library were obtained using Hiseq 2500 (Illumina). For biological replication, two libraries were constructed and sequenced from RNAs extracted from two independent exponential phase cultures of *V. vulnificus*.

III-2-3. Strand-specific cDNA library construction and RNA-seq.

The reads obtained from RNA-seq were mapped to the *V. vulnificus* FORC_016 reference genome (GenBank accession numbers CP011775 and CP011776, www.ncbi.nlm.nih.gov) using CLC Genomics Workbench 7.5.1 (CLC Bio). The relative transcript abundance was measured in reads per kilobase of transcript per million mapped sequence reads (RPKM) (Mortazavi, et al. 2008). The fold changes of RPKM values and their significance were assigned and the genes with 2 or greater

fold change with *P*-values < 0.05 were considered to be differentially expressed. To avoid outlier ratios that can result from a small number of reads, genes with fewer than 2 RPKM were sorted out. The graphs describing the results of RNA-seq, component analysis (PCA) plot and scatter plot, were created using CLC Genomics Workbench 7.5.1 (CLC Bio). The rectangular heat maps were generated by gitools (http://www.gitools.org) based on the fold changes of RPKM values of each genes.

III-2-4. Quantitative real-time (qRT) PCR

Using the RNAs which isolated from *V. vulnificus* incubated with VFMG or VFMG containing crabs as template, cDNA was synthesized using iScript™ cDNA Synthesis Kit (Bio-Rad). Real-time PCR amplification of the cDNA was performed by using the Chromo 4 real-time PCR detection system (Bio-Rad) with a pair of specific primers listed in Table III-1 as described previously (Lim et al. 2014). Relative expression levels of the specific transcripts were calculated by using the 16S rRNA expression level as the internal reference for normalization.

Table III-1. Oligonucleotides used in qRT-PCR[a]

	Sequence (5' → 3')	
Locus-tag	**Forward**	**Reverse**
FORC16_0204	AATCGGTCGTAAAGTGGGCA	ATTGCTGCATAGCCGTCAGT
FORC16_0230	ACAGTGTTGCTAACCGTCGT	TTGGAGCTTTGTCACCAGCA
FORC16_0310	TTCGGACGAGTGTGCAATGA	CATGAGAGCGGCTGAAAGGA
FORC16_0397	GCCAGTTAGCGATCCGAGAA	TCATCGGGTGCCACATTCAA
FORC16_0413	ACCTCGATGACGGGGTATCA	GAGATCGCGAATCACAAGGC
FORC16_0427	GGGAACTCGGTCTTGCAGAA	AGCACCTAATAGCGTTGCGA
FORC16_0682	GGTTATGCTCGCCAAGATCG	AATCGTCAGAACGCGGTCAA
FORC16_0741	TCTCGAAACACCTCACGCTC	CTTGGGCGTCCAGAGAACAT
FORC16_0778	TTGTTGATTCGTGCAACGGC	ACAGAAGCGAGAGCAAGCAT
FORC16_0815	GGTGATTGGCGCAACCAAAT	TAAGCCAGCCACTTCTTCCG
FORC16_0852	CGTCGTTTCGATGGTTTCCG	ACCCGCTGGGTTGATCTTTT
FORC16_0934	GCATTACCCGGATTGTTGGC	CCAGAGCACTATGATCGCGT
FORC16_0948	AGCCAGAAAACTTCGTCGGT	CAACCGCGTTTTCGATTGGT
FORC16_0949	TTGCGCTGCATTGGGATCTA	GGTAGCTCAACCCTTTCGCT
FORC16_1047	CTGATTTGCGACGAACCCAC	ATATCTCCGCAACGACACCG
FORC16_1056	GTGGGGCTTTCTCCAACTCC	AACAAACACGAGCAACGAGG
FORC16_1084	CGGCGATGGCTTATGGTACA	GTACTTCTGATGGCCCAGCG
FORC16_1117	TCATCGGCCACGACTTAACC	GCTGCGGTATAGGGATGCTT
FORC16_1281	CGCTTTACCGCTCTGCAATC	AAAACCTTGGCCGTCGTAGT
FORC16_1362	GTTGGCAACTATTGGCACAGT	AGCCTCAACAGATTCCACGA
FORC16_1777	GTAGCCCAGAGCAAGTGTGT	GAAGTGCCATGCGTGTTGAG
FORC16_1940	GTGACGCATGAAATGGCGTT	AGCGCTCTGAATCAGGGTTA
FORC16_2057	CAGAAGTTGGTCAGCGCCTA	CGGAACAAGTCTGGCAGGAT
FORC16_2196	CTCTAGCGGGTCCTGTTGTG	GTAAGCGTGAGGACCTGTGG
FORC16_2330	GTATTTTCGCAGCATGGCGT	GGGAACCAACCAAGACCGAT
FORC16_2366	GCAGAAGCGGCTCCAGTA	TGATGGAATCGCCAACAGCC
FORC16_2410	GAGCTACGTGACGGTGACAA	GTGCCGTCTAGCTCGATCAT
FORC16_2482	GAAAGAGTTTGTGCTGGCGG	ATCCTGCGCATGAACCATGA
FORC16_2670	GCGCCTAGAAGCGATCAAAC	GTTCAAACCGAACTGCGGAC
FORC16_2821	TCAGCGTGTAGTCATTGCGA	ATAGCTCGCGGATCAGGTTG

FORC16_2859	TAAACTGCGTCATGCCAATGC	GTGTTGTCCGGCATGAGGT
FORC16_2877	AGTCCGGCGCGGTTATTTTT	CGCTCTCGCTCCTACAAACA
FORC16_2933	GGTGTGGGTCACGACAAGAT	GACCAGGGCGCATGAAGTTA
FORC16_3007	TGACGGTTTCTACTTCGAATAAACG	AAGTCGATCTCCCCCGCTT
FORC16_3055	CCTGATTGTCACCCAAGGCA	AGCACACGCAAATGATCACC
FORC16_3086	CTAGGCTCACTAACAACGGCG	AACAGGTGACTGCGACGAT
FORC16_3108	AGCCATCACCGTTTGCAGTA	GATCAACTCACCCAGTGCGA
FORC16_3199	AGATTGCCAGTGGCGAAGAA	CAGATAAAGCGCACAGACGC
FORC16_3449	AATAGCGACAAACCTGGGCA	GGTAAAGGTCTGCTTCCCCC
FORC16_3636	AGCCTAGCCAACAAAGGCAT	AGCATAAGCCGGCCACTAAG
FORC16_3643	GCAGTACTTGATGGCACGGA	TGCCGAGATCATCGAGGAGA
FORC16_3766	ATCATTCTGTCGTTGGCGGT	TTTCGCTAACGGTGCCAAAC
FORC16_3789	CACAAAGGCGACAACAGTGG	GGCACGCCAATGCTCTTAAA
FORC16_3797	TGAAGAGCTGGCTTACGCTT	GTTATGGAAGCGCAGCATGT
FORC16_3872	GGCTAGTGAGGAGCGTCTTG	GACCAATGCCAACCCCAAAC
FORC16_3887	CTTGCACGTTACGGCATACG	CATCCACTTCCAGCACTCGT
FORC16_3891	TGAGGTGCTCAAAGAGGCTG	GTCATAAAGGCGGTGGTGGA
FORC16_3893	GTTTACCGTTGCACCCGTTT	TCACTTTATCCGCGGCCAG
FORC16_4076	TTACCTCAAACGTCGCGGAA	TGGACGCTTTAAACGGCTCT
FORC16_4120	AGATCCTTGGGCTCCGTTTG	ATTCAAGGCTCTGGTCCACG
FORC16_4245	ACGCATTAAACGCTCAGGGA	ATAGGTTTCATCGGCCGCAA
FORC16_4394	GGGTGCTGTGGGTCAGTTTA	CTTCATCACCGCTTTCCAGC
FORC16_4407	AGTGATCAAGCCAGACGCAA	GTTGCGGTTCATGCCTTTCC

*The oligonucleotides were designed using the *V. vulnificus* FORC_016 genomic sequence (GenBank accession number CP011775 and CP011776, www.ncbi.nlm.nih.gov).

III-3. Results and Discussion

III-3-1. Identification of differentially expressed genes.

A mean of 56.7 million reads were obtained per each sample, of which ~88.9% were mapped to a single location of *V. vulnificus* FORC_016 reference genome. To identify relationships among the transcriptome of each samples, the similarity of the transcriptomes was analyzed by principal component analysis (PCA) (Fig. II-1). Although each samples were clearly separated into 4 groups depending on their incubation condition, the samples exposed to crabs were closely related to each other, suggesting that the exposure to crab was significantly affect the transcriptome of *V. vulnificus*. Therefore, the differentially expressed genes by exposure to crab incubated for 1 and 4 h were further analyzed.

The differentially expressed genes following each conditions were identified. Average RPKM values from the biological duplicate samples were used to represent the expression level of each gene. The scatter plots showed that a number of genes are differentially expressed with significance (P-value < 0.05, 2 fold threshold) (Fig. III-2). Compare to cells incubated in VFMG for 1h, a total 1,327 genes were identified to be differentially expressed in cells incubated in VFMG containing crab for 1h; 405 up-regulated and 992 down-regulated. In the case of samples incubated

in VFMG or VFMG containing crab for 4 h, a total 791 genes were identified to be differentially expressed; 143 genes up-regulated and 648 gene down-regulated in cells incubated on VFGM containing crab. For further analysis, the differentially expressed genes were clustered into functionally related groups using the Cluster of Orthologous Groups (COG) database for the *V. vulnificus* FORC_016 genome (http://weizhong-lab.ucsd.edu/metagenomic-analysis/server/cog/) which showed that the genes with various functions were differentially expressed (Fig. III-3).

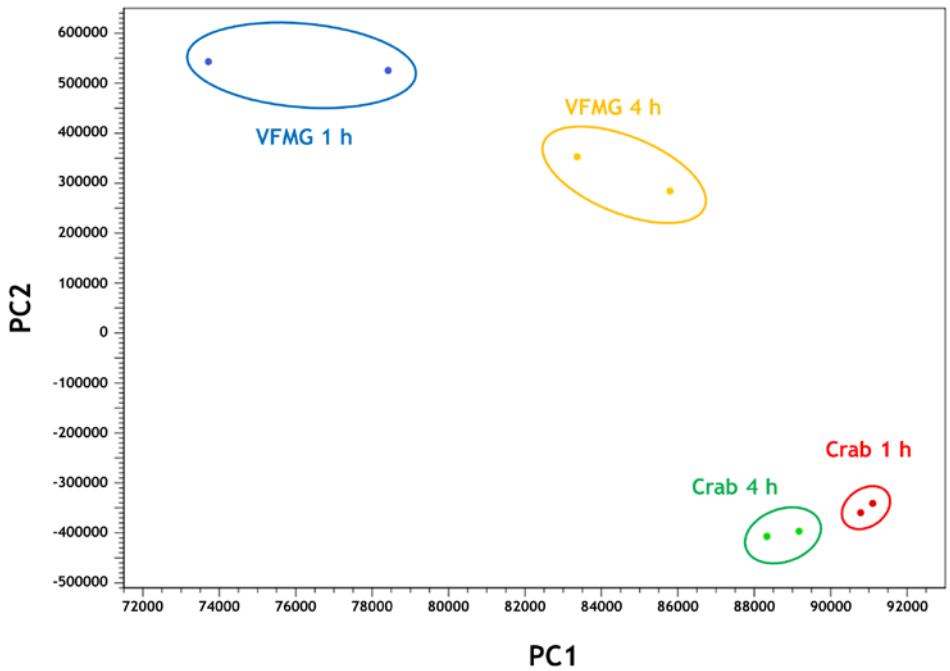

Figure III-1. Principal component analysis (PCA) of the transcriptomes. PCA analysis was performed using RPKM values from the RNA-seq analyses. Each samples incubated in VFMG or VFMG containing crab for 1 or 4 h were plotted in two dimensional plots across the first two principal components (PC). Samples for each condition were denoted by a different color. Blue dots, RNAs from cells incubated in VFMG for 1 h; yellow dots, RNAs from cells incubated in VFMG for 4 h; red dots, RNAs cells incubated in VFMG containing crab for 1 h; green dots, RNAs cells incubated in VFMG containing crab for 4 h.

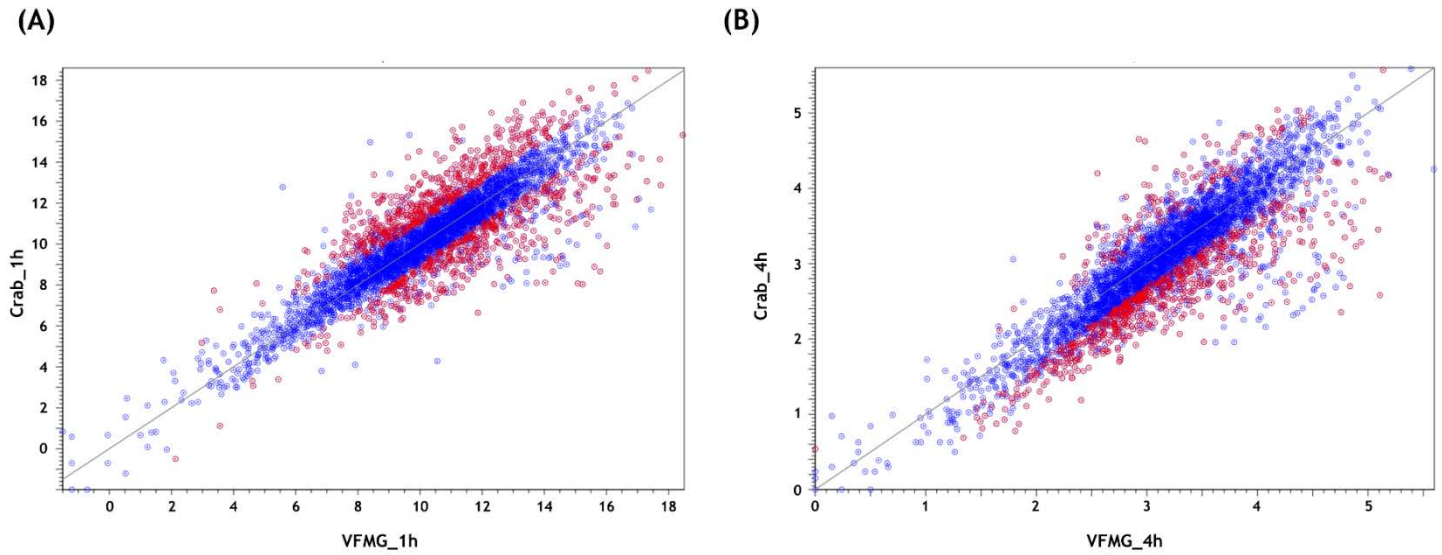
(A)
Crab_1h
VFMG_1h
0
2
4
6
8
10
12
14
16
18
(B)
Crab_4h
VFMG_4h
0
1
2
3
4
5

Figure III-2. Transcriptome comparisons of the RNA-seq samples. Scatter-plot of genes differentially expressed between the cells incubated in VFMG or VFMG containing crab for (A) 1 h and (B) 4 h was generated. Numbers on the X- and Y-axis represent the transformed RPKM (log2) of each sample. Red dots represent the differentially expressed genes.

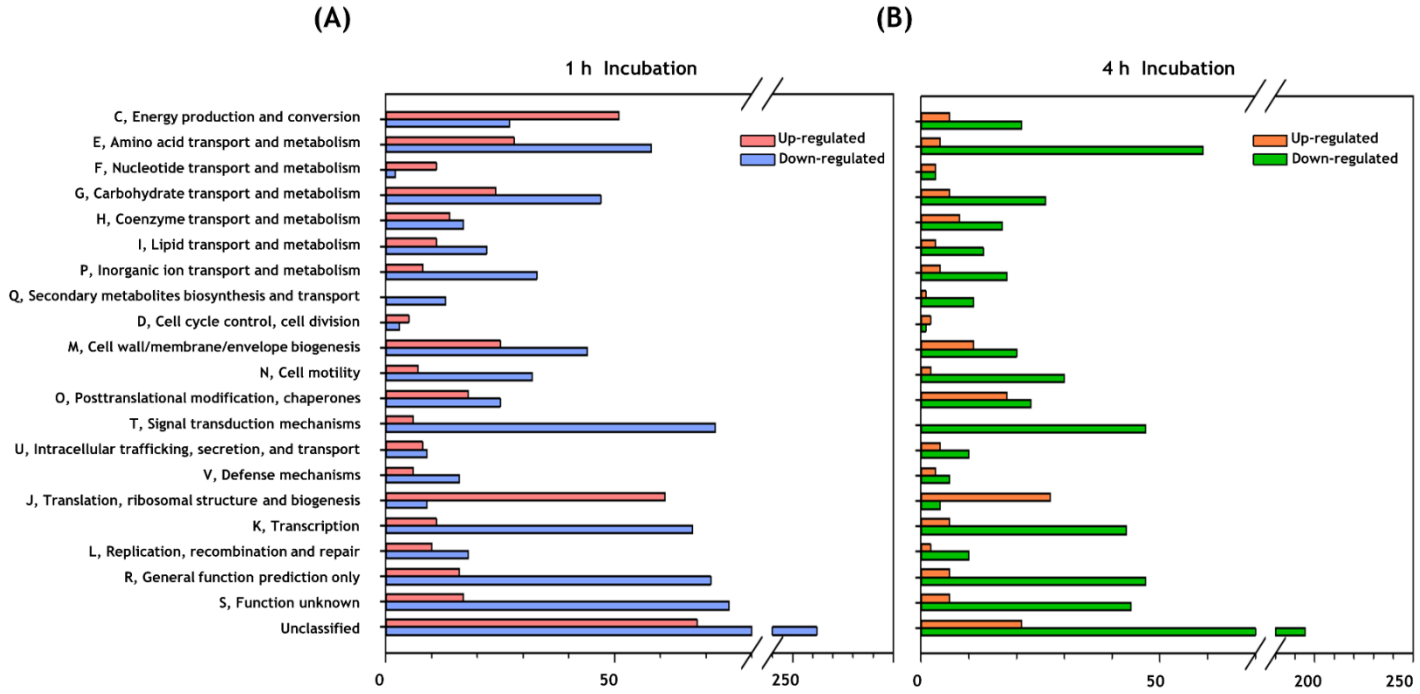
(A)
(B)
1 h Incubation
4 h Incubation
C, Energy production and conversion
E, Amino acid transport and metabolism
F, Nucleotide transport and metabolism
G, Carbohydrate transport and metabolism
H, Coenzyme transport and metabolism
I, Lipid transport and metabolism
P, Inorganic ion transport and metabolism
Q, Secondary metabolites biosynthesis and transport
D, Cell cycle control, cell division
M, Cell wall/membrane/envelope biogenesis
N, Cell motility
O, Posttranslational modification, chaperones
T, Signal transduction mechanisms
U, Intracellular trafficking, secretion, and transport
V, Defense mechanisms
J, Translation, ribosomal structure and biogenesis
K, Transcription
L, Replication, recombination and repair
R, General function prediction only
S, Function unknown
Unclassified
Up-regulated
Down-regulated
Up-regulated
Down-regulated
0
50
250
0
50
200
250

Figure III-3. Functional categorization of differentially expressed genes. The differentially expressed genes (*P*-value < 0.05, 2-fold threshold) were functionally categorized based on the COG database for the *V. vulnificus* FORC_016 genome, which was retrieved from GenBank (accession numbers CP011775 and CP011776). Genes up and down regulated by crab exposure for 1 h (A) and for 4 h (B) were represented.

III-3-2. Identification of differentially expressed genes under exposure to crab.

To identify the effect of exposure time to crab on *V. vulnificus* FORC_016, the differentially expressed genes with specialized function following the exposure to crab for 1h and 4h were compared. The differentially expressed genes with specialized function was summarized in Table III-2 and Figure III-4 to III-7. Selected categories of genes were further described below.

Amino acid metabolism

Most of genes involved in the amino acids biosynthesis and specific amino-acid transport were down-regulated in both of 1 h and 4 h incubation samples (Fig. III-4). Instead, the expression level of oligopeptide transporter (FORC16_0948-0952, FORC16_1044-1048, and FORC16_1116-1119) was increased, suggesting that the bacterium chooses to uptake peptides for supply of amino acids. Because the crab is an abundant source of peptides, it would be more effective for the bacterium of energy conservation aspect to uptake peptides rather than to synthesize the single amino-acids.

Interestingly, although most of the genes associated with single amino acid synthesis and transport was down-regulated in response to crab exposure, genes related with glycine cleavage system (FORC16_3199, FORC16_3200, FORC16_3264,

FORC16_3625, and FORC16_3626) were significantly up-regulated in 1 h incubation sample. The glycine cleavage system is a novel ATP generation pathway which is responsible for net ATP generation of glycolysis, suggesting that this bacterium demanded high energy (Vazquez, et al. 2011). Consistently, the genes encoding ATP synthase (FORC16_2870-2877), electron transport complex (FORC16_0932-0934), cytochrome c oxidase (FORC_1362-1365), cytochrome c biogenesis protein (FORC_2053-2058), and NADH-quinone reductase (FORC16_2191-2196) which is related with energy production were up-regulated in 1 h incubation sample (Fig. III-5C).

Along with genes encoding glycine cleavage system, genes associated with proline metabolism (FORC16_4407, FORC16_4408, and FORC16_4409) were also up-regulated in cells incubated with crab (FIG. III-4A). Proline permease and proline dehydrogenase, which were encoded by FORC16_4409 and FORC16_4407 respectively, have been considered as converting proline into glutamate for assimilation of glutamate and for resistance to osmotic stress (Lee, et al. 2003). Because expression level of genes involved in glutamate metabolism (FORC16_0424-0427) and glutamate transport (FORC16_1278-1281 and FORC16_2818 to 2821) were decreased in cells incubated with crab, increase of

genes related with proline metabolism would be due to the high osmolality stress, rather than deficiency of glutamate.

The expression level of genes involved in nitrogen metabolism and also decreased. Bacteria take up nitrate (NO_3^-) and nitrite (NO_2^-) from environment and subsequently reduced them to ammonia for nitrogen assimilation (Moreno-Vivián, et al. 1999, Richardson, et al. 2001). Transport of nitrate or nitrite is an energy-consuming process because they are charged molecules that could not pass through biological membranes (Moir, et al. 2001). Considering that the one of the important reasons of nitrogen assimilation is amino acid synthesis, the nitrogen metabolism might be down-regulated because the demands of amino acid were satisfied by uptake of peptides so down-regulation on nitrogen metabolism would be benefit to bacteria in energy saving aspect.

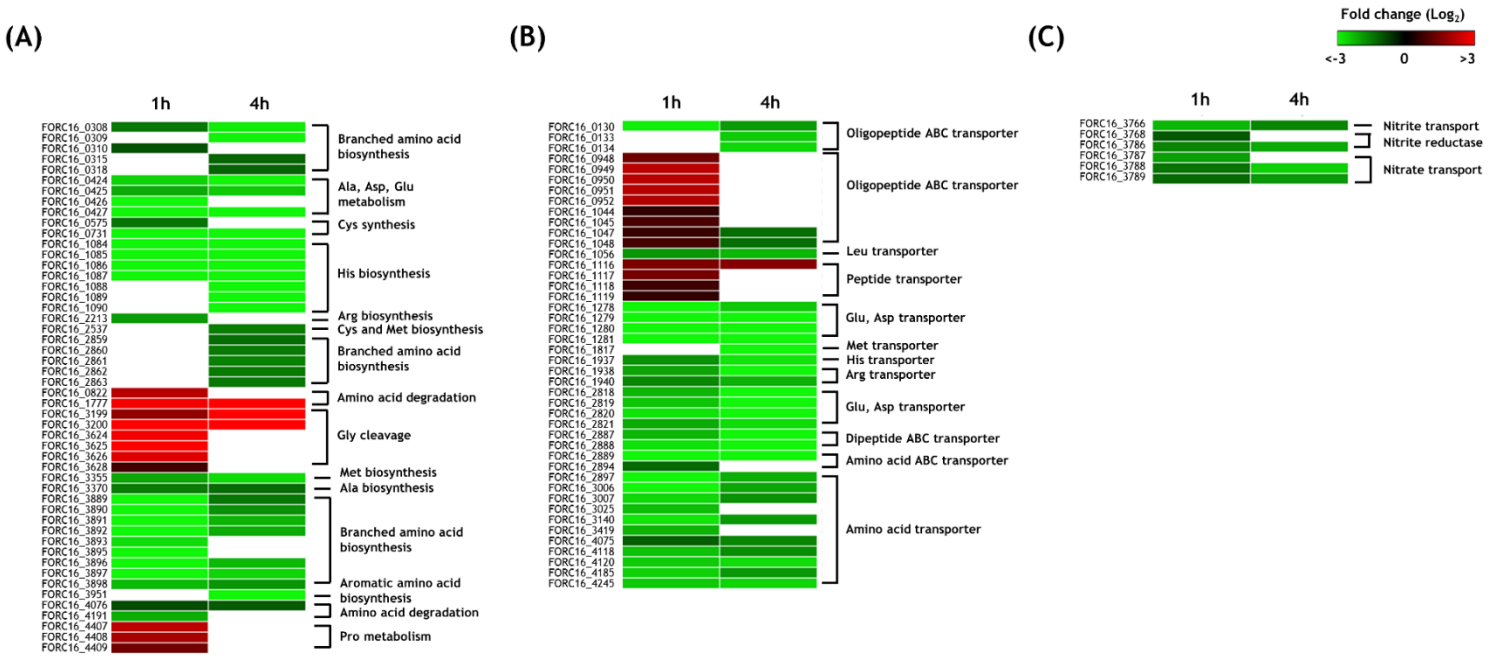
(A)
1h
4h
FORC16_0308
FORC16_0309
FORC16_0310
FORC16_0315
FORC16_0318
FORC16_0424
FORC16_0425
FORC16_0426
FORC16_0427
FORC16_0575
FORC16_0731
FORC16_1084
FORC16_1085
FORC16_1086
FORC16_1087
FORC16_1088
FORC16_1089
FORC16_1090
FORC16_2213
FORC16_2537
FORC16_2859
FORC16_2860
FORC16_2861
FORC16_2862
FORC16_2863
FORC16_0822
FORC16_1777
FORC16_3199
FORC16_3200
FORC16_3624
FORC16_3625
FORC16_3626
FORC16_3628
FORC16_3355
FORC16_3370
FORC16_3889
FORC16_3890
FORC16_3891
FORC16_3892
FORC16_3893
FORC16_3895
FORC16_3896
FORC16_3897
FORC16_3898
FORC16_3951
FORC16_4076
FORC16_4191
FORC16_4407
FORC16_4408
FORC16_4409
Branched amino acid biosynthesis
Ala, Asp, Glu metabolism
Cys synthesis
His biosynthesis
Arg biosynthesis
Cys and Met biosynthesis
Branched amino acid biosynthesis
Amino acid degradation
Gly cleavage
Met biosynthesis
Ala biosynthesis
Branched amino acid biosynthesis
Aromatic amino acid biosynthesis
Amino acid degradation
Pro metabolism
(B)
1h
4h
FORC16_0130
FORC16_0133
FORC16_0134
FORC16_0948
FORC16_0949
FORC16_0950
FORC16_0951
FORC16_0952
FORC16_1044
FORC16_1045
FORC16_1047
FORC16_1048
FORC16_1056
FORC16_1116
FORC16_1117
FORC16_1118
FORC16_1119
FORC16_1278
FORC16_1279
FORC16_1280
FORC16_1281
FORC16_1817
FORC16_1937
FORC16_1938
FORC16_1940
FORC16_2818
FORC16_2819
FORC16_2820
FORC16_2821
FORC16_2887
FORC16_2888
FORC16_2889
FORC16_2894
FORC16_2897
FORC16_3006
FORC16_3007
FORC16_3025
FORC16_3140
FORC16_3419
FORC16_4075
FORC16_4118
FORC16_4120
FORC16_4185
FORC16_4245
Oligopeptide ABC transporter
Oligopeptide ABC transporter
Leu transporter
Peptide transporter
Glu, Asp transporter
Met transporter
His transporter
Arg transporter
Glu, Asp transporter
Dipeptide ABC transporter
Amino acid ABC transporter
Amino acid transporter
(C)
Fold change (Log2)
<-3
0
>3
1h
4h
FORC16_3766
FORC16_3768
FORC16_3786
FORC16_3787
FORC16_3788
FORC16_3789
Nitrite transport
Nitrite reductase
Nitrate transport

(D)

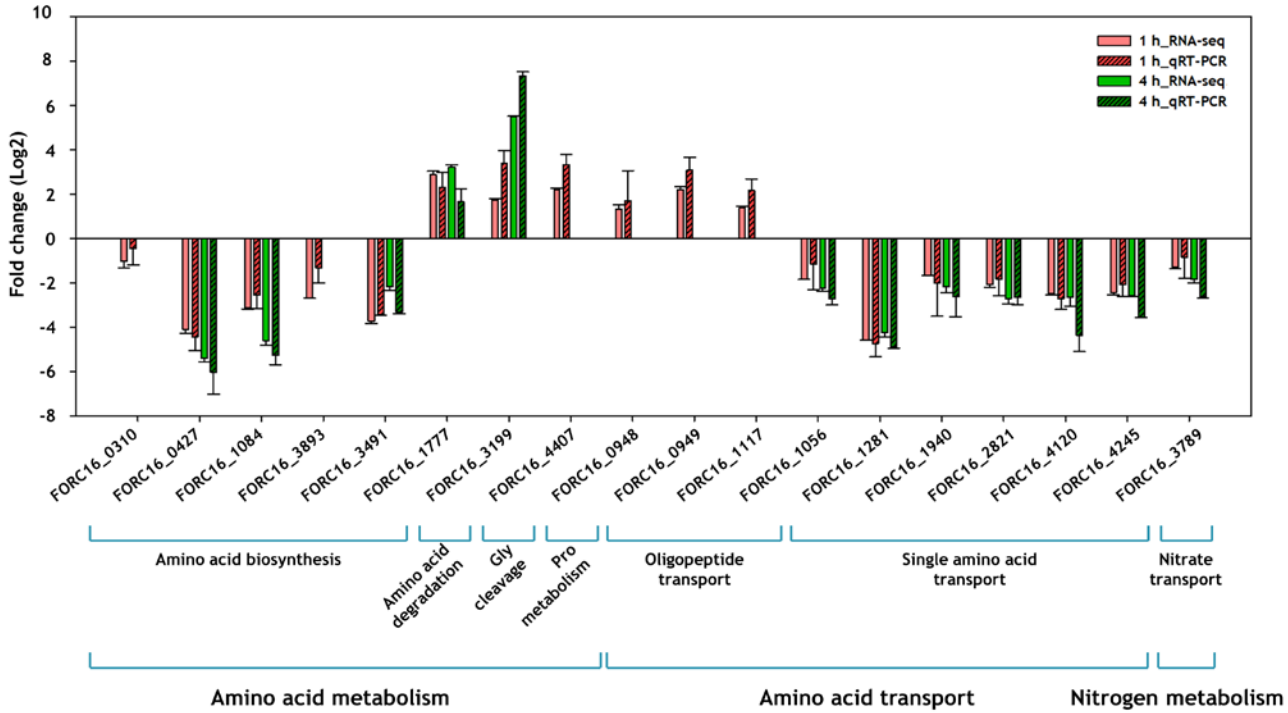
Fold change (Log2)
10
8
6
4
2
0
-2
-4
-6
-8
1 h_RNA-seq
1 h_qRT-PCR
4 h_RNA-seq
4 h_qRT-PCR
FORC16_0310
FORC16_0427
FORC16_1084
FORC16_3893
FORC16_3491
FORC16_1777
FORC16_3199
FORC16_4407
FORC16_0948
FORC16_0949
FORC16_1117
FORC16_1056
FORC16_1281
FORC16_1940
FORC16_2821
FORC16_4120
FORC16_4245
FORC16_3789
Amino acid biosynthesis
Amino acid degradation
Gly cleavage
Pro metabolism
Oligopeptide transport
Single amino acid transport
Nitrate transport
Amino acid metabolism
Amino acid transport
Nitrogen metabolism

Figure III-4. Heat maps of genes related with amino acid metabolism. The expression ratio of genes related with amino acid metabolism between cells incubated with VFMG and VFMG containing crab for 1h and 4h were calculated from RNA- seq. results and demonstrated as heat maps ($P < 0.05$) (A, B, and C). The results from RNA-seq. were verified using qRT-PCR (D). A, Genes related with amino acid transport; B, genes related with amino acid synthesis; C, genes related with nitrogen metabolism. The green-to-red color scale represented fold-change (log_2).

Carbon metabolism and energy production

Chitin, a polymer of *N*-acetylglucosamine (GlcNAc), is one of the most abundant carbon source in crab (Yen, et al. 2009). Although chitin is a highly insoluble carbon source, it is rapidly break down to GlcNAc by marine bacterium, a favorable sugar for attachment and colonization (Chang, et al. 2004, Keyhani, et al. 1999, Yu, et al. 1991). Previous studies reported that *Vibrio* species also have chitinolytic activities, therefore it could catabolite chitins (Wortman, et al. 1986, Yen, et al. 2009, Yu, et al. 1991). Although chitins would be one of the major carbon sources for *V. vulnificus* FORC_016 in VFMG containing crabs, the expression level of genes related with chitin transport (FORC16_2330-2331) and genes encoding two putative chitinases (FORC16_2933 and FORC16_3652) were significantly down-regulated regardless of incubation time (Fig III-5B). Furthermore, genes associated chitin utilization (FORC16_2334 and FORC16_2336) were also down-regulated in cells contact with crab, suggesting that *V. vulnificus* FORC_016 did not use chitin as carbon source. Most of bacteria utilize prefer carbon selectively by carbon catabolite repression, and extracellular chitinase expression is also catabolite repressed (Görke, et al. 2008, Keyhani, et al. 1999). Therefore, the down-regulation of chitinase expression level might be due to the existence of favorable carbon source, such as glucose. The carbohydrate composition analysis of blood tissue of green crab revealed that glucose and glycogen were predominant sugar and polysaccharide in crab tissue,

respectively (Johnston, et al. 1972). Therefore, the increased expression level of genes related with starch metabolism (FORC16_3686, FORC16_3796, and FORC16_3797), fructose, mannose metabolism (FORC16_3636), and glycolysis (FORC16_0769, FORC_2410 and FORC16_2447) and decreased expression of genes related with other sugar metabolism would be due to high presence of glucose in swimming crab (Table III-2 and Fig. III-5A). Consistent with this, the expression level of genes related with TCA cycle were up-regulated only in 1 h incubation sample with significance ($P < 0.05$), suggesting that *V. vulnificus* FORC_016 produced energy during incubation by metabolizing the sugars derived by tissue of swimming crab.

Cell growth

The expression of genes related with nucleotide metabolism (FORC16_0814-0815) and genes encoding ribosomal proteins (FORC16_0203-230) were significantly increased in both of 1 and 4 h incubation sample. In addition, the gene encoding cell division protein FtsI (FORC16_0397), cell division topological specificity factor (FORC16_803), and cell division trigger factor (FORC16_0852) were up-regulated, while the gene encoding cell division inhibitor (FORC16_0741) were down-regulated. The combined result suggested that the bacterium was in proliferation state when exposure to crab for 1 and 4 h, by utilizing organic compounds such as

oligopeptide and carbon sources from swimming crab as described above.

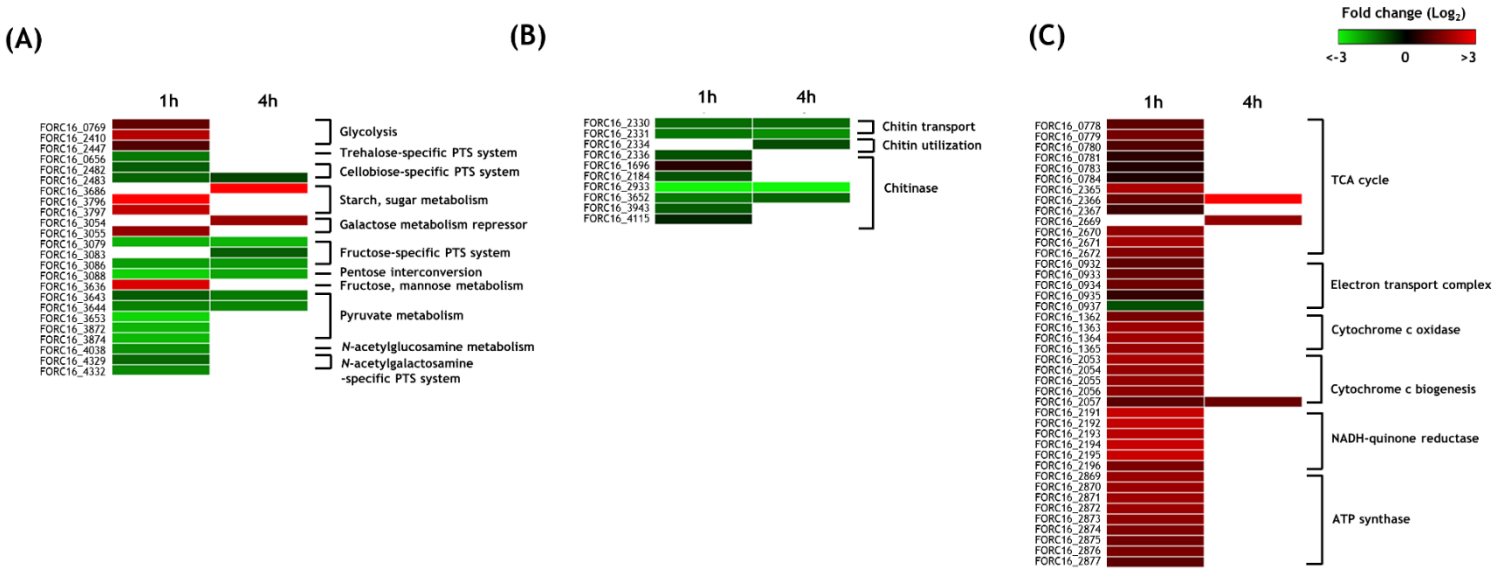
(A)
1h
4h
FORC16_0769
FORC16_2410
FORC16_2447
FORC16_0656
FORC16_2482
FORC16_2483
FORC16_3686
FORC16_3796
FORC16_3797
FORC16_3054
FORC16_3055
FORC16_3079
FORC16_3083
FORC16_3086
FORC16_3088
FORC16_3636
FORC16_3643
FORC16_3644
FORC16_3653
FORC16_3872
FORC16_3874
FORC16_4038
FORC16_4329
FORC16_4332
Glycolysis
Trehalose-specific PTS system
Cellobiose-specific PTS system
Starch, sugar metabolism
Galactose metabolism repressor
Fructose-specific PTS system
Pentose interconversion
Fructose, mannose metabolism
Pyruvate metabolism
N-acetylglucosamine metabolism
N-acetylgalactosamine -specific PTS system
(B)
1h
4h
FORC16_2330
FORC16_2331
FORC16_2334
FORC16_2336
FORC16_1696
FORC16_2184
FORC16_2933
FORC16_3652
FORC16_3943
FORC16_4115
Chitin transport
Chitin utilization
Chitinase
(C)
Fold change (Log2)
<-3
0
>3
1h
4h
FORC16_0778
FORC16_0779
FORC16_0780
FORC16_0781
FORC16_0783
FORC16_0784
FORC16_2365
FORC16_2366
FORC16_2367
FORC16_2669
FORC16_2670
FORC16_2671
FORC16_2672
FORC16_0932
FORC16_0933
FORC16_0934
FORC16_0935
FORC16_0937
FORC16_1362
FORC16_1363
FORC16_1364
FORC16_1365
FORC16_2053
FORC16_2054
FORC16_2055
FORC16_2056
FORC16_2057
FORC16_2191
FORC16_2192
FORC16_2193
FORC16_2194
FORC16_2195
FORC16_2196
FORC16_2869
FORC16_2870
FORC16_2871
FORC16_2872
FORC16_2873
FORC16_2874
FORC16_2875
FORC16_2876
FORC16_2877
TCA cycle
Electron transport complex
Cytochrome c oxidase
Cytochrome c biogenesis
NADH-quinone reductase
ATP synthase

(D)

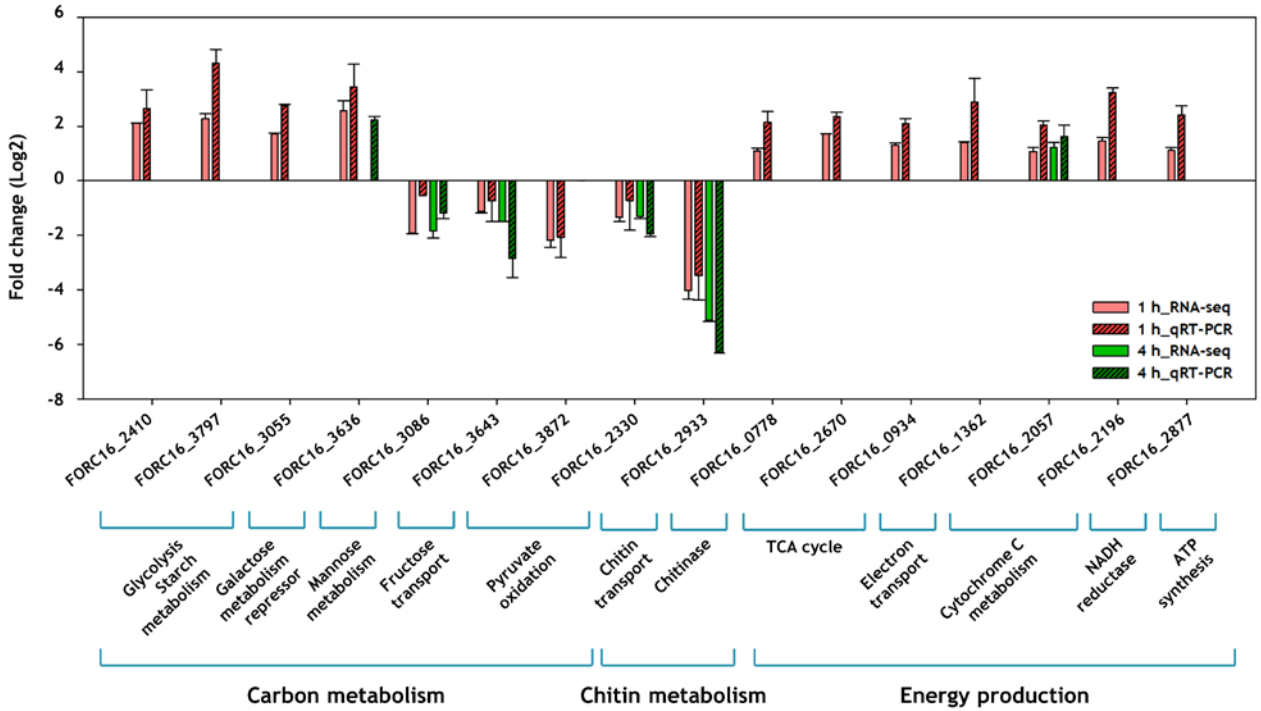
Fold change (Log2)
6
4
2
0
-2
-4
-6
-8
1 h_RNA-seq
1 h_qRT-PCR
4 h_RNA-seq
4 h_qRT-PCR
FORC16_2410
FORC16_3797
FORC16_3055
FORC16_3636
FORC16_3086
FORC16_3643
FORC16_3872
FORC16_2330
FORC16_2933
FORC16_0778
FORC16_2670
FORC16_0934
FORC16_1362
FORC16_2057
FORC16_2196
FORC16_2877
Glycolysis
Starch metabolism
Galactose metabolism repressor
Mannose metabolism
Fructose transport
Pyruvate oxidation
Chitin transport
Chitinase
TCA cycle
Electron transport
Cytochrome C metabolism
NADH reductase
ATP synthesis
Carbon metabolism
Chitin metabolism
Energy production

Figure III-5. Heat maps of genes related with carbon metabolism and energy production. The expression ratio of genes related with carbon metabolism between cells incubated with VFMG and VFMG containing crab for 1h and 4h were calculated from RNA- seq. results and demonstrated as heat maps ($P < 0.05$) (A, B, and C). The results from RNA-seq. were verified using qRT-PCR (D). A, Genes related with carbon metabolism; B, genes related with chitin metabolism; C, genes related with energy production. The green-to-red color scale represented fold-change (log_2).

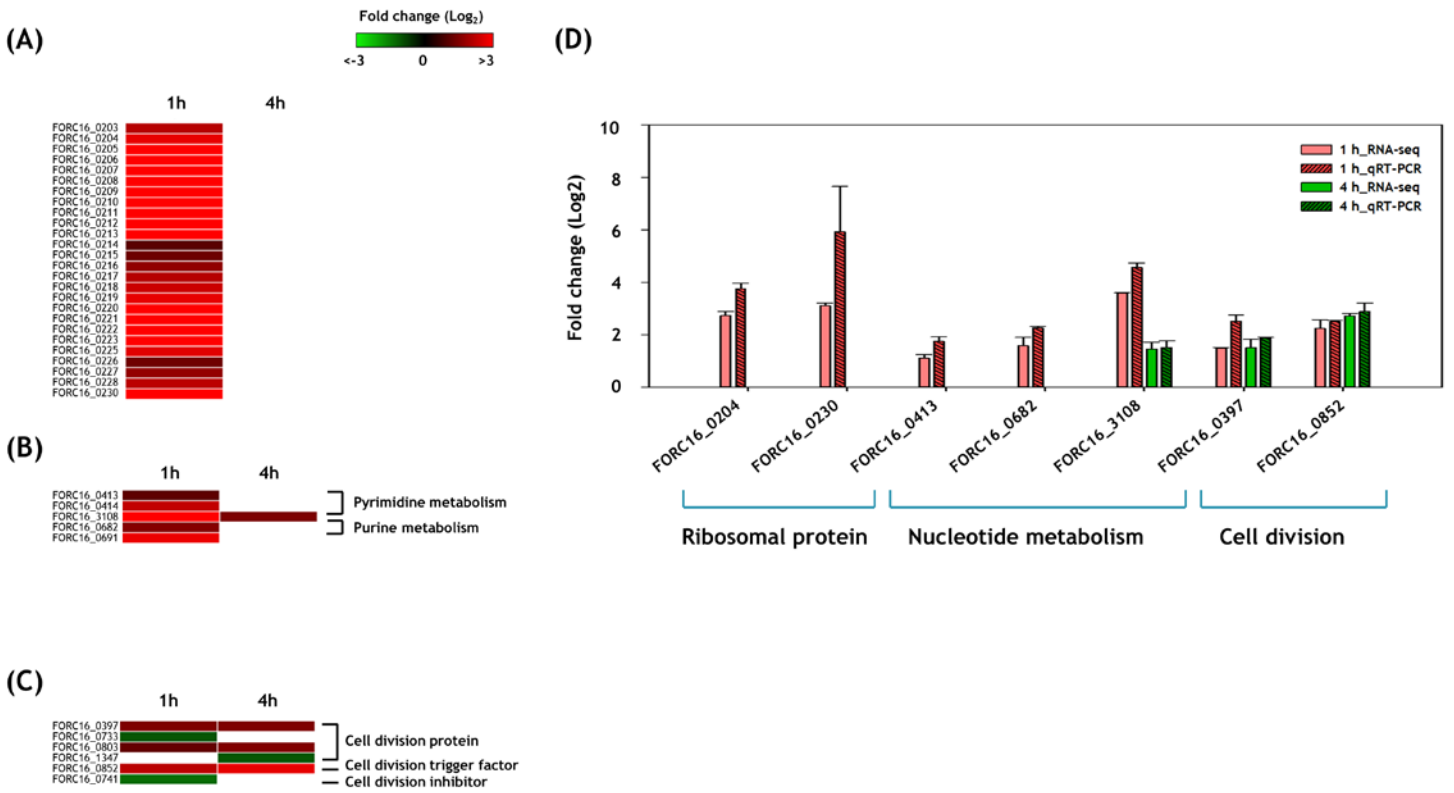
(A)
Fold change (Log2)
<-3
0
>3
1h
4h
FORC16_0203
FORC16_0204
FORC16_0205
FORC16_0206
FORC16_0207
FORC16_0208
FORC16_0209
FORC16_0210
FORC16_0211
FORC16_0212
FORC16_0213
FORC16_0214
FORC16_0215
FORC16_0216
FORC16_0217
FORC16_0218
FORC16_0219
FORC16_0220
FORC16_0221
FORC16_0222
FORC16_0223
FORC16_0225
FORC16_0226
FORC16_0227
FORC16_0228
FORC16_0230
(B)
1h
4h
FORC16_0413
FORC16_0414
FORC16_3108
FORC16_0682
FORC16_0691
Pyrimidine metabolism
Purine metabolism
(C)
1h
4h
FORC16_0397
FORC16_0733
FORC16_0803
FORC16_1347
FORC16_0852
FORC16_0741
Cell division protein
Cell division trigger factor
Cell division inhibitor
(D)
Fold change (Log2)
10
8
6
4
2
0
1 h_RNA-seq
1 h_qRT-PCR
4 h_RNA-seq
4 h_qRT-PCR
FORC16_0204
FORC16_0230
FORC16_0413
FORC16_0682
FORC16_3108
FORC16_0397
FORC16_0852
Ribosomal protein
Nucleotide metabolism
Cell division

Figure III-6. Heat maps of genes related with cell growth. The expression ratio of genes related with energy production and cell growth between cells incubated with VFMG and VFMG containing crab for 1h and 4h were calculated from RNA-seq. results and demonstrated as heat maps ($P < 0.05$) (A, B, and C). The results from RNA-seq. were verified using qRT-PCR (D). A, genes encoding ribosomal proteins; B, genes related with nucleotide metabolism; C, genes related with cell division. The green-to-red color scale represented fold-change (log_2).

Virulence genes

Regardless of incubation time, most genes encoding pili which is related with adhesion of *V. vulnificus* were down-regulated under exposure to crab (Table III-2). Otherwise, the expression level of gene encoding chitin binding protein (FORC16_3424) was increased in cells incubated with crab for 1 h, suggesting that it had important role in adherence of *V. vulnificus* in early stage of exposure to crab. The genes encoding major toxin of *V. vulnificus* such as RTX toxins (FORC16_3881-3885) and metalloproteases (FORC16_1262, FORC16_3415, and FORC16_4281) were down-regulated under crab exposure condition, suggesting that down-regulation of such toxin genes might be a strategy for conservation of the energy for proliferated bacteria. These results suggested that *V. vulnificus* might be not a life-threatening pathogen for swimming crab, and the role of swimming crab in foodborne illness is a reservoir of *V. vulnificus*.

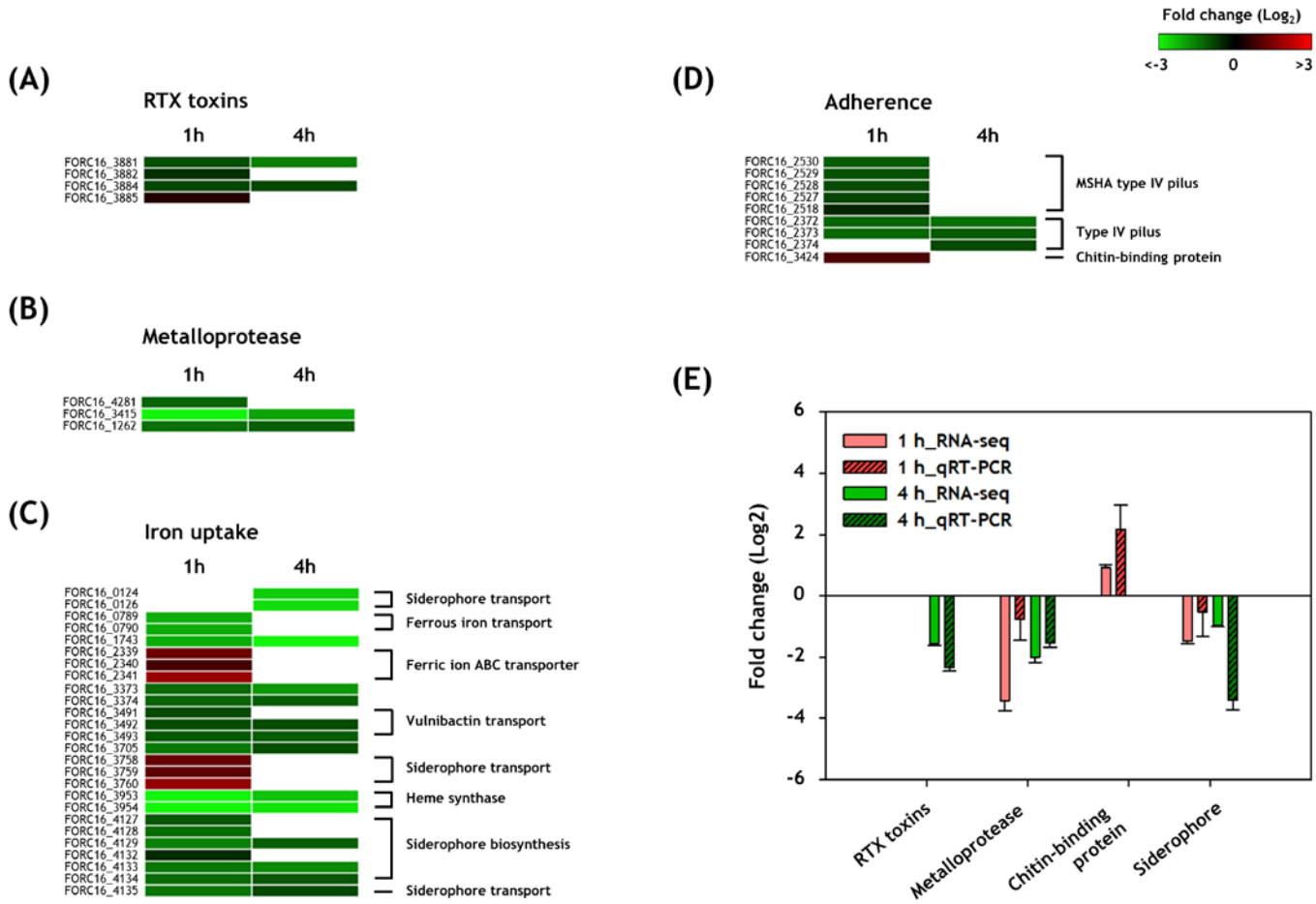
(A)
RTX toxins
1h
4h
FORC16_3881
FORC16_3882
FORC16_3884
FORC16_3885
(B)
Metalloprotease
1h
4h
FORC16_4281
FORC16_3415
FORC16_1262
(C)
Iron uptake
1h
4h
FORC16_0124
FORC16_0126
FORC16_0789
FORC16_0790
FORC16_1743
FORC16_2339
FORC16_2340
FORC16_2341
FORC16_3373
FORC16_3374
FORC16_3491
FORC16_3492
FORC16_3493
FORC16_3705
FORC16_3758
FORC16_3759
FORC16_3760
FORC16_3953
FORC16_3954
FORC16_4127
FORC16_4128
FORC16_4129
FORC16_4132
FORC16_4133
FORC16_4134
FORC16_4135
Siderophore transport
Ferrous iron transport
Ferric ion ABC transporter
Vulnibactin transport
Siderophore transport
Heme synthase
Siderophore biosynthesis
Siderophore transport
Fold change (Log2)
<-3
0
>3
(D)
Adherence
1h
4h
FORC16_2530
FORC16_2529
FORC16_2528
FORC16_2527
FORC16_2518
FORC16_2372
FORC16_2373
FORC16_2374
FORC16_3424
MSHA type IV pilus
Type IV pilus
Chitin-binding protein
(E)
Fold change (Log2)
6
4
2
0
-2
-4
-6
1 h_RNA-seq
1 h_qRT-PCR
4 h_RNA-seq
4 h_qRT-PCR
RTX toxins
Metalloprotease
Chitin-binding protein
Siderophore

Figure III-7. Heat maps of virulence genes. The expression ratio of genes related with pathogenesis between cells incubated with VFMG and VFMG containing crab for 1h and 4h were calculated from RNA- seq. results and demonstrated as heat maps ($P < 0.05$) (A, B, C, and D). The results from RNA-seq. were verified using qRT-PCR (E). A, genes encoding RTX toxins; B, genes encoding metalloprotease; C, genes related with iron uptake; D, genes related with adherence. The green-to-red color scale represented fold-change (log_2).

Table III-2. List of genes differentially expressed by exposure crab.

Locus tag[a]	Gene product	1h		4h	
		Fold change	*P* value	Fold change	*P* value
Amino metabolism					
FORC16_0308	3-isopropylmalate dehydratase small subunit	-1.466	0.031	-2.881	0.026
FORC16_0309	3-isopropylmalate dehydratase large subunit			-2.947	0.044
FORC16_0310	3-isopropylmalate dehydrogenase	-1.009	0.044		
FORC16_0315	Probable transcriptional activator for leuABCD operon			-1.244	0.014
FORC16_0318	Acetolactate synthase small subunit			-1.209	0.049
FORC16_0424	Glutamate synthase (NADPH) small chain	-2.578	0.013	-3.569	0.003
FORC16_0425	Glutamate synthase (NADPH) large chain	-2.068	0.01	-2.475	0.026
FORC16_0426	Glutamate synthase (NADPH) small chain	-3.762	0.031		
FORC16_0427	Glutamate synthase (NADPH) large chain	-4.078	0.029	-5.427	0.017
FORC16_0575	D-amino acid dehydrogenase small subunit	-1.423	0.008		
FORC16_0731	Cysteine synthase	-3.784	0.009	-5.444	0.011
FORC16_0822	Putative histidine ammonia-lyase protein	2.169	0.006		
FORC16_1084	Histidinol dehydrogenase	-3.117	0.013	-4.65	0.043
FORC16_1085	Histidinol-phosphate aminotransferase	-3.54	0.004	-5.213	0.029
FORC16_1086	Histidinol-phosphatase / Imidazoleglycerol-phosphate dehydratase	-3.778	0.02	-5.469	0.031
FORC16_1087	Imidazole glycerol phosphate synthase amidotransferase subunit	-3.787	0.039	-5.579	0.025

FORC16_1088	Phosphoribosylformimino-5-aminoimidazole carboxamide ribotide isomerase			-5.638	0.023
FORC16_1089	Imidazole glycerol phosphate synthase cyclase subunit			-5.521	0.02
FORC16_1090	Phosphoribosyl-AMP cyclohydrolase / Phosphoribosyl-ATP pyrophosphatase			-5.374	0.016
FORC16_1777	L-serine dehydratase, beta subunit / L-serine dehydratase, alpha subunit	2.871	0.001	3.214	0.029
FORC16_2213	N-acetylglutamate synthase	-1.899	0.006		
FORC16_2537	Aspartokinase			-1.531	0.021
FORC16_2859	Acetolactate synthase large subunit			-1.33	0.007
FORC16_2860	Acetolactate synthase small subunit			-1.503	0.019
FORC16_2861	Branched-chain amino acid aminotransferase			-1.579	0.024
FORC16_2862	Dihydroxy-acid dehydratase			-1.503	0.017
FORC16_2863	Threonine dehydratase biosynthetic			-1.467	0.037
FORC16_3199	2-amino-3-ketobutyrate coenzyme A ligase	1.733	0.019	5.501	0.015
FORC16_3200	L-threonine 3-dehydrogenase	3.024	0.021	5.768	0.014
FORC16_3355	Peptide methionine sulfoxide reductase MsrA / Peptide methionine sulfoxide reductase MsrB	-2.032	0.009	-2.67	0.003
FORC16_3370	4-aminobutyrate aminotransferase	-1.51	0.004	-1.322	0.022
FORC16_3624	glycine dehydrogenase	2.846	0.023		
FORC16_3625	Glycine cleavage system H protein	3.086	0.013		
FORC16_3626	Serine hydroxymethyltransferase	2.612	0.018		
FORC16_3889	Enoyl-CoA hydratase (valine, isoleucine degradation)	-3.667	0.042	-1.449	0.028
FORC16_3890	Enoyl-CoA hydratase (valine, isoleucine degradation)	-4.048	0.022	-1.775	0.005
FORC16_3891	Branched-chain acyl-CoA dehydrogenase	-3.746	0.039	-2.196	0.005

FORC16_3892	Methylmalonate-semialdehyde dehydrogenase	-3.304	0.019	-2.087	0.022
FORC16_3893	3-ketoacyl-CoA thiolase (isoleucine degradation)	-2.692	0.002		
FORC16_3895	Isovaleryl-CoA dehydrogenase	-3.854	0.001		
FORC16_3896	Methylcrotonyl-CoA carboxylase carboxyl transferase subunit	-4.031	0.013	-2.271	0.003
FORC16_3897	Methylglutaconyl-CoA hydratase	-3.143	0.008	-2.608	0.013
FORC16_3898	Hydroxymethylglutaryl-CoA lyase	-2.277	0.008	-1.844	0.008
FORC16_3951	2-keto-3-deoxy-D-arabino-heptulosonate-7- phosphate synthase I alpha			-3.026	0.002
FORC16_4076	Glutamine amidotransferases class-II	-0.935	0.049	-1.121	0.016
FORC16_4191	hypothetical protein	-2.121	0.012		
FORC16_4407	Proline:sodium symporter PutP / Propionate:sodium symporter	2.185	7.3405 E-05		
FORC16_4408	Delta 1-pyrroline-5-carboxylate dehydrogenase domain protein	1.972	0.005		
FORC16_4409	Proline dehydrogenase (Proline oxidase) / Delta-1-pyrroline-5-carboxylate dehydrogenase	1.337	0.003		
Sulfur metabolism					
FORC16_0944	Molybdenum cofactor biosynthesis protein MoaB	2.111	0.006		
FORC16_0945	Molybdenum cofactor biosynthesis protein MoaC	1.565	0.005		
FORC16_0946	Molybdenum cofactor biosynthesis protein MoaD	1.822	0.015		
FORC16_0947	Molybdenum cofactor biosynthesis protein MoaE	1.748	0.005		
Iron uptake					
FORC16_0126	Ferric siderophore transport system, biopolymer transport protein ExbB			-2.721	0.043
FORC16_0789	Ferrous iron transport protein B	-2.132	0.003		

FORC16_0790	Ferrous iron transport protein C	-2.097	0.01		
FORC16_1743	Non-specific DNA-binding protein Dps / Iron-binding ferritin-like antioxidant protein / Ferroxidase	-2.107	0.008		
FORC16_2339	Ferric iron ABC transporter, ATP-binding protein	1.284	0.003		
FORC16_2341	Ferric iron ABC transporter, iron-binding protein	1.82	0.0004 3705		
FORC16_3373	Ferric iron ABC transporter, ATP-binding protein	-1.275	0.014	-1.856	0.005
FORC16_3374	Ferric iron ABC transporter, permease protein	-1.239	0.032	-1.16	0.047
FORC16_3493	Ferric vibriobactin, enterobactin transport system, ATP-binding protein	-1.1	0.047		
FORC16_3705	TonB-dependent heme and hemoglobin receptor HutA ; TonB-dependent hemin , ferrichrome receptor	-1.47	0.001		
FORC16_3758	Ferric siderophore transport system, periplasmic binding protein TonB	1.212	0.0001 9298		
FORC16_3759	Biopolymer transport protein ExbD/TolR	1.096	0.0001 8819		
FORC16_3760	Ferric siderophore transport system, biopolymer transport protein ExbB	1.726	0.001		
FORC16_3953	Heme O synthase, protoheme IX farnesyltransferase COX10-CtaB	-3.803	0.004	-2.401	0.003
FORC16_3954	Heme A synthase, cytochrome oxidase biogenesis protein Cox15-CtaA	-3.974	0.009	-2.797	0.003
FORC16_4127	2,3-dihydro-2,3-dihydroxybenzoate dehydrogenase	-1.067	0.002		
FORC16_4128	Isochorismate synthase of siderophore biosynthesis	-1.316	0.028		
FORC16_4129	2,3-dihydroxybenzoate-AMP ligase	-1.583	0.016	-1.165	0.032
FORC16_4133	2,3-dihydroxybenzoate-AMP ligase	-1.477	0.012	-1.691	0.011
FORC16_4134	Aryl carrier domain	-1.319	0.011		

FORC16_4135	Catechol siderophore ABC transporter, substrate-binding protein			-0.885	0.041
Amino acid transport					
FORC16_0130	Oligopeptide transport system permease protein OppB	-2.891	0.044	-1.897	0.035
FORC16_0133	Oligopeptide transport ATP-binding protein OppD			-2.483	0.034
FORC16_0134	Oligopeptide transport ATP-binding protein OppF			-2.626	0.016
FORC16_0948	Oligopeptide ABC transporter, periplasmic oligopeptide-binding protein OppA	1.322	0.007		
FORC16_0949	Oligopeptide transport system permease protein OppB	2.186	0.003		
FORC16_0950	Oligopeptide transport system permease protein oppC	2.179	0.003		
FORC16_0951	Oligopeptide transport ATP-binding protein OppD	2.157	0.004		
FORC16_0952	Oligopeptide transport ATP-binding protein OppF	2.078	0.003		
FORC16_1047	Oligopeptide transport ATP-binding protein OppD	0.671	0.026	-1.336	0.043
FORC16_1048	Oligopeptide transport ATP-binding protein OppF	0.815	0.03	-1.351	0.027
FORC16_1056	Leucine-responsive regulatory protein, regulator for leucine (or lrp) regulon and high-affinity branched-chain amino acid transport system	-1.839	0.018	-2.235	0.014
FORC16_1116	Peptide transport system ATP-binding protein SapF	1.476	0.004	1.574	0.05
FORC16_1117	Peptide transport system ATP-binding protein SapD	1.376	0.002		
FORC16_1278	ABC-type polar amino acid transport system, ATPase component	-2.99	0.039	-2.457	0.004

FORC16_1279	Glutamate Aspartate transport system permease protein GltK	-3.351	0.035	-3.159	0.007
FORC16_1280	Glutamate Aspartate transport system permease protein GltJ	-3.784	0.016	-3.68	0.001
FORC16_1281	Glutamate Aspartate periplasmic binding protein precursor GltI	-4.584	0.009	-4.245	0.011
FORC16_1817	Methionine ABC transporter ATP-binding protein			-3.301	0.001
FORC16_1937	Histidine ABC transporter, permease protein HisM	-1.779	0.012	-2.789	0.005
FORC16_1938	Arginine/ornithine ABC transporter, permease protein AotQ	-1.996	0.002	-3.158	0.009
FORC16_1940	Arginine/ornithine ABC transporter, ATP-binding protein AotP	-1.652	0.0003 5081	-2.169	0.027
FORC16_2818	Dipeptide transport system permease protein DppC	-2.204	0.001	-3.344	0.003
FORC16_2819	ABC transporter permease	-2.407	0.009	-3.603	0.002
FORC16_2820	Dipeptide-binding ABC transporter, periplasmic substrate-binding component	-2.759	0.017	-3.789	0.023
FORC16_2821	Dipeptide transport ATP-binding protein DppD	-2.093	0.037	-2.695	0.022
FORC16_2887	ABC-type polar amino acid transport system, ATPase component	-2.228	0.035	-3.136	0.005
FORC16_2888	Amino acid ABC transporter, permease protein	-2.76	0.016	-4.076	0.002
FORC16_2889	Amino acid ABC transporter, periplasmic amino acid-binding portion	-3.463	0.043	-5.568	0.003
FORC16_2894	Peptide ABC transporter, ATP-binding protein	-1.296	0.007		
FORC16_2897	ABC-type amino acid transport/signal transduction system	-3.344	0.037	-2.132	0.011
FORC16_3006	ABC-type amino acid transport/signal transduction system	-3.255	0.012	-2.031	0.002

FORC16_3007	ABC-type amino acid transport/signal transduction system	-2.64	0.004	-1.78	0.009
FORC16_3025	Oligopeptide transport system permease protein OppB	-2.311	0.002		
FORC16_3140	ABC-type amino acid transport, signal transduction systems, periplasmic component/domain	-2.795	0.005	-1.872	0.015
FORC16_3419	Serine transporter	-2.2	0.028		
FORC16_4075	Amino acid transporter	-1.148	0.018	-1.646	0.013
FORC16_4118	ABC-type amino acid transport/signal transduction systems	-2.359	0.025	-1.719	0.014
FORC16_4120	Putative amino acid ABC transporter, periplasmic amino acid-binding protein	-2.487	0.025	-2.683	0.047
FORC16_4185	ABC-type amino acid transport/signal transduction system	-2.558	0.037	-1.848	0.009
FORC16_4245	ABC-type branched-chain amino acid transport system, periplasmic component	-2.458	0.025	-2.592	0.008
Fatty acide metabolism					
FORC16_0801	Long-chain-fatty-acid--CoA ligase	1.701	0.002		
FORC16_0814	3-oxoacyl-[ACP] synthase	2.615	0.013	2.061	0.04
FORC16_0815	3-oxoacyl-(ACP) reductase	2.447	0.015	1.912	0.044
FORC16_0817	3-oxoacyl-(ACP) synthase FabV like	0.9	0.029	0.477	0
FORC16_1015	Malonyl CoA-acyl carrier protein transacylase	0.281	0.006		
FORC16_2047	3-ketoacyl-CoA thiolase / Acetyl-CoA acetyltransferase	2.337	0.003		
FORC16_3449	Fatty acid desaturase; Delta-9 fatty acid desaturase	-1.891	0.023	-3.246	0.003
FORC16_3509	Fatty acid cis/trans isomerase	-0.931	0.001		
FORC16_3679	Long-chain fatty acid transport protein	-1.805	0.004		
FORC16_3696	lysophospholipase L1			-1.071	0.043
FORC16_3887	3-oxoacyl-(acyl-carrier protein) reductase	-3.45	0.031	-1.638	0.048

FORC16_4175	Long-chain fatty acid transport protein			-1.212	0.004
Nucleotide metabolism					
FORC16_0413	carbamoyl-phosphate synthase small chain	1.11	0.007		
FORC16_0414	Carbamoyl-phosphate synthase large chain	2.287	0.002		
FORC16_0682	Ribose-phosphate pyrophosphokinase	1.58	0.02		
FORC16_0691	UDP-sugar hydrolase; 5'-nucleotidase	2.773	0.001		
FORC16_3108	N-Ribosylnicotinamide phosphorylase	3.582	0.00047421	1.471	0.015
Nitrogen metabolism					
FORC16_3766	Nitrite transporter from formate/nitrite family	-2.241	0.004	-1.645	0.006
FORC16_3768	Nitrite reductase (NAD(P)H) large subunit	-1.089	0.046		
FORC16_3786	Nitrite reductase (NAD(P)H) large subunit	-1.622	0.035	-2.079	0.003
FORC16_3787	Nitrate ABC transporter, ATP-binding protein	-1.952	0.003		
FORC16_3788	Nitrate ABC transporter, permease protein	-1.397	0.034	-2.522	0.013
FORC16_3789	Nitrate ABC transporter, nitrate-binding protein	-1.291	0.001	-1.851	0.035
Cell cycle					
FORC16_0397	cell division protein FtsI	1.491	0.027	1.497	0.03
FORC16_0733	Cell division protein ZipA	-1.045	0.019		
FORC16_0741	Cell division inhibitor Slr1223	-1.327	0.005		
FORC16_0803	Cell division topological specificity factor MinE	1.186	0.027	1.517	0.046
FORC16_0852	Cell division trigger factor	2.205	0.005	2.714	0.03
FORC16_1347	cell division protein ZapC			-1.055	0.034
Carbon metabolism					
FORC16_0769	Phosphoglucomutase	1.166	0.016		

FORC16_2410	Enolase	2.122	0.001		
FORC16_0656	PTS system, trehalose-specific IIB component / PTS system, trehalose-specific IIC component	-1.47	0.033		
FORC16_2482	PTS system, cellobiose-specific IIA component	-1.128	0.024		
FORC16_2483	PTS system, cellobiose-specific IIC component	-1.216	0.006	-0.842	0.045
FORC16_3686	Glucan 1,6-alpha-glucosidase			4.006	0.024
FORC16_3796	Glycosidase	3.239	0.0001 3838		
FORC16_3797	Glycosidase	2.294	0.016		
FORC16_3054	Galactose operon repressor, GalR-LacI family of transcriptional regulators			1.827	0.033
FORC16_3055	Galactose/methyl galactoside ABC transport system, permease protein MglC	1.728	0.039		
FORC16_3079	PTS system, fructose-specific IIA component / PTS system, fructose-specific IIB component / PTS system, fructose-specific IIC component	-2.176	0.002	-2.208	0.001
FORC16_3083	PTS system, fructose-specific IIA component / PTS system, fructose-specific IIB component / PTS system, fructose-specific IIC component			-1.139	
FORC16_3086	PTS system, fructose-specific IIBC component	-1.92	0.005	-1.84	0.005
FORC16_3088	4-deoxy-L-threo-5-hexosulose-uronate ketol-isomerase	-2.561	0.009	-2.034	0.017
FORC16_3636	Tagatose-6-phosphate kinase / 1-phosphofructokinase	2.57	0.047		
FORC16_3643	Pyruvate kinase	-1.126	0.002	-1.485	0.018
FORC16_3644	Phosphoglycerate transporter protein PgtP	-1.582	0.003	-1.644	0.002

FORC16_3653	Glucose-1-phosphate adenylyltransferase	-2.602	0.022		
FORC16_3872	Branched-chain alpha-keto acid dehydrogenase, E1 component, alpha subunit	-2.209	0.026		
FORC16_3874	Dihydrolipoamide acyltransferase component of branched-chain alpha-keto acid dehydrogenase complex	-2.273	0.008		
FORC16_4038	N-acetylmannosamine-6-phosphate 2-epimerase	-1.744	0.023		
FORC16_4329	N-acetylglucosamine-6-phosphate deacetylase	-1.255	0.046		
FORC16_4332	PTS system, N-acetylgalactosamine-specific IIC component	-1.653	0.046		
FORC16_4394	Ascorbate-specific PTS system, EIIC component	-1.136	0.037	-1.585	0.022
Energy production					
FORC16_0778	Succinate dehydrogenase hydrophobic membrane anchor protein	1.098	0.012		
FORC16_0779	Succinate dehydrogenase flavoprotein subunit	1.389	0.001		
FORC16_2365	Dihydrolipoamide dehydrogenase of pyruvate dehydrogenase complex	2.03	0.0003 1143		
FORC16_2366	Dihydrolipoamide acetyltransferase component of pyruvate dehydrogenase complex	1.241	0.004	2.963	0.039
FORC16_2669	Succinate dehydrogenase flavoprotein subunit			1.742	0.046
FORC16_2670	Succinate dehydrogenase iron-sulfur protein	1.721	0.001		
FORC16_2671	Fumarate reductase subunit C	1.936	0.0001 5635		
FORC16_2672	Fumarate reductase subunit D	1.553	1.7703 E-05		

FORC16_0932	Electron transport complex protein RnfE	1.112	0.004		
FORC16_0933	Electron transport complex protein RnfG	1.192	0.002		
FORC16_0934	Electron transport complex protein RnfD	1.299	0.001		
FORC16_1362	Cytochrome c oxidase subunit CcoN	1.414	0.008		
FORC16_1363	Cytochrome c oxidase subunit CcoO	1.834	0.013		
FORC16_1364	Cytochrome c oxidase subunit CcoQ	1.892	0.014		
FORC16_1365	Cytochrome c oxidase subunit CcoP	1.827	0.009		
FORC16_2053	Cytochrome c heme lyase subunit CcmH	1.987	0.001		
FORC16_2054	Cytochrome c heme lyase subunit CcmL	1.774	0.0003 0488		
FORC16_2055	Cytochrome c-type biogenesis protein CcmG/DsbE, thiol:disulfide oxidoreductase	1.74	0.001		
FORC16_2056	Cytochrome c heme lyase subunit CcmF	1.653	0.0004 0254		
FORC16_2057	Cytochrome c-type biogenesis protein CcmE, heme chaperone	1.059	0.026	1.244	0.022
FORC16_2191	Na(+)-translocating NADH-quinone reductase subunit F	2.347	0.002		
FORC16_2192	Na(+)-translocating NADH-quinone reductase subunit E	2.31	0.001		
FORC16_2193	Na(+)-translocating NADH-quinone reductase subunit D	2.193	0.002		
FORC16_2194	Na(+)-translocating NADH-quinone reductase subunit C	2.34	0.003		
FORC16_2195	Na(+)-translocating NADH-quinone reductase subunit B	2.364	0.001		
FORC16_2196	Na(+)-translocating NADH-quinone reductase subunit A	1.468	0.003		
FORC16_2869	ATP synthase epsilon chain	1.812	0.005		

FORC16_2870	ATP synthase beta chain	1.806	0.005
FORC16_2871	ATP synthase gamma chain	1.859	0.004
FORC16_2872	ATP synthase alpha chain	1.812	0.005
FORC16_2873	ATP synthase delta chain	1.67	0.009
FORC16_2874	ATP synthase B chain	1.489	0.011
FORC16_2875	ATP synthase F0 sector subunit c	1.34	0.022
FORC16_2876	ATP synthase F0 sector subunit a	1.438	0.017
FORC16_2877	ATP synthase protein I2	1.099	0.038
Ribosomal protein			
FORC16_0203	SSU ribosomal protein S10p (S20e)	2.147	1.028 E-04
FORC16_0204	LSU ribosomal protein L3p (L3e)	2.726	4.496 E-04
FORC16_0205	LSU ribosomal protein L4p (L1e)	3.315	1.305 E-04
FORC16_0206	LSU ribosomal protein L23p (L23Ae)	3.568	2.265 E-04
FORC16_0207	LSU ribosomal protein L2p (L8e)	3.749	1.901 E-04
FORC16_0208	MULTISPECIES: 30S ribosomal protein S19	3.892	2.583 E-04
FORC16_0209	LSU ribosomal protein L22p (L17e)	4.123	8.171 E-05
FORC16_0210	SSU ribosomal protein S3p (S3e)	4.222	2.250 E-05
FORC16_0211	LSU ribosomal protein L16p (L10e)	4.435	1.930 E-04
FORC16_0212	LSU ribosomal protein L29p (L35e)	4.348	2.585 E-04
FORC16_0213	SSU ribosomal protein S17p (S11e)	4.366	7.545 E-05
FORC16_0214	LSU ribosomal protein L14p (L23e)	1.063	1.850 E-04
FORC16_0215	LSU ribosomal protein L24p (L26e)	1.285	0.002

FORC16_0216	LSU ribosomal protein L5p (L11e)	1.704	6.860 E-05		
FORC16_0217	SSU ribosomal protein S14p (S29e) / SSU ribosomal protein S14p (S29e), zinc-independent	2.136	2.865 E-05		
FORC16_0218	SSU ribosomal protein S8p (S15Ae)	2.393	3.853 E-04		
FORC16_0219	LSU ribosomal protein L6p (L9e)	2.721	2.788 E-04		
FORC16_0220	LSU ribosomal protein L18p (L5e)	3.012	1.407 E-04		
FORC16_0221	SSU ribosomal protein S5p (S2e)	3.185	0.001		
FORC16_0222	LSU ribosomal protein L30p (L7e)	3.25	7.540 E-05		
FORC16_0223	LSU ribosomal protein L15p (L27Ae)	3.026	0.001		
FORC16_0225	LSU ribosomal protein L36p	2.647	6.654 E-05		
FORC16_0226	SSU ribosomal protein S13p (S18e)	1.319	0.0003		
FORC16_0227	SSU ribosomal protein S11p (S14e)	1.745	0.001		
FORC16_0228	SSU ribosomal protein S4p (S9e)	2.217	7.322 E-07		
FORC16_0230	LSU ribosomal protein L17p	3.105	0.001		
Chitine metabolism					
FORC16_2330	(GlcNAc)2 ABC transporter, permease component 1	-1.312	0.027	-1.303	0.028
FORC16_2331	(GlcNAc)2 ABC transporter, permease component 2	-1.445	0.047	-1.739	0.042
FORC16_2184	Chitinase	-1.04	0.017		
FORC16_2933	Chitinase	-4.054	0.01	-5.125	0
FORC16_3652	Chitodextrinase precursor	-1.467	0.011	-1.226	0.018
FORC16_3943	Chitinase	-1.128	0.03	-0.86	0.083
Adherence					
FORC16_2530	MSHA biogenesis protein MshH	-1.14	0.002		
FORC16_2529	MSHA biogenesis protein MshI	-1.008	0.002		

FORC16_2528	MSHA biogenesis protein MshJ	-0.937	0.005		
FORC16_2527	MSHA biogenesis protein MshK	-0.872	0.011		
FORC16_2372	type IV pilin	-1.23	0.011	-1.371	0.029
FORC16_2373	Type IV fimbrial assembly, ATPase PilB	-1.277	0.008	-1.139	0.014
FORC16_2374	Type IV fimbrial assembly protein PilC			-0.913	0.038
FORC16_3424	Chitin binding protein	0.925	0.005		
Metalloproteases					
FORC16_4281	Vibriolysin, extracellular zinc protease	-1.225	0.003		
FORC16_3415	Zinc metalloprotease			-2.007	0.013
FORC16_1262	Putative trypsin			-1.172	0.016
Quorum sensing					
FORC16_2364	Quorum-sensing regulator of virulence	-2.167	0.009	-1.239	0.003
FORC16_0940	Regulatory protein LuxO	-1.059	0.001		
FORC16_0941	Phosphorelay protein LuxU			-1.019	0.04
FORC16_4055	Autoinducer 2 sensor kinase/phosphatase LuxQ	1.153	0.021		
RTX toxin					
FORC16_3881	RTX toxins determinant A and related Ca2+-binding proteins	-0.981	0.046	-1.557	0.013
FORC16_3884	RTX toxin transporter	-0.868	0.004		

[a] Locus tags are based on the database for the *V. vulnificus* FORC_016 genome, which was retrieved from GenBank (CP011775 and CP011776, www.ncbi.nlm.nih.gov).

III-3-3. Growth of *V. vulnificus* in VFMG and VFMG containing crabs.

The combined RNA-seq. results suggested that contact and incubation with crab resulted in rapid growth of *V. vulnificus* FORC_016. In order to identify whether *V. vulnificus* could grow more rapidly in the VFMG containing crab than in VFMG, the bacterial growth in each RNA-seq. sampling conditions was observed. The growth of *V. vulnificus* was measured by counting colony forming unit (CFU)/ ml from serial dilutions plated onto LBS agar. The CFU/ml of cells incubated with crab was increased 1.5-log after 1 h incubation, while that of cells incubated in VFMG was not altered during incubation (Fig. III-8). After 4 h incubation, CFU/ml of *V. vulnificus* was increased about 0.2 log compare to 1 h incubation. These combined results were consistence with the results from RNA-seq. suggesting that *V. vulnificus* could rapidly grow using crab as nutrients, therefore contamination with *V. vulnificus* resulted in deterioration of crab and increase in possibility of foodborne illness.

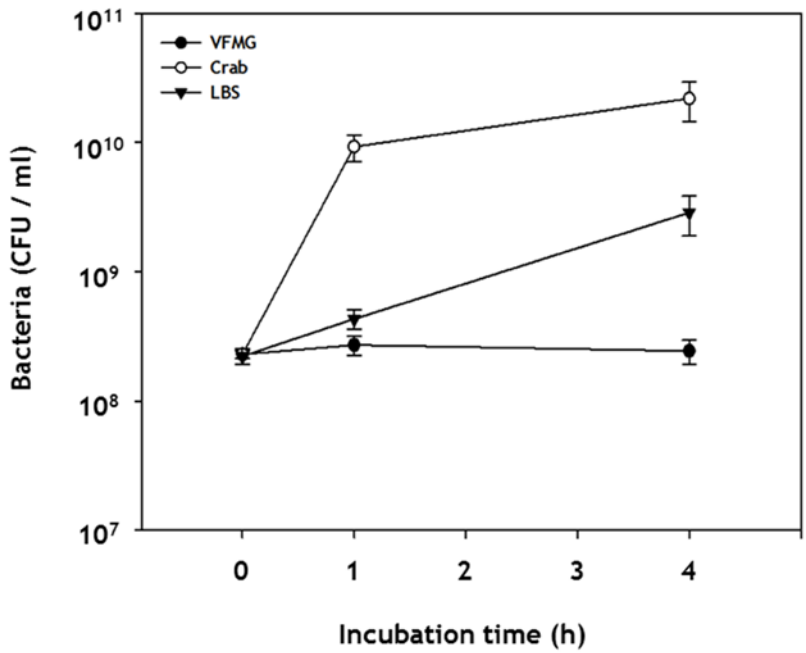

Figure III-8. Growth of *V. vulnificus* on crab. *V. vulnificus* grown to A_{600} of 0.8 was harvested and washed, and subsequently inoculated in VFMG, VFMG containing crab, or LBS. Cell growth was measured on 1 h and 4 h by CFU counting. Open circle, cells grown in VFMG; closed circle, cells grown in VFMG containing crab; closed triangle, cells grown in LBS.

Chapter IV.

Seasonal and Local Variation of Microbial Composition in Swimming Crab

IV-1. Introduction

The swimming crab, *Portunus trituberculatus,* which is widely distributed in Indic and West Pacific Oceans, is an important commercial species in Southeast and East Asia including Korea, Japan, and China. The global productions for *P. trituberculatus* have been increased from the 1970's, and recently 503,855 t of *P. trituberculatus* was captured in 2013 (FAO 2013). Especially, the catch of *P. trituberculatus* and its daily consumption rate was located on the upper ranks in South Korea in recent years, indicating that the swimming crab is one of the largely consumed seafood in South Korea (Moon, et al. 2009, Zhang, et al. 2014). The consumption of food accompanied intake of bacterial communities on food, and the microbiota on food could influence the human gut microbiome (Hehemann, et al. 2010). Furthermore, it has been reported that the bacterial foodborne illness occasionally occurred via consumption of crab over the world (Altekruse, et al. 2000, Kwon, et al. 2000, Matulkova, et al. 2013, Park, et al. 2008). Therefore, it is necessary to identify the bacterial members in swimming crabs to understand the possible effect of crab microbiota on human health and prevent the foodborne illness by intake of crab. However, there have been little information about the bacterial communities in *P. trituberculatus.*

It is important that the accurate understanding about the causative bacteria of food poisoning to prevent the foodborne illness. Most of detection methods for causative foodborne pathogens are culture-based, and it has been developed for rapid and accurate detection for decades (Feng 1997, Harwood, et al. 2004, Jokerst, et al. 2012, Taskila, et al. 2012). However, the culture-based methods are time-consuming techniques which take at least more than 3-5 days to identify the pathogens, and moreover, they only can detect the culturable bacteria (Arthur, et al. 2005, Kulkarni, et al. 2002, Wade 2002). The bacteria that can be grown in the laboratory are only a small fraction of the total diversity that exists in nature, so our understanding about microorganisms from the standard culture-based methods is so limited (Riesenfeld, et al. 2004, Stewart 2012). In South Korea, above 30% of foodborne outbreak cases was reported as having occurred by unknown bacteria in each year, so it is needed to use a method that could analyze whole bacteria including unculturable species for accurate understanding and prevention of foodborne illness (MFDS 2015). Metagenomics is a powerful genomic tool that analyze microorganisms in genomic level by direct extraction from accessible microorganisms (Handelsman 2004, Riesenfeld, et al. 2004). The 16S rRNA sequence-based analysis allows whole microbial composition analysis including unculturable bacteria, providing diverse information about microbial composition in food which would be helpful for establishment of appropriate strategy to prevent foodborne outbreaks.

In this study, I analyzed the bacterial communities in swimming crabs to understand the crab microbiome. Considering the consumption patterns of swimming crabs in South Korea, 65 swimming crabs were sampled from different seasons and locations. The composition of bacterial community in each swimming crabs was identified using pyrosequencing with targeted V1-V3 regions of 16S rRNA genes. The diversity and composition of bacterial communities in swimming crab were characterized and compared to identify the seasonal and local differences of bacterial communities in swimming crab.

IV-2. Materials and Methods

IV-2-1. Crab sample collection

To identify the effect of season and location on the microbial communities in swimming crab, the crab samples were collected from locations of maximum production of swimming crab on spring (S1 to S6) and autumn (A1 to A7) in Yellow sea (Table IV-1) (Oh 2011). Five crabs from each location were collected and immediately transported in icebox to the laboratory and stored at -80 ^{o}C until further processing.

Table IV-1. Crab samples analyzed in this study

Sample name	Sampling location	Sampling date
S1	Bieungdo	June, 2015
S2	Gunsan 1	June, 2015
S3	Gunsan 2	June, 2015
S4	Kyokpo	June, 2015
S5	Yeonpyeng island	June, 2015
S6	Daecheong island	June, 2015
A1	Bieungdo	October, 2014
A2	Gunsan 1	October, 2014
A3	Gunsan 2	October, 2014
A4	Kyokpo	October, 2014
A5	Yeonpyeng island	October, 2014
A6	Daecheong island	October, 2014
A7	Seocheon	October, 2014

IV-2-2. Metagenomic DNA extraction

To extract the metagenomic DNAs in crab, the bacteria on the crab surface were detached and collected by using SPINDLE as previously described (Kim, et al. 2012). The crab samples of which crab shells, pincers, and legs were removed were put with 225 ml of buffered peptone water in sterile sample bags and treated with SPINDLE for 2 min at 7000 g for detaching of bacteria in crab. After detachment, the buffered peptone water which containing bacterial cells was centrifuged at 4 ºC for 15 min at 9,000 rpm and the pellets were harvested. For the lysis of cells, the pellets were resuspended in 400 μl of lysis buffer (10 mM Tris-HCl (pH 8.0), 1 mM EDTA) and treated with 50 μl of lysozyme (100 mg/ml) for 1 h at 37 ºC. After lysozyme treatment, one freeze-thaw step was performed, and then the proteinase K mixture (140 μl of 0.5 M EDTA, 20 μl of Proteinase K (20 mg/ml), 40 μl of 10% SDS) was added to sample for 1 h at 37ºC. To inactivate proteinase K, 100 μl of 5 M NaCl and 80 μl of CTAB/NaCl solution (0.7 M NaCl, 0.27 M CTAB) were added to lysates and incubated for 10 min at 65 ºC. After incubation, 650 μl of phenol/chloroform/isoamylalcohol (25:24:1, pH 8.0) was added to lysates, and the samples were subsequently centrifuged at 4 ºC for 5 min at 5,000 rpm. The upper aqueous phase was transferred to a new clean 1.5 ml tube, then 10 μl of RNase A (30 mg/ml) was added and incubated for 1 h at 37 ºC to digest the RNA. The metagenomic DNA which was contained in aqueous phase was purified and

concentrated by ethanol precipitation. To remove the PCR inhibitors, the extracted DNAs were cleaned up using PowerClean ProDNA Clean-Up kit (Mo Bio Laboratories, Solana Beach, CA) according to the manufacturer's protocol. The concentration of the purified genomic DNA was determined using a NanoVue spectrophotometer (GE Healthcare).

IV-2-3. Pyrosequencing

To analyze microbiota in crab, hypervariable regions (V1-V3) of the bacterial 16S rRNA genes were amplified from the extracted DNA using barcoded fusion primers (Hur, et al. 2011). The amplification conditions were as follows: initial denaturation at 94 ^{o}C for 5 min; followed by 30 cycles of denaturation (30 s, 94 ^{o}C), primer annealing (30 s, 55 ^{o}C), and extension (30 s, 72 ^{o}C); with a final extension step of 7 min at 72 ^{o}C. The amplified V1-V3 region of 16S rRNA genes were purified using the QIAquick PCR purification kit (Qiagen, Valencia, CA) and quantified using the PicoGreen dsDNA Assay kit (Invitrogen, Carlsbad, CA). The quantified amplicons was pooled equal concentration, and was sequenced using 454 pyrosequencing Titanium FLX plus system (Roche/454 Life Sciences, Branford, CT) according to the manufacturer's protocol.

IV-2-4. Data analysis

Sequence reads obtained using a pyrosequencing were analyzed according to previous descriptions (Jeon, et al. 2013). Briefly, sequence reads from each sample were separated by unique barcodes, and low quality reads (average quality score < 25 or read length < 300 bp) were removed. The primer sequences were removed by pairwise alignment, and clustered sequences by 97% similarity to correct sequencing errors. The representative sequences in each cluster were selected for taxonomic assignment. A BLAST search for each representative sequence was conducted using the EzTaxon-e database (http://eztaxon-e.ezbiocloud.net), and the taxonomic positions of each read were determined according to the highest pairwise similarity among the top five BLAST hits. Possible chimera sequences were removed using the UCHIME program (Edgar, et al. 2011). The number of sequencing reads in each samples were normalized by random subsampling, and the community richness (Chao 1) and diversity index (Shannon index) were calculated using the Mothur program (Schloss, et al. 2009).

IV-2-5. Statistical analysis

The community richness estimators, diversity index, and proportion of each bacterial phyla, and genera in crab samples were represented as average of 5 crabs from same locations. The results were represented as mean ± standard deviation (mean ± SD).

Comparison of diversity indices was performed using analysis of variance (ANOVA). Significance of differences between samples was accepted at a P value of <0.05.

IV-3. Results

IV-3-1. The comparison of microbiota diversity in swimming crabs.

A total of 1,037.176 reads with an average length of 451.74 ± 54.17 bp were obtained from pyrosequencing of 65 crabs. The number of sequence reads of each sample were varied from 4,526 to 39,774, thus 4,000 sequences were randomly subsampled from each sample for comparison of diversity of bacterial communities. The good's coverage of normalized reads were 0.91 ± 0.06 (ranged 0.84 to 0.97), and the detailed information about the pyrosequencing were summarized in Table IV-2.

The bacterial community diversity were analyzed by calculating the diversity index (Shannon) and community richness estimator (Chao 1) (Table IV-2). The diversity indices were represented as the average of the five crabs from each locations. The diversity indices of spring crabs (S1-S6) and autumn crabs (A1-A7) were compared to determine the seasonal effect on bacterial diversity. As shown in Table 2, the average observed OTUs and estimated OTUs (Chao 1) of microbiota obtained at autumn were approximately 3-times higher than those of spring crabs, indicated that the bacterial communities in crab would be more diverse in autumn than in spring. Likewise, the Shannon diversity index of autumn crabs (ranged 5.15 to 5.78) were significantly different with those of spring crabs (ranged 3.78 to 4.43) ($P < 0.001$).

The diversity of bacterial communities depending on locations was also compared. In spring crab, the average observed numbers of OTUs were not significantly different between locations (ranged 285.60 to 429.40). Furthermore, diversity indices of bacterial communities in spring crab from different locations were also similar to each other (Table IV-2). Likewise, there were no significant differences in OTUs (ranged 735.00 to 1027.40) and diversity indices among the bacterial community in autumn crabs, although the bacterial community is more diverse in autumn than in spring.

Table IV-2. Summary of statistics of pyrosequencing obtained from crabs.

	# of reads (total)	# of reads (average)[a]	Average read length (bp)[a]	Observed OTUs[a]	Chao1[a]	Shannon[a]	Good's coverage[a]
Total	1,037,176	15956.55 ± 4545.33	451.74 ± 54.17				0.91 ± 0.06
S1	85,474	17094.80 ± 1918.49	409.52 ± 16.27	302.20 ± 56.41	542.36 ± 108.47	3.85 ± 0.54	0.97 ± 0.01
S2	68,416	13683.20 ± 2112.65	405.01 ± 8.04	293.60 ± 64.20	551.30 ± 159.65	3.79 ± 0.27	0.97 ± 0.01
S3	68,896	13779.20 ± 4218.09	407.46 ± 23.70	325.80 ± 89.90	604.44 ± 190.90	3.94 ± 0.46	0.96 ± 0.01
S4	71,386	14277.20 ± 1126.71	375.64 ± 6.57	285.60 ± 36.85	551.77 ± 103.21	3.78 ± 0.34	0.97 ± 0.01
S5	56,468	11293.60 ± 2394.45	370.16 ± 11.01	429.40 ± 94.09	853.81 ± 255.07	4.43 ± 0.35	0.95 ± 0.02
S6	84,925	16985.00 ± 1781.44	416.21 ± 20.18	300.80 ± 65.09	565.70 ± 90.84	3.92 ± 0.57	0.97 ± 0.01
A1	85,043	17008.60 ± 2370.55	492.75 ± 10.83	735.00 ± 170.89	1567.69 ± 344.46	5.15 ± 0.53	0.90 ± 0.03
A2	62,933	12586.60 ± 6978.44	486.56 ± 16.86	947.20 ± 122.96	1994.81 ± 710.18	5.78 ± 0.26	0.87 ± 0.04
A3	80,987	16197.40 ± 2822.50	498.39 ± 20.37	918.20 ± 168.84	2111.45 ± 270.00	5.58 ± 0.28	0.86 ± 0.02
A4	80,405	16081.00 ± 3469.31	493.19 ± 9.52	1027.40 ± 169.11	2422.60 ± 434.87	5.70 ± 0.45	0.84 ± 0.04
A5	89,156	17831.20 ± 2749.24	507.50 ± 7.37	924.2 ± 173.50	2257.84 ± 498.74	5.38 ± 0.49	0.87 ± 0.05
A6	99,149	19829.80 ± 4736.41	506.65 ± 15.77	839.20 ± 248.41	1865.51 ± 633.92	5.21 ± 0.69	0.85 ± 0.03
A7	103,938	20787.60 ± 11008.55	503.65 ± 14.87	956.40 ± 192.97	2362.66 ± 561.72	5.46 ± 0.45	0.86 ± 0.03

[a] The values were represented in means of 5 crabs of each locations.

IV-3-2. Composition analysis of seasonal bacterial communities in swimming crab.

The compositions of bacterial communities on crab were analyzed and compared at the phylum level (Fig. IV-1). In spring, the two phyla, *Proteobacteria* and *Firmicutes,* were dominant in bacterial community in all crabs (Fig. IV-1A). *Firmicutes* was predominant phylum in bacterial communities in sample S2 (94.6 ± 5.26%), S4 (91.79 ± 12.45%), and S5 (68.21 ± 19.7%), whereas *Proteobacteria* was predominant in S1 (65.67 ± 20.13%), S3 (63.08 ± 19.73%), and S6 (64.55 ± 15.54%). In contrast to spring crabs, the bacterial communities in autumn crabs (A1 to A7) were more diverse (Fig. IV-1B). In all autumn crab samples, *Proteobacteria* was predominant phylum (57.22 to 80.22 %). *Bacteroidetes* was second most dominant phylum in most of autumn crabs except A5 (7.5 to 17.73%). The third dominant phylum was more variable among the samples A1 to A7; *Firmicutes* in A1 (5.22 ± 4.79%), A2 (13.43 ± 13.90%), A4 (7.33 ± 7.77%), and A7 (8.82 ± 6.84%), and *Actinobacteria* in A3 (10.52 ± 6.05%) and A6 (4.39 ± 3.81%), and *Bacteroidetes* in A5 (10.02 ± 8.73%). *Tenericutes* was second abundant phylum in A5 (16.56 ± 19.94%), but its proportion in other samples was comparatively low (1.35 ± 0.71% in A3, 1.95 ± 2.66% in A4, 1.03 ± 1.08 in A6, and < 1% in A1, A2 and A7). The candidate division of TM7 (1.69 ± 1.05% in A3 and <1% in the others), and *Planctomycetes* (2.98 ± 2.7% in A2, 1.04 ± 0.72% in A3, 1.44 ± 1.91% in A6 and

<1% in the others) were detected in autumn crabs. Interestingly, the proportion of each bacterial phylum were various among the five crabs from same location, indicating that there was individual variation in composition of bacterial community in autumn crabs.

For further identification of bacterial communities in crab, the bacterial composition were analyzed at genus level (Fig. IV-2). In spring, *Psychrobacter* was most abundant genus in half of the crab samples (61.80 ± 20.23% in S1, 56.94 ± 22.39% in S3 and 58.96 ± 18.37% in S6) (Fig. IV-2A**)**. *Carnobacterium* was the second dominant genus in S1 (12.96 ± 10.13%), S2 (37.69 ± 16.81%), S3 (15.21 ± 7.74 %), and S6 (14.56 ± 8.16%). The predominant genus of bacterial communities in S2, S4, and S5 were different. *Vagococcus* (42.86 ± 17.77%) was predominant in S2, while *Lactococcus* (34.46 ± 24.89%) and *Shewanella* (10.67 ± 6.50%) were dominant genera in S5. Interestingly, *Streptococcus* (40.11 ± 26.54%), which were known to relate with foodborne poisoning (Katzenell, et al. 2001), was predominant genus in S4 followed by *Lactococcus* (29.89 ± 27.29 %).

The composition of bacterial communities in autumn crabs were quietly different from those of spring crabs at genus level (Fig. IV-2B). At first, the proportion of unculturable bacteria were higher in autumn (20.17 to 40.61%) than in spring (0.15

to 8.47%). *Psychrobacter*, the predominant genus in spring crabs, was also one of the dominant genera in bacterial community of most of autumn crab samples, but the proportions of this genus were relatively low in autumn crabs (8.11% in average) compared to spring crabs (31.17% in average). *Roseovarius* was identified as predominant bacterial genus in A4 (15.22 ± 7.54%), A5 (18.09 ± 12.29%), A6 (24.67 ± 11.81%), and A7 (17.74 ± 10.19%), whereas *Psychrobacter* and *Arcobacter* were predominant in A1 (35.71 ± 25.48%) and A3 (18.59 ± 15.86%), respectively. In A2, the uncultured family *Clostridiales* AB118592_g, a member of *Firmicutes*, was predominant (9.14 ± 12.04%) followed by *Formosa* (9.12 ± 6.96%) and *Roseovarius* (5.22 ± 2.39%).

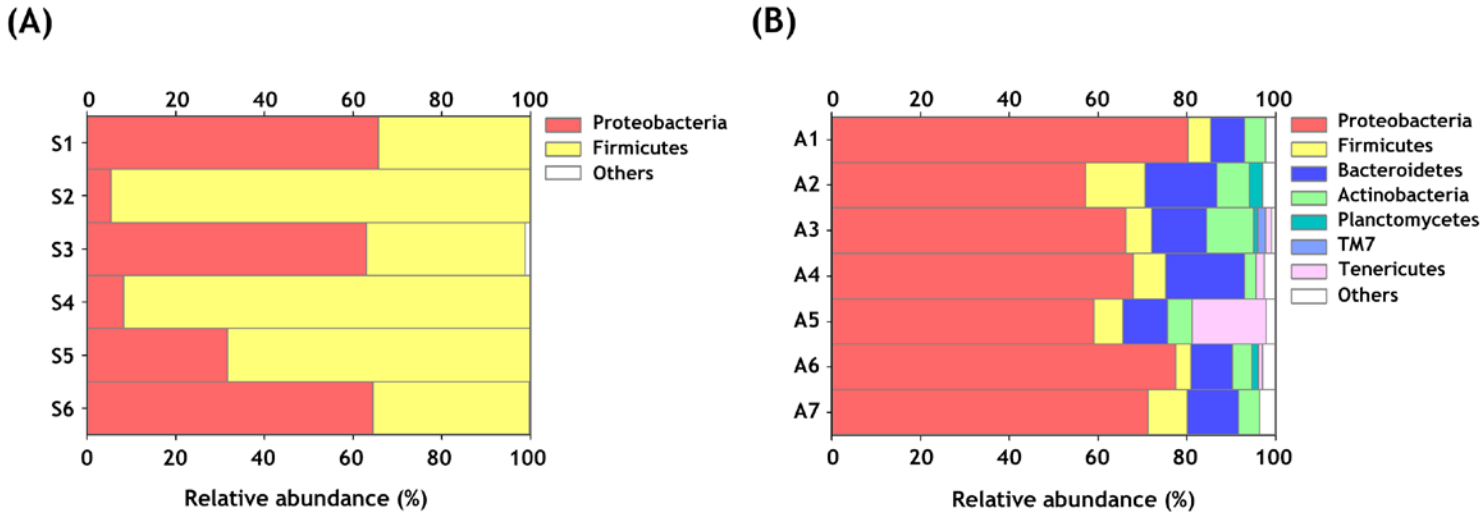

Figure IV-1. Relative abundance of bacterial phyla in crabs. The average composition of bacterial communities in spring (A) and autumn (B) crabs were represented as relative abundance in phylum level. The phyla whose abundance was less than 1% were exhibited as “Others”.

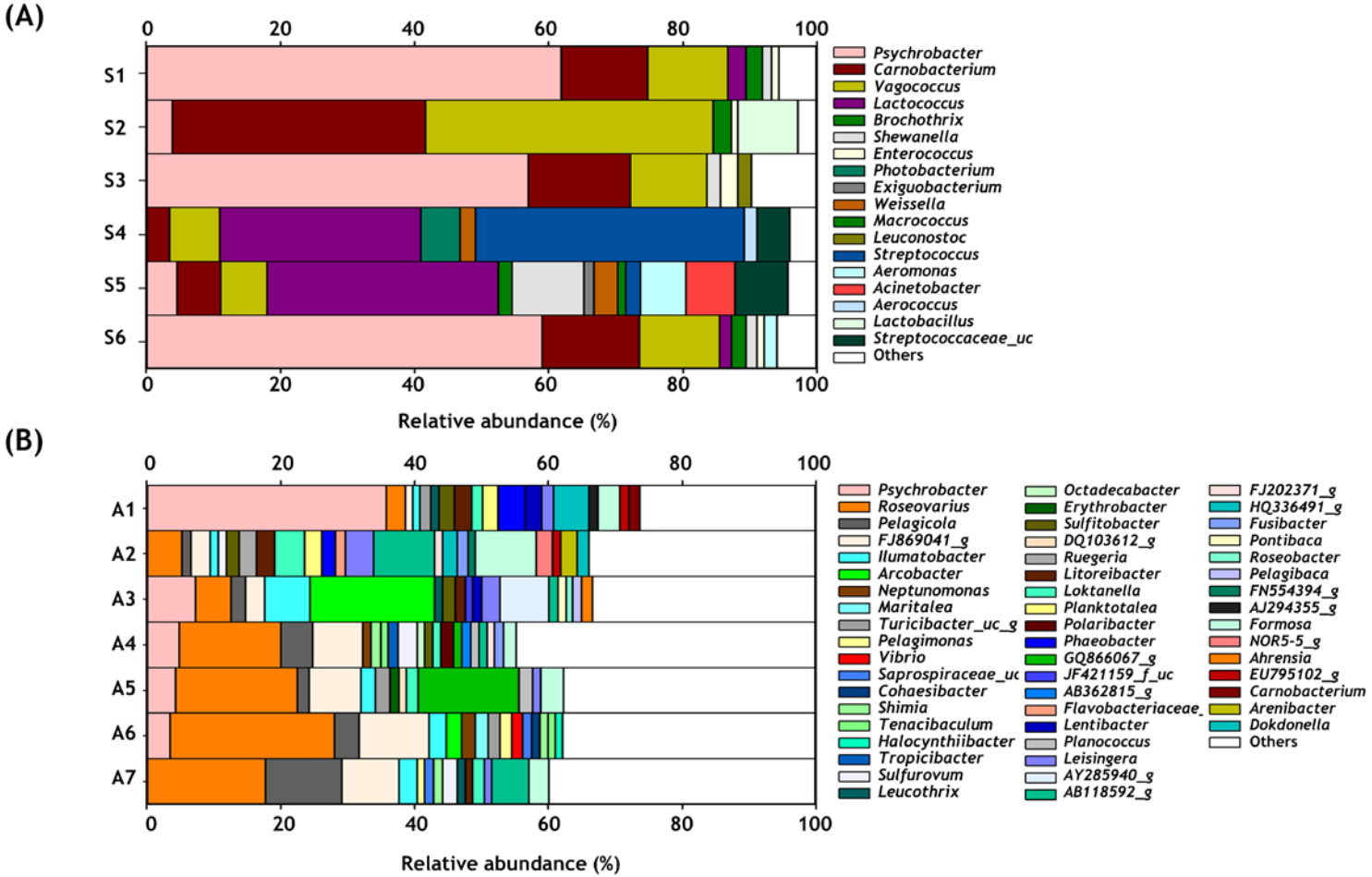
(A)
0
20
40
60
80
100
S1
S2
S3
S4
S5
S6
Psychrobacter
Carnobacterium
Vagococcus
Lactococcus
Brochothrix
Shewanella
Enterococcus
Photobacterium
Exiguobacterium
Weissella
Macrococcus
Leuconostoc
Streptococcus
Aeromonas
Acinetobacter
Aerococcus
Lactobacillus
Streptococcaceae_uc
Others
Relative abundance (%)
(B)
A1
A2
A3
A4
A5
A6
A7
Psychrobacter
Roseovarius
Pelagicola
FJ869041_g
Ilumatobacter
Arcobacter
Neptunomonas
Maritalea
Turicibacter_uc_g
Pelagimonas
Vibrio
Saprospiraceae_uc
Cohaesibacter
Shimia
Tenacibaculum
Halocynthiibacter
Tropicibacter
Sulfurovum
Leucothrix
Octadecabacter
Erythrobacter
Sulfitobacter
DQ103612_g
Ruegeria
Litoreibacter
Loktanella
Planktotalea
Polaribacter
Phaeobacter
GQ866067_g
JF421159_f_uc
AB362815_g
Flavobacteriaceae_
Lentibacter
Planococcus
Leisingera
AY285940_g
AB118592_g
FJ202371_g
HQ336491_g
Fusibacter
Pontibaca
Roseobacter
Pelagibaca
FN554394_g
AJ294355_g
Formosa
NOR5-5_g
Ahrensia
EU795102_g
Carnobacterium
Arenibacter
Dokdonella
Others
Relative abundance (%)

Figure IV-2. Relative abundance of bacterial genera in crab. The average composition of bacterial communities in spring (A) and autumn (B) crabs were represented as relative abundance in genus level. The genera whose abundance was less than 1% were exhibited as “Others”.

To identify the relationship of the bacterial communities in each crab samples, the differences among the bacterial communities in 65 crabs were determined using a Principal Coordinated Analysis (PCoA) (Fig. 3). The PCoA were performed based on the UniFrac distance matrix, and the first (PC1) and second (PC2) component of the PCoA explained 50.84% and 18.79% of the total variation, respectively. The bacterial communities of spring crabs (S1-S6) and autumn crabs (A1-A7) were clearly separated on PCoA plot, indicating that the bacterial community compositions in crabs were similar depending on season. However, the spring crabs were subdivided into two groups, *Firmicutes*-dominated group 1 (S2, 24, and S5) and *Proteobacteria*-dominated group 2 (S1, S3, and S6) on PCoA plot, revealing that there are differences among the crabs from different locations.

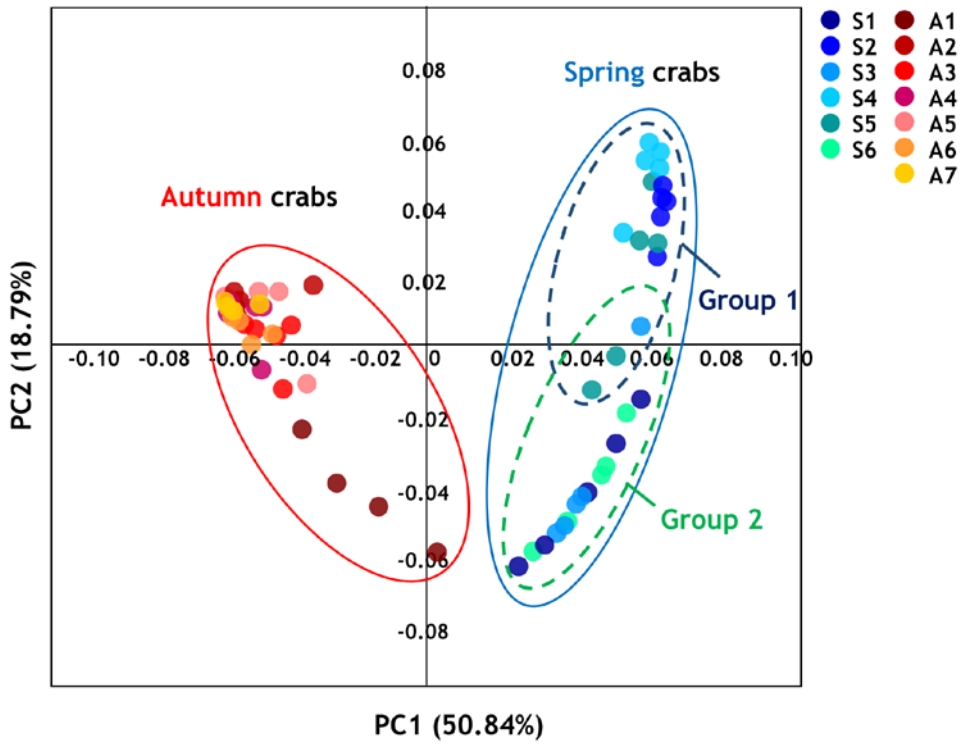

Figure IV-3. Principal coordinate analysis (PCoA) of swimming crabs. Dissimilarities among the bacterial communities in crab samples were compared on a PCoA plot. The distance matrix was calculated using the Fast UniFrac.

IV-3-3. *Vibrio* in swimming crab.

For identification of abundance of the genus *Vibrio* in swimming crabs, the proportion of *Vibrio* species in swimming crabs was analyzed (Fig. IV-4). The analysis revealed that the average proportion of *Vibrio* was higher in autumn (0.43 ± 0.57%) than in spring (0.20 ± 0.17%), although the *Vibrio* was less abundant in most crab samples except A6 (< 1%). In spring, the proportion of *Vibrio* was highest in S5 (0.47 ± 0.49%) and lowest in S3 (< 0.01%). A6 had relatively high proportion of *Vibrio* (1.64 ± 2.74%) among the autumn crab samples, whereas A2 had lowest proportion of *Vibrio* (0.01 ± 0.01%). To identify the presence of pathogenic *Vibrio* species such as *V. vulnificus, V. cholerae*, and *V. parahaemolyticus,* the proportion of pathogenic *Vibrio* was further analyzed at species level, revealing that only *V. vulnificus* was detected in S5 and A4 but their proportion was significantly low (< 0.01%).

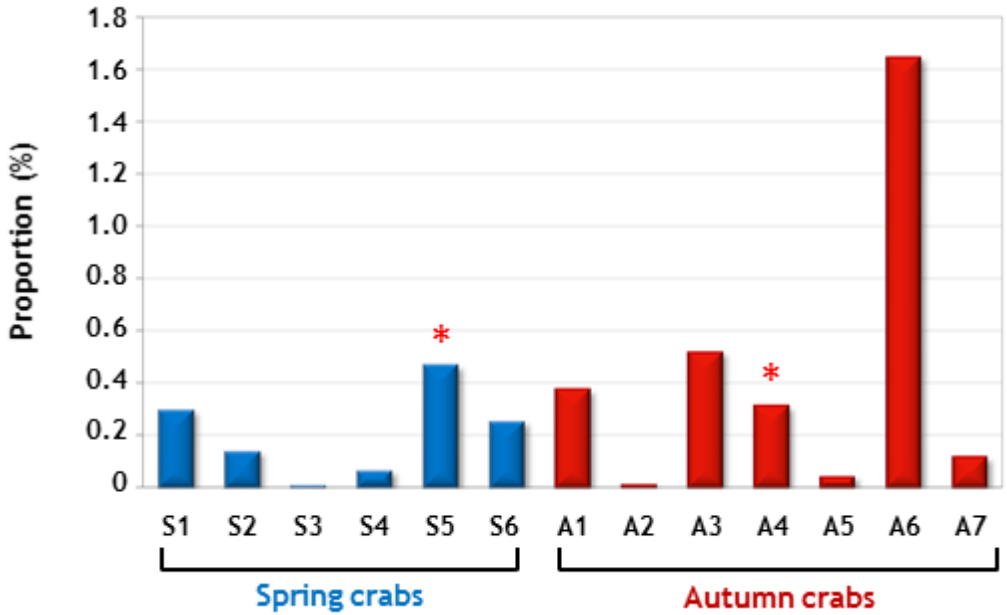

Figure IV-4. Proportion of Vibrio in swimming crab. The average proportion of genus *Vibrio* in each sample was analyzed and represented as bar graph. Crab samples collected in spring and autumn were represented as blue and red bar, respectively. Crab samples containing pathogenic *Vibrio* species were represented by asterisk.

IV-4. Discussion

IV-4-1. Seasonal and local effect on bacterial community in swimming crab.

The diversity indices of microbiota in crab were significantly different between the spring and autumn crabs, whereas those of crabs from different locations were similar in the same sampling time (Table IV-2). The Shannon diversity index, of microbiota in crab was higher in autumn (5.47 ± 0.48) than those in spring (3.95 ± 0.45). This result suggested that bacterial community in crab was more diverse in autumn than in spring, and the diversity of bacterial community in crab was considerably influenced by season. The compositions of bacterial community in crab were different between spring and autumn (Fig. IV-1). *Proteobacteria* and *Firmicutes* were predominant phyla in spring, whereas there are 7 dominant phyla including *Proteobacteria*, *Firmicutes*, *Bacteriodetes*, *Actinobacteria*, *Planctomycetes*, TM7, and *Tenericutes* (> 1% abundance) in autumn. These differences between sampling times were also investigated in PCoA plot (Fig. IV-3). The results indicated that the microbiota in crab was strongly influenced by sampling time rather than the location, and the key factors effecting on bacterial community in crab might be the seasonal variation of ocean, including temperature, salinity, or other factors.

It had been reported that the temperature and salinity of Yellow Sea was influenced by seasonal variations in circulation of currents such as Kuroshio Current, Taiwan Warm Current, and Tsushima Warm Current, *etc* (Ichikawa, et al. 2002, Teague, et al. 2003). The observation of temperature and salinity of Yellow Sea revealed that the temperature of Yellow Sea was highest in August (24.80 to 25.10 ^{o}C) and lowest in February (3.00 to 4.10 ^{o}C), while the salinity was not significantly altered during a year (29.30 to 31.49 ‰) (KOOFS 2015). Therefore, the seasonal change in temperature in Yellow Sea would be a key factor that influenced diversity and composition of bacterial community in crab. The high diversity of autumn crabs also could be explained by the seasonal temperature change in Yellow Sea, because the microflora in crabs might become more diverse during summer in which temperature is relatively high. The seasonal variation of currents circulation also influenced the nutrient conditions in Yellow Sea, which was one of the major factor determining the size and composition of phytoplankton communities (Agawin, et al. 2000, Chen 2009, Fu, et al. 2009, Shen 2001, Wang, et al. 2003, Zhou, et al. 2008). Previous studies reported that the size and composition of phytoplankton could affect the composition of the marine bacterial community, because the phytoplankton is a major source of carbon flux in ocean (Liu, et al. 2013, Taylor, et al. 2014). Thus, the seasonal variation of nutrient flux and phytoplankton communities might be one

reason for different composition between bacterial communities in spring and autumn crabs.

IV-4-2. Seasonal variation in bacterial community composition in swimming crab.

From the taxonomic composition analysis, it was revealed that *Proteobacteria* was dominant bacterial phylum in the most crabs regardless of season (5.38 to 65.67% and 57.22 to 80.22% in spring and autumn, respectively) (Figs. IV-1). However, the other dominant phyla were different between spring and autumn crabs. The bacterial community in crabs was dominated by *Firmicutes* (34.26 to 91.79%) in spring, but its proportion was decreased in autumn (3.38 to 13.43%). Instead, *Bacteroidetes* (7.5 to 17.73%) and *Actinobacteria* (2.61 to 10.52%) were identified as the second and third dominant phylum in autumn crabs. These results were consistent with previous studies which reported that *Proteobacteria* was most abundant phylum in gut and surface of various crabs (Givens, et al. 2013, Goffredi, et al. 2008, Li, et al. 2007, Li, et al. 2012, Watsuji, et al. 2009, Zhang, et al. 2016). Along with *Proteobacteria*, *Bacteroidetes* and *Firmicutes* were revealed as the dominant phyla in gut microbiome of crab, which contribute to digestion and nutrient availability by providing bacterial enzymes (Givens, et al. 2013, Harris 1993, Li, et al. 2007, Li, et al. 2012). *Actinobacteria*, which was known to widely occur in soil and oceans, was

commonly identified in gills of crab because gills were constantly contact with bacteria present in ocean (Manivasagan, et al. 2013, Zhang, et al. 2016). The analysis on seasonal variation in bacterial community of Yellow Sea revealed that the *Actinobacteria* was one of the most abundant phyla in Yellow Sea water, but its abundance significantly decreased in spring (Park, et al. 2014). This result was consistent with results of this study, which was lower abundance of *Actinobacteria* in spring crabs (< 1%) compare to in autumn crabs (2.61 to 10.52%).

The compositions of genera in crabs were also different between spring and autumn (Fig. IV-2). Most of the relative abundant genera (>1%) of microbiota in spring crabs were belonging to phylum *Firmicutes*, but those of autumn crabs were belonging to the phylum *Proteobacteria.* Although the composition of bacterial communities was different between spring and autumn crabs at genus level, *Psychrobacter* was revealed as dominant genus in both of spring (S1, S2, S3, S4 and S6) and autumn (A1, A3, A4, A5, and A6) crabs. The genus *Psychrobacter*, within *Proteobacteria*, has been reported that it could grow at relatively low temperature, and have cold-adapted proteome to survive under zero temperature (Ayala-del-Río, et al. 2010, Feller, et al. 1997). Because the circulation of currents was varied depending on season, the monthly mean temperature of Yellow Sea was significantly altered, ranged from 3.00 ^{o}C (Febraury) to 25.10 ^{o}C (August) (KOOFS 2015). Therefore, it

was reasonable that the genus *Psychrobacter* was dominant in swimming crabs regardless of season, because the ability of adapt to low temperature would be beneficial for survival.

In spring, *Carnobacteirum* and *Vagococcus* were dominated in all crabs along with *Psychrobacter* (3.51 to 37.69% for *Carnobacteirum*, 6.40 to 42.86% for *Vagococcus*) (Fig. IV-2A). The genera *Carnobacterium* and *Vagococcus* have been known as probiotics of marine fishes which contribute to cellular immune response by inhibiting growth of pathogens, so their roles in crab microbiome might be protection of swimming crab from the bacterial crab disease (Leisner, et al. 2007, Román, et al. 2012, Sorroza, et al. 2012). Consistent with this, *Vagococcus fluvialis*, a well-known immunostimulants of aquatic organisms, was predominated among the genera *Vagococcus* in all crabs (3.98 to 7.24%) except the crabs from S2 (2.67 ± 2.26%) (Table IV-3). Instead, *Vagococcus salmoninarum* was revealed as the most abundant species belonging to *Vagococcus* in S2 (17.72 ± 7.36%). Some Gram-positive cocci species such as *Streptococcus parauberis*, *Lactococcus garvieae, Lactococcus piscium*, and *V. salmoninarum* have been recognized as fish pathogens causing septicemic fish disease streptococcosis, which are related with significant loss of fish production (Hasson, et al. 2009, Ruiz-Zarzuela, et al. 2005, Vendrell, et al. 2006, Wang, et al. 2007)**.** Infection with these bacteria lead to spoilage and deterioration of

food quality during storage, and furthermore, could cause foodborne illness (Aguado-Urda, et al. 2011, Fernández-No, et al. 2012, Wang, et al. 2007). *Streptococcus* and *Lactococcus* were predominated in S4 (40.11 ± 26.54%) and S5 (34.46 ± 24.89%), respectively, and the further species analysis on these genera revealed that the pathogenic *S. parauberis* (39.49 ± 26.33% in S4) and *L. garvieae* (33.55 ± 24.84% in S5) were predominant in S4 and S5 (Table IV-3). It is noticeable that the proportion of *Psychrobacter* was significantly low in the pathogenic cocci-dominated crabs (S2, S4, and S5, < 1 to 4.61%) compared to others (S1, S3, and S6, 56.94 to 61.8%). These data suggested that the high proportion of pathogenic bacteria would affect the microbiome in crabs by causing the competition for survival, then could result in the altered composition of bacterial communities. The crab microflora of crabs with high proportion of pathogenic bacteria (S2, S4, and S5) was also distinguished from others on PCoA plots, indicating that there are differences between them (Fig. IV-3).

In the case of autumn crabs, *Roseovarius* was predominant in A4 (15.22 ± 7.54%), in A5 (18.09 ± 12.29%), in A6 (24.67 ± 11.81%) and in A7 (17.74 ± 10.19%) (Fig. IV-2B). The genus *Roseovarius* is a member of *Roseobacter* clade which were important in the heterotrophic bacterial community due to their ability for utilization of low molecular weight organic compounds such as dimethysulfoniopropionate

(DMSP) (Buchan, et al. 2005, Fuse, et al. 2003, González, et al. 2000, Kirkwood, et al. 2010). Previous reports revealed that the some cases of phytoplankton bloom in ocean positively associated with rapid growth of *Roseobacter* clade because of their DMSP-utilizing ability (Buchan, et al. 2005, Pinhassi, et al. 2005, Tan, et al. 2015). It was also reported that the order Rhodobacterales, which contains *Roseovarius*, increased during harmful phytoplankton bloom which was caused by *Cochlodinium polykrikoides* in South Korean costal ocean (Park, et al. 2015). The harmful phytoplankton bloom occur annually from July to October in which the temperature of ocean was relatively high, therefore, the abundance of *Roseovarius* in autumn crabs might be caused by these seasonal phytoplankton bloom (NIFS 2013). In addition to *Roseovarius*, 163 genera belonging to Rhodobacterales were identified in autumn crabs, and their high proportion in crab microflora (30.85 to 59.24% in A1-A7) suggested that the diverse and different composition of bacterial communities in autumn crabs also would be associated with the bloom events.

The analysis for *Vibrio* species revealed that the genus *Vibrio* existed in swimming crabs regardless of season (Fig. IV-4). The *Vibrio* species have known to be commonly identified in gut of aquatic invertebrates, and their role in gut microbiome have been supposed to contribute to osmoregulation (Harris 1993). However, the proportion of *Vibrio* was significantly low in most of the crab samples (< 0.01 to

1.64 %). The genus composition analysis revealed that various genera presented and dominated in crab microbiome depending on the seasonal variation in ocean temperature, therefore the low proportion of *Vibrio* in swimming crab might be due to the competition among the bacteria in swimming crab. However, although the genus *Vibrio* was not dominant genus in crab microflora, the pathogenic *V. vulnificus* was detected in S5 and A4, suggesting that consumption of swimming crab could cause foodborne illness.

Table IV-3. Composition of predominant genera in spring crabs (%) [a]

	S1	S2	S3	S4	S5	S6
Vagococcus						
fluvialis	4.13 ± 4.57	2.67 ± 2.26	6.96 ± 7.65	6.17 ± 5.36	3.98 ± 1.28	7.24 ± 6.05
salmoninarum	2.59 ± 2.84	17.72 ± 7.36	2.54 ± 1.79	0.17 ± 0.29	0.7 ± 0.35	1.84 ± 1.24
fessus	2.64 ± 2.64	16.49 ± 10.08	0.97 ± 0.61	0.37 ± 0.29	0.71 ± 0.55	1.23 ± 0.85
carniphilus	0.31 ± 0.37	0.08 ± 0.1	0.24 ± 0.19	0.19 ± 0.2	0.35 ± 0.1	0.88 ± 1.22
penaei	0.19 ± 0.13	0.3 ± 0.2	0.34 ± 0.36	0.1 ± 0.08	0.62 ± 0.61	0.31 ± 0.3
lutrae	0.01 ± 0.01	0.01 ± 0.02	0.01 ± 0.01	0.02 ± 0.05	0.01 ± 0.01	0.02 ± 0.01
acidifermentans	0.02 ± 0.04	0.01 ± 0.02	0.02 ± 0.01	0.01 ± 0.01	0.01 ± 0.01	0.02 ± 0.02
entomophilus	0.01 ± 0.02	0 ± 0.01	0.01 ± 0.02			
unculturable	0.16 ± 0.22	5.4 ± 3.38	0.08 ± 0.07	0.36 ± 0.35	0.45 ± 0.14	0.23 ± 0.4
Carnobacterium						
jeotgali	8.89 ± 5.24	25.1 ± 15.24	7.19 ± 6.2	2.82 ± 4.32	4.87 ± 2.11	9.99 ± 5.98
iners	1.64 ± 2.21	5.87 ± 3.68	2.76 ± 0.62	0.1 ± 0.12	0.52 ± 0.42	2 ± 1.18
maltaromaticum	1.11 ± 2.03	2.04 ± 0.9	3.27 ± 4.66	0.24 ± 0.15	0.5 ± 0.38	0.87 ± 0.6
alterfunditum group	0.66 ± 0.87	0.92 ± 0.47	0.58 ± 0.43	0.07 ± 0.08	0.19 ± 0.12	0.45 ± 0.24
mobile	0.33 ± 0.38	0.52 ± 0.32	0.82 ± 1.51	0.07 ± 0.07	0.1 ± 0.05	0.22 ± 0.14
inhibens	0.13 ± 0.23	0.01 ± 0.01	0.37 ± 0.68	0.04 ± 0.09	0.01 ± 0.01	0.83 ± 1.1
funditum	0.03 ± 0.03	0.11 ± 0.07	0.04 ± 0.02	0.01 ± 0.02	0.03 ± 0.02	0.02 ± 0.01
viridans	0.04 ± 0.04	0.01 ± 0.01	0.03 ± 0.02			0.05 ± 0.05

gallinarum	0.01 ± 0.02	0 ± 0.01	0.01 ± 0.01	0.05 ± 0.1	0.01 ± 0.01	0 ± 0.01
divergens	0.01 ± 0.01					0.05 ± 0.1
unculturable	0.07 ± 0.07	2.88 ± 1.47	0.04 ± 0.04	0.09 ± 0.04	0.18 ± 0.09	0.04 ± 0.01
Lacococcus						
garvieae	1.95 ± 2.62	0.02 ± 0.03	0.12 ± 0.26	27.81 ± 25.34	33.55 ± 24.84	1.3 ± 1.82
lactis subsp. cremoris group	0.73 ± 0.94	0.05 ± 0.11	0.31 ± 0.56	0 ± 0.01	0.23 ± 0.19	0.23 ± 0.19
piscium	0.03 ± 0.03	0.03 ± 0.02	0.32 ± 0.42	0 ± 0.01	0.01 ± 0.01	0.07 ± 0.09
raffinolactis	0.03 ± 0.05		0.05 ± 0.06		0.04 ± 0.04	0.14 ± 0.22
formosensis	0.01 ± 0.01			0.04 ± 0.03	0.03 ± 0.03	0 ± 0.01
chungangensis	0.02 ± 0.03				0.01 ± 0.01	0.02 ± 0.03
taiwanensis	0.02 ± 0.03		0 ± 0.01			0.01 ± 0.01
plantarum			0.02 ± 0.03			
lactis group	0 ± 0.01		0 ± 0.01			
unculturable	0.01 ± 0.01			2.03 ± 1.93	0.58 ± 0.26	
Streptococcus						
parauberis	0.26 ± 0.21	0.05 ± 0.03	0.8 ± 1.08	39.49 ± 26.33	2.15 ± 0.8	0.09 ± 0.06
iniae				0.01 ± 0.01		
unculturable	0 ± 0.01			0.6 ± 0.5	0.06 ± 0.04	

[a] The values were represented in means of 5 crabs of each location (mean ± SD).

Chapter V.

Conclusion

V. vulnificus and *V. parahaemolyticus* are well-known foodborne pathogen causing gastroenteritis and primary septicemia via consumption of contaminated seafoods, respectively. However, overall virulence factors and pathogenesis are not clearly understood even in recent genomic era. To extend our knowledge about its genomic characteristics as well as virulence factors of *V. vulnificus* and *V. parahaemolyticus* in South Korea, the genomes of *V. vulnificus* FORC_016 which isolated from blood of food-poisoning patient and *V. parahaemolyticus* FORC_008 which isolated from a flounder fish were completely sequenced and analyzed. The genomic analysis revealed that the *V. vulnificus* FORC_016 have RTX toxins, cytolysin, and metalloprotease that have been considered to major virulence factors of *V. vulnificus*. *V. parahaemolyticus* FORC_008 did not have the gene encoding TDH and TRH, but contained genes encoding other virulence factors such as putative hemolysins and secretion systems. Phylogenetic tree analysis using 16S rRNA sequences and further ANI analysis revealed that the strain FORC_016 and strain FORC_008 are the most closely related to the clinical isolate strains, suggesting that these strains may be potential pathogens. Furthermore, comparative analysis revealed that *V. vulnificus* FORC_016 and *V. parahaemolyticus* FORC_008 contains several unique virulence factors contributing to the survival in the host.

To identify the transcriptomic profile alteration and differentially expressed virulence genes under exposure to foods, the transcriptome profiles under exposure to crab were identified in *Vibrio vulnificus* by RNA-seqs. The transcriptome analysis indicated that genes involved in oligopeptide uptake, glucose utilization, cell growth, and energy production were up-regulated suggesting that *V. vulnificus* can utilize and metabolize the nutrient from the crab. Most of virulence factors were down-regulated during crab incubation, suggesting that the swimming crab is a good reservoir of *V. vulnificus* and crab-mediated *V. vulnificus* outbreak could be occurred when consumed the *V. vulnificus* FORC_016 contaminated crab.

In this study, I analyzed the composition of bacterial communities in swimming crab, *P. trituberculatus,* from different seasons and locations using pyrosequencing to identify the seasonal and local effect on crab microbiome. The pyrosequencing results indicated that the bacterial community in swimming crab were more diverse in autumn than in spring, and their composition was strongly influenced by season. The composition of bacterial communities in swimming crab were significantly different between in spring and in autumn, but the phylum *Proteobacteria* which was dominated by genus *Psycrobacter* was dominant in crab regardless of seasons. The composition analysis was also revealed that along with *Psycrobacter*, the genera *Carnobacterium* and *Vagococcus* was abundant in spring whereas *Roseovarius* was

most dominant genus in autumn, and the infection with pathogenic bacteria could affect the composition of crab microbiome. Additional *Vibrio species* analysis indicated that intake of crab have possibilities to cause foodborne illness. This report provides extended understanding on the variation of bacterial communities in swimming crab, therefore it would be helpful for handling of swimming crabs and prevention of foodborne illness via consumption of swimming crab.

In conclusion, the genomic and transcriptomic analysis of *V. vulinifcus* FORC_016 provides genomic insights into the genomic properties as well as virulence factors of *V. vulnificus*, and give a basis of regulation strategy by providing information about the genes differentially expressed exposure to crab. Also, the metagenomics on crab microbiome provides the insights into the seasonal and local microbial dynamics on crab. This useful for further understanding of its pathogenesis and even for prevention of foodborne outbreaks via contaminated foods, especially crab, by *V. vulnificus* in South Korea.

References

Agawin NS, Duarte CM, Agusti S. 2000. Nutrient and temperature control of the contribution of picoplankton to phytoplankton biomass and production. Limnology and Oceanography **45**: 591-600.

Aguado-Urda M, López-Campos GH, Blanco MM *et al.* 2011. Genome sequence of *Lactococcus garvieae* 21881, isolated in a case of human septicemia. Journal of Bacteriology **193**: 4033-4034.

Altekruse S, Bishop R, Baldy L *et al.* 2000. *Vibrio* gastroenteritis in the US Gulf of Mexico region: the role of raw oysters. Epidemiology and Infection **124**: 489-495.

Altermann E, Klaenhammer TR. 2003. GAMOLA: a new local solution for sequence annotation and analyzing draft and finished prokaryotic genomes. Omics A Journal of Integrative Biology **7**: 161-169.

Arthur TM, Bosilevac JM, Nou X *et al.* 2005. Evaluation of culture-and PCR-based detection methods for *Escherichia coli* O157: H7 in inoculated ground beef. Journal of Food Protection® **68**: 1566-1574.

Ayala-del-Río HL, Chain PS, Grzymski JJ *et al.* 2010. The genome sequence of *Psychrobacter arcticus* 273-4, a psychroactive Siberian permafrost bacterium, reveals mechanisms for adaptation to low-temperature growth. Applied and Environmental Microbiology **76**: 2304-2312.

Aziz RK, Bartels D, Best AA *et al.* 2008. The RAST Server: rapid annotations using subsystems technology. BMC Genomics **9**: 75.

Besemer J, Lomsadze A, Borodovsky M. 2001. GeneMarkS: a self-training method for prediction of gene starts in microbial genomes. Implications for finding sequence motifs in regulatory regions. Nucleic Acids Research **29**:

2607-2618.

Beuchat LR. 1973. Interacting effects of pH, temperature, and salt concentration on growth and survival of *Vibrio parahaemolyticus*. Applied Microbiology **25**: 844-846.

Brenner DJ, Krieg NR, Staley JT *et al.* *The Proteobacteria: Part A Introductory Essays*: Springer, 2005.

Buchan A, González JM, Moran MA. 2005. Overview of the marine Roseobacter lineage. Applied and Environmental Microbiology **71**: 5665-5677.

Cabanillas-Beltrán H, LLausás-Magaña E, Romero R *et al.* 2006. Outbreak of gastroenteritis caused by the pandemic *Vibrio parahaemolyticus* O3: K6 in Mexico. FEMS microbiology letters **265**: 76-80.

Chang AK, Kim HY, Park JE *et al.* 2005. *Vibrio vulnificus* secretes a broad-specificity metalloprotease capable of interfering with blood homeostasis through prothrombin activation and fibrinolysis. Journal of Bacteriology **187**: 6909-6916.

Chang D-E, Smalley DJ, Tucker DL *et al.* 2004. Carbon nutrition of *Escherichia coli* in the mouse intestine. Proceedings of the National Academy of Sciences of the United States of America **101**: 7427-7432.

Chatzidaki-Livanis M, Jones MK, Wright AC. 2006. Genetic variation in the *Vibrio vulnificus* group 1 capsular polysaccharide operon. Journal of Bacteriology **188**: 1987-1998.

Chen C-TA. 2009. Chemical and physical fronts in the Bohai, Yellow and East China seas. Journal of Marine Systems **78**: 394-410.

Chen C-Y, Wu K-M, Chang Y-C *et al.* 2003. Comparative genome analysis of *Vibrio vulnificus*, a marine pathogen. Genome Research **13**: 2577-2587.

Chen L, Xiong Z, Sun L *et al.* 2011. VFDB 2012 update: toward the genetic diversity and molecular evolution of bacterial virulence factors. Nucleic Acids Research: gkr989.

Croucher NJ, Thomson NR. 2010. Studying bacterial transcriptomes using RNA-seq. Current Opinion in Microbiology **13**: 619-624.

Daniels NA, MacKinnon L, Bishop R *et al.* 2000. *Vibrio parahaemolyticus* infections in the United States, 1973–1998. Journal of Infectious Diseases **181**: 1661-1666.

Dikow RB, Smith WL. 2013. Genome-level homology and phylogeny of Vibrionaceae (Gammaproteobacteria: Vibrionales) with three new complete genome sequences. BMC Microbiology **13**: 1.

Dryselius R, Kurokawa K, Iida T. 2007. Vibrionaceae, a versatile bacterial family with evolutionarily conserved variability. Research in Microbiology **158**: 479-486.

Edgar RC, Haas BJ, Clemente JC *et al.* 2011. UCHIME improves sensitivity and speed of chimera detection. Bioinformatics **27**: 2194-2200.

Egan ES, Waldor MK. 2003. Distinct replication requirements for the two *Vibrio cholerae* chromosomes. Cell **114**: 521-530.

FAO. 2013. Food and Agriculture Organization of the United Nations. URL http://www.fao.org/fishery/species/2630/en (accessed 3.3.16).

Farmer III J. The family Vibrionaceae *The prokaryotes*: Springer, 2006, 495-507.

Farmer Iii J, Hickman-Brenner F. The genera *Vibrio* and *Photobacterium*. *The prokaryotes*: Springer, 2006, 508-563.

Feller G, Zekhnini Z, Lamotte-Brasseur J *et al.* 1997. Enzymes from Cold-

Adapted Microorganisms—The Class C β-lactamase from the Antarctic Psychrophile *Psychrobacter Immobilis* A5. European Journal of Biochemistry **244**: 186-191.

Felsenstein J. 1985. Confidence limits on phylogenies: an approach using the bootstrap. Evolution: 783-791.

Feng P. 1997. Impact of molecular biology on the detection of foodborne pathogens. Molecular Biotechnology **7**: 267-278.

Fernández-No IC, Böhme K, Calo-Mata P *et al.* 2012. Isolation and characterization of Streptococcus parauberis from vacuum-packaging refrigerated seafood products. Food Microbiology **30**: 91-97.

Fluit A, Schmitz FJ. 2004. Resistance integrons and super-integrons. Clinical Microbiology and Infection **10**: 272-288.

Food, Administration D. 2005. *Vibrio parahaemolyticus* risk assessment: quantitative risk assessment on the public health impact of pathogenic *Vibrio parahaemolyticus* in raw oysters. Food and Drug Administration, Washington, DC http://www. fda. gov. pallas2. tcl. sc edu/Food/ScienceResearch/ResearchAreas/RiskAssessmentSafetyAssessment/ucm050421.htm (accessed 10.2.16).

Fu M, Wang Z, Li Y *et al.* 2009. Phytoplankton biomass size structure and its regulation in the Southern Yellow Sea (China): Seasonal variability. Continental Shelf Research **29**: 2178-2194.

Fuse H, Inoue H, Murakami K *et al.* 2003. Production of free and organic iodine by Roseovarius spp. FEMS Microbiology Letters **229**: 189-194.

Görke B, Stülke J. 2008. Carbon catabolite repression in bacteria: many ways to make the most out of nutrients. Nature Reviews Microbiology **6**: 613-624.

Gao B, Mohan R, Gupta RS. 2009. Phylogenomics and protein signatures elucidating the evolutionary relationships among the Gammaproteobacteria. International Journal of Systematic and Evolutionary Microbiology **59**: 234-247.

Givens CE, Burnett KG, Burnett LE *et al.* 2013. Microbial communities of the carapace, gut, and hemolymph of the Atlantic blue crab, *Callinectes sapidus*. Marine Biology **160**: 2841-2851.

Goffredi SK, Jones WJ, Erhlich H *et al.* 2008. Epibiotic bacteria associated with the recently discovered Yeti crab, *Kiwa hirsuta*. Environmental Microbiology **10**: 2623-2634.

González JM, Simó R, Massana R *et al.* 2000. Bacterial community structure associated with a dimethylsulfoniopropionate-producing North Atlantic algal bloom. Applied and Environmental Microbiology **66**: 4237-4246.

Gray LD, Kreger AS. 1987. Mouse skin damage caused by cytolysin from *Vibrio vulnificus* and by *V. vulnificus* infection. Journal of Infectious Diseases **155**: 236-241.

Gulig PA, Bourdage KL, Starks AM. 2005. Molecular pathogenesis of *Vibrio vulnificus*. Journal of Microbiology **43**: 118-131.

Gupta RS. 2000. The phylogeny of proteobacteria: relationships to other eubacterial phyla and eukaryotes. FEMS Microbiology Reviews **24**: 367-402.

Handelsman J. 2004. Metagenomics: application of genomics to uncultured microorganisms. Microbiology and Molecular Biology Reviews **68**: 669-685.

Harris JM. 1993. The presence, nature, and role of gut microflora in aquatic invertebrates: a synthesis. Microbial Ecology **25**: 195-231.

Harwood VJ, Gandhi JP, Wright AC. 2004. Methods for isolation and confirmation of *Vibrio vulnificus* from oysters and environmental sources: a review. Journal of Microbiological Methods **59**: 301-316.

Hasson KW, Wyld EM, Fan Y *et al.* 2009. Streptococcosis in farmed *Litopenaeus vannamei*: a new emerging bacterial disease of penaeid shrimp. Diseases of Aquatic Organisms **86**: 93-106.

Hehemann J-H, Correc G, Barbeyron T *et al.* 2010. Transfer of carbohydrate-active enzymes from marine bacteria to Japanese gut microbiota. Nature **464**: 908-912.

Honda T, Ni Y, Miwatani T. 1988. Purification and characterization of a hemolysin produced by a clinical isolate of Kanagawa phenomenon-negative *Vibrio parahaemolyticus* and related to the thermostable direct hemolysin. Infection and Immunity **56**: 961-965.

Hor LI, Gao CT, Wan L. 1995. Isolation and Characterization of *Vibrio vulnificus* Inhabiting the Marine Environment of the Southwestern Area of Taiwan. Journal of Biomedical Science **2**: 384-389.

Horseman MA, Surani S. 2011. A comprehensive review of *Vibrio vulnificus*: an important cause of severe sepsis and skin and soft-tissue infection. International journal of infectious diseases : IJID : official publication of the International Society for Infectious Diseases **15**: e157-166.

Hueck CJ. 1998. Type III protein secretion systems in bacterial pathogens of animals and plants. Microbiology and Molecular Biology Reviews **62**: 379-433.

Hur M, Kim Y, Song H-R *et al.* 2011. Effect of genetically modified poplars on soil microbial communities during the phytoremediation of waste mine tailings. Applied and Environmental Microbiology **77**: 7611-7619.

Ichikawa H, Beardsley RC. 2002. The current system in the Yellow and East China Seas. Journal of Oceanography **58**: 77-92.

Jensen RV, DePasquale SM, Harbolick EA *et al.* 2013. Complete genome sequence of prepandemic *Vibrio parahaemolyticus* BB22OP. Genome Announcements **1**: e00002-00012.

Jeon Y-S, Chun J, Kim B-S. 2013. Identification of household bacterial community and analysis of species shared with human microbiome. Current Microbiology **67**: 557-563.

Jeong HG, Satchell KJ. 2012. Additive function of *Vibrio vulnificus* MARTX(Vv) and VvhA cytolysins promotes rapid growth and epithelial tissue necrosis during intestinal infection. PLoS Pathogens **8**: e1002581.

Jeong KC, Jeong HS, Rhee JH *et al.* 2000. Construction and phenotypic evaluation of a *Vibrio vulnificus vvpE* mutant for elastolytic protease. Infection and immunity **68**: 5096-5106.

Johnston MA, Davies PS. 1972. Carbohydrates of the hepatopancreas and blood tissues of *Carcinus*. Comparative Biochemistry and Physiology Part B: Comparative Biochemistry **41**: 433-443.

Jokerst JC, Adkins JA, Bisha B *et al.* 2012. Development of a paper-based analytical device for colorimetric detection of select foodborne pathogens. Analytical Chemistry **84**: 2900-2907.

Jones MK, Oliver JD. 2009. *Vibrio vulnificus*: disease and pathogenesis. Infection and Immunity **77**: 1723-1733.

Joseph SW, Colwell RR, Kaper JB. 1982. *Vibrio parahaemolyticus* and related halophilic *Vibrios*. Critical Reviews in Microbiology **10**: 77-124.

Jun JW, Kim JH, Choresca Jr CH *et al.* 2012. Isolation, molecular characterization,

and antibiotic susceptibility of *Vibrio parahaemolyticus* in Korean seafood. Foodborne Pathogens and Disease **9**: 224-231.

Kalburge S, Polson S, Crotty KB *et al.* 2014. Complete genome sequence of *Vibrio parahaemolyticus* environmental strain UCM-V493. Genome Announcements **2**: e00159-00114.

Kaneko T, Colwell RR. 1973. Ecology of *Vibrio parahaemolyticus* in Chesapeake bay. Journal of Bacteriology **113**: 24-32.

Kang MK, Jhee EC, Koo BS *et al.* 2002. Induction of nitric oxide synthase expression by *Vibrio vulnificus* cytolysin. Biochemical and Biophysical Research Communications **290**: 1090-1095.

Kaspar C, Tamplin M. 1993. Effects of temperature and salinity on the survival of *Vibrio vulnificus* in seawater and shellfish. Applied and Environmental Microbiology **59**: 2425-2429.

Katzenell U, Shemer J, Bar-Dayan Y. 2001. Streptococcal contamination of food: an unusual cause of epidemic pharyngitis. Epidemiology and Infection **127**: 179-184.

Keyhani NO, Roseman S. 1999. Physiological aspects of chitin catabolism in marine bacteria. Biochimica et Biophysica Acta (BBA)-General Subjects **1473**: 108-122.

Kim BS, Kim JS. 2002. Cholesterol induce oligomerization of *Vibrio vulnificus* cytolysin specifically. Experimental and Molecular Medicine **34**: 239-242.

Kim HR, Rho HW, Jeong MH *et al.* 1993. Hemolytic mechanism of cytolysin produced from *Vibrio vulnificus*. Life Sci **53**: 571-577.

Kim S, Bang YJ, Kim D *et al.* 2014. Distinct characteristics of OxyR2, a new OxyR-type regulator, ensuring expression of Peroxiredoxin 2 detoxifying low

levels of hydrogen peroxide in *Vibrio vulnificus*. Molecular microbiology **93**: 992-1009.

Kim SM, Park JH, Lee HS *et al.* 2013. LuxR homologue SmcR is essential for *Vibrio vulnificus* pathogenesis and biofilm detachment, and its expression is induced by host cells. Infection and Immunity **81**: 3721-3730.

Kim Y, Lee S, Sagong H *et al.* 2012. Development and evaluation of a new device to effectively detach micro-organisms from food samples. Letters in Applied Microbiology **55**: 256-262.

Kim YR, Lee SE, Kim CM *et al.* 2003a. Characterization and pathogenic significance of *Vibrio vulnificus* antigens preferentially expressed in septicemic patients. Infection and Immunity **71**: 5461-5471.

Kim YR, Lee SE, Kook H *et al.* 2008. *Vibrio vulnificus* RTX toxin kills host cells only after contact of the bacteria with host cells. Cell Microbiology **10**: 848-862.

Kim YR, Rhee JH. 2003b. Flagellar basal body *flg* operon as a virulence determinant of *Vibrio vulnificus*. Biochemical and Biophysical Research Communications **304**: 405-410.

Kirkwood M, Le Brun NE, Todd JD *et al.* 2010. The *dddP* gene of *Roseovarius nubinhibens* encodes a novel lyase that cleaves dimethylsulfoniopropionate into acrylate plus dimethyl sulfide. Microbiology **156**: 1900-1906.

KOOFS. 2015. Korea Ocean Observing And Forecasting System. http://www.khoa.go.kr/koofs/kor/oldobservation/obs_past_search_statistic do (accessed 15.4.16).

Kulkarni S, Lever S, Logan J *et al.* 2002. Detection of Campylobacter species: a comparison of culture and polymerase chain reaction based methods. Journal of Clinical Pathology **55**: 749-753.

Kwon KB, Yang JY, Ryu DG *et al.* 2001. *Vibrio vulnificus* cytolysin induces superoxide anion-initiated apoptotic signaling pathway in human ECV304 cells. The Journal of Biological Chemistry **276**: 47518-47523.

Kwon SR, Oh YJ, Eum HS *et al.* 2000. Estimated magnitude of an outbreak of *Vibrio parahaemolyticus* enteritis in Inchon, Korea. Korean Journal of Infectious Diseases **32**: 100-107.

Lüdeke CH, Kong N, Weimer BC *et al.* 2015. Complete genome sequences of a clinical isolate and an environmental isolate of *Vibrio parahaemolyticus*. Genome Announcements **3**: e00216-00215.

Lee BC, Kim SH, Choi SH *et al.* 2005. Induction of interleukin-8 production via nuclear factor-kappaB activation in human intestinal epithelial cells infected with *Vibrio vulnificus*. Immunology **115**: 506-515.

Lee JH, Kim MW, Kim BS *et al.* 2007. Identification and characterization of the *Vibrio vulnificus rtxA* essential for cytotoxicity *in vitro* and virulence in mice. Journal of Microbiology **45**: 146-152.

Lee JH, Park NY, Lee MH *et al.* 2003. Characterization of the *Vibrio vulnificus putAP* operon, encoding proline dehydrogenase and proline permease, and its differential expression in response to osmotic stress. Journal of Bacteriology **185**: 3842-3852.

Lee JH, Rho JB, Park KJ *et al.* 2004. Role of flagellum and motility in pathogenesis of *Vibrio vulnificus*. Infection and Immunity **72**: 4905-4910.

Leisner JJ, Laursen BG, Prévost H *et al.* 2007. Carnobacterium: positive and negative effects in the environment and in foods. FEMS Microbiology Reviews **31**: 592-613.

Li K, Guan W, Wei G *et al.* 2007. Phylogenetic analysis of intestinal bacteria in the Chinese mitten crab (*Eriocheir sinensis*). Journal of Applied Microbiology

103: 675-682.

Li S, Sun L, Wu H *et al.* 2012. The intestinal microbial diversity in mud crab (*Scylla paramamosain*) as determined by PCR-DGGE and clone library analysis. Journal of Applied Microbiology **113**: 1341-1351.

Lim JG, Choi SH. 2014. IscR is a global regulator essential for pathogenesis of *Vibrio vulnificus* and induced by host cells. Infection and Immunity **82**: 569-578.

Linkous DA, Oliver JD. 1999. Pathogenesis of *Vibrio vulnificus*. FEMS Microbiology Letters **174**: 207-214.

Litwin CM, Byrne BL. 1998. Cloning and characterization of an outer membrane protein of *Vibrio vulnificus* required for heme utilization: regulation of expression and determination of the gene sequence. Infection and Immunity **66**: 3134-3141.

Liu M, Xiao T, Sun J *et al.* 2013. Bacterial community structures associated with a natural spring phytoplankton bloom in the Yellow Sea, China. Deep Sea Research Part II: Topical Studies in Oceanography **97**: 85-92.

Lo W-S, Chen H, Chen C-Y *et al.* 2014. Complete genome sequence of *Vibrio vulnificus* 93U204, a bacterium isolated from diseased tilapia in Taiwan. Genome Announcements **2**: e01005-01014.

Lynch T, Livingstone S, Buenaventura E *et al.* 2005. *Vibrio parahaemolyticus* disruption of epithelial cell tight junctions occurs independently of toxin production. Infection and Immunity **73**: 1275-1283.

Majiduddin FK, Materon IC, Palzkill TG. 2002. Molecular analysis of beta-lactamase structure and function. International Journal of Medical Microbiology **292**: 127-137.

Makino K, Oshima K, Kurokawa K *et al.* 2003. Genome sequence of *Vibrio parahaemolyticus*: a pathogenic mechanism distinct from that of *Vibrio cholerae*. The Lancet **361**: 743-749.

Manivasagan P, Venkatesan J, Kim S-K. 2013. Introduction to marine actinobacteria. Marine microbiology: bioactive compounds and biotechnological applications **1**: 1-19.

Matulkova P, Gobin M, Taylor J *et al.* 2013. Crab meat: a novel vehicle for *E. coli* O157 identified in an outbreak in South West England, August 2011. Epidemiology and Infection **141**: 2043-2050.

McCarter L. 1999. The multiple identities of *Vibrio parahaemolyticus*. Journal of Molecular Microbiology and Biotechnology **1**: 51-57.

Merkel SM, Alexander S, Zufall E *et al.* 2001. Essential role for estrogen in protection against *Vibrio vulnificus*-induced endotoxic shock. Infection and Immunity **69**: 6119-6122.

MFDS. 2015. Ministry of Food and Drug Satety in South Korea URL http://www.foodsafetykorea.go.kr/portal/mainhtml (accessed 4.10.16).

Miyoshi S-I, Sultan SZ, Yasuno Y *et al.* 2006. Growth phase-dependent production of a toxic metalloprotease by *Vibrio vulnificus*. Toxin Reviews **25**: 19-30.

Moir J, Wood N. 2001. Nitrate and nitrite transport in bacteria. Cellular and Molecular Life Sciences **58**: 215-224.

Moon H-B, Kim H-S, Choi M *et al.* 2009. Human health risk of polychlorinated biphenyls and organochlorine pesticides resulting from seafood consumption in South Korea, 2005–2007. Food and Chemical Toxicology **47**: 1819-1825.

Moreno-Vivián C, Cabello P, Martínez-Luque M *et al.* 1999. Prokaryotic nitrate

reduction: molecular properties and functional distinction among bacterial nitrate reductases. Journal of Bacteriology **181**: 6573-6584.

Mortazavi A, Williams BA, McCue K *et al.* 2008. Mapping and quantifying mammalian transcriptomes by RNA-Seq. Nature Methods **5**: 621-628.

NIFS. 2013. National institute of Fisheries Science, Red Tide information. http://www.nifs.go.kr/redtide/webpage/environment/genesis_02_2012jsp (accessed 27.4.16)

Nishibuchi M, Kaper JB. 1995. Thermostable direct hemolysin gene of *Vibrio parahaemolyticus*: a virulence gene acquired by a marine bacterium. Infection and Immunity **63**: 2093.

Oh C-W. 2011. Population biology of the swimming crab *Portunus trituberculatus* (Miers, 1876)(Decapoda, Brachyura) on the western coast of Korea, Yellow Sea. Crustaceana **84**: 1251.

Okada K, Iida T, Kita-Tsukamoto K *et al.* 2005. *Vibrios* commonly possess two chromosomes. Journal of Bacteriology **187**: 752-757.

Oliver JD. *Vibrio vulnificusOceans and health: pathogens in the marine environment*: Springer, 2005a, 253-276.

Oliver JD. 2005b. Wound infections caused by *Vibrio vulnificus* and other marine bacteria. Epidemiology and Infection **133**: 383-391.

Osaka K, Komatsuzaki M, Takahashi H *et al.* 2004. *Vibrio vulnificus* septicaemia in Japan: an estimated number of infections and physicians' knowledge of the syndrome. Epidemiology and Infection **132**: 993-996.

Ottemann KM, Miller JF. 1997. Roles for motility in bacterial-host interactions. Molecular Microbiolgy **24**: 1109-1117.

Palasuntheram C. 1981. The halophilic properties of *Vibrio parahaemolyticus*. Microbiology **127**: 427-428.

Paranjpye RN, Lara JC, Pepe JC *et al.* 1998. The type IV leader peptidase/N-methyltransferase of *Vibrio vulnificus* controls factors required for adherence to HEp-2 cells and virulence in iron-overloaded mice. Infection and Immunity **66**: 5659-5668.

Paranjpye RN, Strom MS. 2005. A *Vibrio vulnificus* type IV pilin contributes to biofilm formation, adherence to epithelial cells, and virulence. Infection and Immunity **73**: 1411-1422.

Park BS, Kim J-H, Kim JH *et al.* 2015. Dynamics of bacterial community structure during blooms of *Cochlodinium polykrikoides* (Gymnodiniales, Dinophyceae) in Korean coastal waters. Harmful Algae **48**: 44-54.

Park JH, Cho Y-J, Chun J *et al.* 2011. Complete genome sequence of *Vibrio vulnificus* MO6-24/O. Journal of Bacteriology **193**: 2062-2063.

Park K-S, Ono T, Rokuda M *et al.* 2004a. Functional characterization of two type III secretion systems of *Vibrio parahaemolyticus*. Infection and Immunity **72**: 6659-6665.

Park KS, Ono T, Rokuda M *et al.* 2004b. Cytotoxicity and enterotoxicity of the thermostable direct hemolysin-deletion mutants of *Vibrio parahaemolyticus*. Microbiology and Immunology **48**: 313-318.

Park SC, Lee JH, Kang JW *et al.* 2014. Seasonal variations in the bacterial community of Gwangyang Bay seawater. 생명과학회지 **24**: 522-531.

Park SD, Kim HD, Won TH *et al.* 2008. Epidemiological studies of *Vibrio vulnificus* sepsis. Korean Journal of Dermatology **46**: 171-180.

Pazhani GP, Bhowmik SK, Ghosh S *et al.* 2014. Trends in the epidemiology of pandemic and non-pandemic strains of *Vibrio parahaemolyticus* isolated from diarrheal patients in Kolkata, India. PLoS Neglected Tropical Diseases **8**: 10.1371.

Pinhassi J, Simó R, González JM *et al.* 2005. Dimethylsulfoniopropionate turnover is linked to the composition and dynamics of the bacterioplankton assemblage during a microcosm phytoplankton bloom. Applied and Environmental Microbiology **71**: 7650-7660.

Raghunath P. 2014. Roles of thermostable direct hemolysin (TDH) and TDH-related hemolysin (TRH) in *Vibrio parahaemolyticus*. Frontiers in Microbiology **5**.

Richardson D, Berks B, Russell D *et al.* 2001. Functional, biochemical and genetic diversity of prokaryotic nitrate reductases. Cellular and Molecular Life Sciences **58**: 165-178.

Riesenfeld CS, Schloss PD, Handelsman J. 2004. Metagenomics: genomic analysis of microbial communities. Annual Review Genetetics **38**: 525-552.

Román L, Real F, Sorroza L *et al.* 2012. The in vitro effect of probiotic *Vagococcus fluvialis* on the innate immune parameters of *Sparus aurata* and *Dicentrarchus labrax*. Fish and Shellfish Immunology **33**: 1071-1075.

Ruiz-Zarzuela I, de Bias I, Gironés O *et al.* 2005. Isolation of *Vagococcus salmoninarum* in rainbow trout, Oncorhynchus mykiss (Walbaum), broodstocks: characterization of the pathogen. Veterinary Research Communications **29**: 553-562.

Saitou N, Nei M. 1987. The neighbor-joining method: a new method for reconstructing phylogenetic trees. Molecular Biology and Evolution **4**: 406-425.

Satchell KJ, Geissler B. The multifunctional-autoprocessing RTX toxins of *Vibrios Microbial toxins: current research and future trends Caister Academic Press, Auckland, New Zealand*. Auckland, New Zealand Caister Academic Press, 2009, 113-126.

Schloss PD, Westcott SL, Ryabin T *et al.* 2009. Introducing mothur: open-source, platform-independent, community-supported software for describing and comparing microbial communities. Applied and Environmental Microbiology **75**: 7537-7541.

Shen Z-L. 2001. Historical changes in nutrient structure and its influences on phytoplantkon composition in Jiaozhou Bay. Estuarine, Coastal and Shelf Science **52**: 211-224.

Shinoda S. 2011. Sixty years from the discovery of *Vibrio parahaemolyticus* and some recollections. Biocontrol Science **16**: 129-137.

Shirai H, Ito H, Hirayama T *et al.* 1990. Molecular epidemiologic evidence for association of thermostable direct hemolysin (TDH) and TDH-related hemolysin of *Vibrio parahaemolyticus* with gastroenteritis. Infection and Immunity **58**: 3568-3573.

Simpson LM, Oliver JD. 1983. Siderophore production by *Vibrio vulnificus*. Infection and Immunity **41**: 644-649.

Simpson LM, White VK, Zane SF *et al.* 1987. Correlation between virulence and colony morphology in *Vibrio vulnificus*. Infection and Immunity **55**: 269-272.

Sorroza L, Padilla D, Acosta F *et al.* 2012. Characterization of the probiotic strain *Vagococcus fluvialis* in the protection of European sea bass (*Dicentrarchus labrax*) against vibriosis by *Vibrio anguillarum*. Veterinary Microbiology **155**: 369-373.

Stewart EJ. 2012. Growing unculturable bacteria. Journal of Bacteriology **194**: 4151-4160.

Stokes Ht, Hall RM. 1989. A novel family of potentially mobile DNA elements encoding site-specific gene-integration functions: integrons. Molecular Microbiology **3**: 1669-1683.

Strom MS, Paranjpye RN. 2000a. Epidemiology and pathogenesis of *Vibrio vulnificus*. Microbes and Infection **2**: 177-188.

Strom MS, Paranjpye RN. 2000b. Epidemiology and pathogenesis of *Vibrio vulnificus*. Microbes and Infection **2**: 177-188.

Su YC, Liu C. 2007. *Vibrio parahaemolyticus*: a concern of seafood safety. Food Microbiology **24**: 549-558.

Tamura K, Stecher G, Peterson D *et al.* 2013. MEGA6: molecular evolutionary genetics analysis version 6.0. Molecular Biology and Evolution **30**: 2725-2729.

Tan S, Zhou J, Zhu X *et al.* 2015. An association network analysis among microeukaryotes and bacterioplankton reveals algal bloom dynamics. Journal of Phycology **51**: 120-132.

Taskila S, Tuomola M, Ojamo H. 2012. Enrichment cultivation in detection of food-borne *Salmonella*. Food Control **26**: 369-377.

Taylor JD, Cottingham SD, Billinge J *et al.* 2014. Seasonal microbial community dynamics correlate with phytoplankton-derived polysaccharides in surface coastal waters. The ISME journal **8**: 245-248.

Teague W, Jacobs G, Ko D *et al.* 2003. Connectivity of the Taiwan, Cheju, and Korea straits. Continental Shelf Research **23**: 63-77.

Thompson JD, Gibson T, Higgins DG. 2002. Multiple sequence alignment using ClustalW and ClustalX. Current Protocols in Bioinformatics: 2.3. 1-2.3. 22.

Vazquez A, Markert EK, Oltvai ZN. 2011. Serine biosynthesis with one carbon catabolism and the glycine cleavage system represents a novel pathway for ATP generation. PLoS One **6**: e25881-e25881.

Vendrell D, Balcázar JL, Ruiz-Zarzuela I *et al.* 2006. *Lactococcus garvieae* in fish: a review. Comparative Immunology, Microbiology and Infectious Diseases **29**: 177-198.

Wade W. 2002. Unculturable bacteria—the uncharacterized organisms that cause oral infections. Journal of the Royal Society of Medicine **95**: 81-83.

Wang B-d, Wang X-l, Zhan R. 2003. Nutrient conditions in the Yellow Sea and the East China Sea. Estuarine, Coastal and Shelf Science **58**: 127-136.

Wang CYC, Shie HS, Chen SC *et al.* 2007. *Lactococcus garvieae* infections in humans: possible association with aquaculture outbreaks. International Journal of Clinical Practice **61**: 68-73.

Watsuji T-o, Nakagawa S, Tsuchida S *et al.* 2009. Diversity and function of epibiotic microbial communities on the galatheid crab, *Shinkaia crosnieri*. Microbes and Environments: 1008060218.

Webster AC, Litwin CM. 2000. Cloning and characterization of vuuA, a gene encoding the *Vibrio vulnificus* ferric vulnibactin receptor. Infection and Immunity **68**: 526-534.

Wortman A, Somerville C, Colwell R. 1986. Chitinase determinants of *Vibrio vulnificus*: gene cloning and applications of a chitinase probe. Applied and Environmental Microbiology **52**: 142-145.

Wright AC, Hill RT, Johnson JA *et al.* 1996. Distribution of *Vibrio vulnificus* in

the Chesapeake Bay. Applied and Environmental Microbiology **62**: 717-724.

Wright AC, Morris JG, Jr. 1991. The extracellular cytolysin of *Vibrio vulnificus*: inactivation and relationship to virulence in mice. Infection and Immunity **59**: 192-197.

Wright AC, Powell JL, Kaper JB *et al.* 2001. Identification of a group 1-like capsular polysaccharide operon for *Vibrio vulnificus*. Infection and Immunity **69**: 6893-6901.

Wright AC, Powell JL, Tanner MK *et al.* 1999. Differential expression of *Vibrio vulnificus* capsular polysaccharide. Infection and Immunity **67**: 2250-2257.

Wright AC, Simpson LM, Oliver JD. 1981. Role of iron in the pathogenesis of *Vibrio vulnificus* infections. Infection and Immunity **34**: 503-507.

Wu S, Zhu Z, Fu L *et al.* 2011. WebMGA: a customizable web server for fast metagenomic sequence analysis. BMC Genomics **12**: 444.

Wu Y, Wen J, Ma Y *et al.* 2014. Epidemiology of foodborne disease outbreaks caused by *Vibrio parahaemolyticus*, China, 2003–2008. Food Control **46**: 197-202.

Xu M, Yamamoto K, Honda T. 1994. Construction and characterization of an isogenic mutant of *Vibrio parahaemolyticus* having a deletion in the thermostable direct hemolysin-related hemolysin gene (*trh*). Journal of Bacteriology **176**: 4757-4760.

Yen M-T, Yang J-H, Mau J-L. 2009. Physicochemical characterization of chitin and chitosan from crab shells. Carbohydrate Polymers **75**: 15-21.

Yoshida S, Ogawa M, Mizuguchi Y. 1985. Relation of capsular materials and colony opacity to virulence of *Vibrio vulnificus*. Infection and Immunity **47**:

446-451.

Yu C, Lee AM, Bassler B *et al.* 1991. Chitin utilization by marine bacteria. A physiological function for bacterial adhesion to immobilized carbohydrates. Journal of Biological Chemistry **266**: 24260-24267.

Yu Y, Yang H, Li J *et al.* 2012. Putative type VI secretion systems of *Vibrio parahaemolyticus* contribute to adhesion to cultured cell monolayers. Archives of Microbiology **194**: 827-835.

Zdobnov EM, Apweiler R. 2001. InterProScan–an integration platform for the signature-recognition methods in InterPro. Bioinformatics **17**: 847-848.

Zhang CI, Lim JH, Kwon Y *et al.* 2014. The current status of west sea fisheries resources and utilization in the context of fishery management of Korea. Ocean & Coastal Management **102**: 493-505.

Zhang L, Orth K. 2013. Virulence determinants for *Vibrio parahaemolyticus* infection. Current Opinion in Microbiology **16**: 70-77.

Zhang M, Sun Y, Chen L *et al.* 2016. Symbiotic bacteria in gills and guts of chinese mitten crab (*Eriocheir sinensis*) differ from the free-living bacteria in water. PloS One **11**: e0148135.

Zhou M-j, Shen Z-l, Yu R-c. 2008. Responses of a coastal phytoplankton community to increased nutrient input from the Changjiang (Yangtze) River. Continental Shelf Research **28**: 1483-1489.

국문초록

패혈증 비브리오균과 장염 비브리오균은 어패류의 생식을 통해 인간을 감염시켜 식중독을 유발하는 기회 감염성 병원성 미생물이다. 최근까지도 패혈증 비브리오균과 장염 비브리오균에 의한 식중독 사례가 빈번하게 보고되고 있으나, 패혈증 비브리오균은 4종, 장염 비브리오균은 5종만이 완벽하게 sequencing 되어 보고되었다. 국내 식중독 사고에서 분리한 패혈증 비브리오균과 장염 비브리오균이 가지는 독성인자를 동정하고 병원성을 확인하기 위하여, 식중독 환자의 혈액에서 분리된 패혈증 비브리오 FORC_016과 식중독 원인 식품인 도다리로부터 분리된 장염 비브리오 FORC_008의 게놈을 완벽하게 분석하였다. 유전체 분석을 통해 패혈증 비브리오 FORC_016의 게놈은 2개의 유전체로 구성되어 있으며 4,461개의 단백질 암호화 유전자와 129개의 tRNA, 34개의 rRNA를 가지고 있음을 밝혀내었다. 또한, 장염 비브리오 FORC_008의 게놈은 2개의 유전체로 구성되어 있으며 4,494개의 단백질 암호화 유전자와 129개의 tRNA, 3개의 rRNA를 가지고 있음을 밝혀내었다. 추가적인 게놈 분석을 통해 패혈증 비브리오 FORC_016이 다수의 독성 유전자를 가지고 있으며 다른 패혈증 비브리오와는 차별화된 독성 유전자를 가지고 있음을 확인하였다. 장염 비브리오 FORC_008의 경우 일반적으로 널리 알려져 있는 주요 독성인자인 두 개의 용혈소를 가지고

있지 않지만 type III secretion system (T3SS)과 용혈소로 예측되는 단백질을 가지고 있음을 밝혀내었다.

더불어 본 연구는 독성 유전자를 다수 보유하고 있는 패혈증 비브리오 FORC_016이 꽃게와 접촉하였을 때 전사체 변화 양상을 RNA-sequencing 기법을 통해 비교 분석하였다. 각 유전자 발현량을 분석한 결과, 꽃게와 접촉하였을 때 접촉 시간에 따라 1시간 접촉 시 1,327개의 유전자가, 4시간 접촉 시 791개의 유전자가 특징적으로 발현이 변화하는 것을 확인하였다 (*P*-value < 0.05, 2 배 기준). 꽃게와 접촉한 시간과는 상관없이, 꽃게에 접촉한 패혈증 비브리오에서 에너지 생성, 세포 성장, 단백질 수송, 포도당 대사와 같은 성장과 관련된 유전자의 발현량이 증가하는 것을 확인하였으며, 이와는 반대로 아미노산 생합성, 질소 대사, 포도당 외의 다른 당류 대사에 관여된 유전자는 발현량이 감소하는 것을 밝혀내어 패혈증 비브리오가 꽃게에 존재하는 영양소를 대사하여 생장할 수 있음을 추측할 수 있었다. 이와는 반대로, 유해 인자들의 발현량은 꽃게와 접촉할 시 감소하였으며, 이로부터 꽃게가 패혈증 비브리오의 저장소의 역할을 할 수 있으며 꽃게가 패혈증 비브리오에 감염된 경우 패혈증 비브리오의 빠른 생장 때문에 꽃게를 먹었을 때 식중독을 유발할 수 있을 것이라 예측할 수 있었다.

또한 모델 식품으로 사용된 꽃게 내 존재 미생물 군집의 계절별, 지역별 차이를 알아보고자 metagenomics를 이용하여 꽃게 내 미생물 군집을 비교 분석 하였다. 그 결과, 꽃게 내 미생물 군집은 지역보다는 계절의 영향을 강력하게 받음을 밝혀내었다. 또한, 미생물 군집의 다양성을 문 (phylum), 속 (genus) 수준에서 분석한 결과, 꽃게 내 미생물 군집은 봄보다 가을에 더 다양하다는 것을 밝혀내었다. 속 수준에서 미생물 군집 구성을 비교하였을 때, 봄에는 *Psychrobacter, Vagococcus, Carnobacterium*이 우점하고 있는 반면, 가을 꽃게에는 *Roseovarius* 속이 우점을 차지하고 있음을 알 수 있었으며 병원성 균주의 비율이 높을 경우 미생물 군집 내 우점속의 비율이 달라지는 것을 확인하였다. 종합하여 볼 때, 꽃게 내 미생물 군집에 가장 큰 영향을 주는 요소는 계절에 따른 온도 변화일 것이라 결론 지을 수 있었다. 또한 비브리오 속의 각 샘플에서의 비율을 비교해본 결과로부터 꽃게의 섭취를 통해 비브리오 감염이 일어날 수 있음을 밝혀내었다.

주요어: 패혈증 비브리오균, 장염 비브리오균, 생물정보학, 유전체학, 전사체학, 메타게놈, 꽃게

학 번: 2010-21225